universität wien

MASTERARBEIT / MASTER'S THESIS

Titel der Masterarbeit / Title of the Master's Thesis

Going back in time to predict the future:

Changes in benthic communities during the Holocene transgression in the northern Adriatic Sea

verfasst von / submitted by

Iason Pifeas BSc

angestrebter akademischer Grad / in partial fulfilment of the requirements for the degree of

Master of Science (MSc)

Wien, 2017 / Vienna 2017

1

TABLE OF CONTENT

INTRODUCTION

The northern Adriatic is particularly suited area to study mechanisms driving long-term eco-system changes under human pressure. Human exploitation goes back to prehistoric times with anthropogenic impact strongly increasing within the recent decades. (Bralic 1990; Lotze et al. 2006). Monitoring of ecological shifts as a response to environmental pressure typically consists of snapshots taken within a timespan of annual or decadal scale. Conservation paleo-biology is a relatively young discipline of research overcoming this limitation by using geo-historical data. This data can be used to define a baseline to estimate impact of environmental disturbances at a time span beyond direct human observation (Birks 1996, 2012; Delcourt & Delcourt 1998; Swetnam et al. 1999; Gorham et al. 2001; Flessa 2002; NRC 2005; Willis & Birks 2006; Froyd & Willis 2008; Gillson et al. 2008; Smol 2008; Dietl & Flessa 2009, 2011; Jackson & Hobbs 2009; Willis & Bhagwat 2010; Willis et al. 2010a, b; Vegas-Vilarrubia et al.2011; CPW 2012; Louys 2012; Lyman 2012a, b; Sayer et al. 2012; Rick & Lockwood 2013; Gillson & Marchant 2014). Conservation paleobiology follows two approaches. The deep time approach evaluates ecological and evolutionary dynamics in time taking advantage of the entire history of life and the near time approach. The latter uses the relatively recent past as a reference to modern-day condition. Hard part remains of different taxa can give hints of past conditions of the environment and differences in community composition can serve as a proxy of environ-mental changes in time (Grotzinger et al. 2008; Hrs-Brenko 2006; Nerlović et al. 2011; Weber & Zuschin, 2013). This approach represents a powerful tool to gain knowledge to restore bio-diversity and ecosystem services under human pressure (Dietl & Flessa 2011, Dietl et al. 2015). The sediment starved northern Adriatic seafloor originates from Pleistocene sand partly blanketed by Holocene mud (Pigorini 1968; Goff et al. 2006). Sediment load of the Po river results in a west-east gradient from mud to sand (Zuschin & Stachowitsch 2009). Macro-ben-thic communities of the northern Adriatic are generally regarded to be most similar to modern biota of the Antarctic shelf and the deep sea. The more oligotrophic east of the northern Adri-atic Sea is characterized by epifaunal suspension feeding organisms, whereas the eutrophic western regions are dominated by infaunal assemblages (McKinney 2003; McKinney & Hage-man 2006; McKinney et al. 2007). Wide spread high biomass macroepibenthic communities with a highly patchy distribution are reported for the northern Adriatic. This distribution re-sults from the need of such assemblages for hard substrate, to establish this epifaunal multi

species clumps (Kidwell & Jablonski 1983; Zuschin et al. 1999). This hard substrate can be provided from dropstones (Oschmann 1990), pebble sized to larger rock grounds (Lee et al. 1997) or biogenic structures (Hurst 1974; Forester 1979; Stachowitsch 1980; Corriero & Pronzato 1987; Bordeaux & Brett 1990; Ward & Thorpe 1991; Lescinsky 1993; Nebelsick *et al.* 1997; Zuschin & Piller 1997). These aggregations can change substrate quality and is a process of biologically induced environmental modification. Substrate stability, availability of small cavities increases and induces diversification of sessile invertebrates and benthic algae (Odum 1971, Begon et al. 1986). This rigid biogenic framework can further develop to facies referred to as "*Coralligène de plateau*" mainly composed of non-geniculate coralline algae (Laborel 1961, Pérès & Picard 1964, Pérès 1982, Laborel 1987, Bellan-Santini et al. 1994).

The northern Adriatic is a very productive ecosystem. Even the comparatively nutrient poor regions can be regarded as highly productive compared to the Mediterranean average (Ott 1992; Stachowitsch 1991). This semi-enclosed continental sea is characterized by high riverine input and a low bathymetric gradient with an average depth less than 50m (Ott 1992; McKinney 2007). Accumulation of dissolved organic matter (DOC) and eutrophication can cause high benthic mortalities by depletion of oxygen in these areas. These events have occurred periodically and became more frequent from 1969 onward (Crema et al. 1991; Barmawidjaja et al. 1995; N'siala et al. 2008; Nerlović et al. 2011). Anoxic and hypoxic events lead to the modification of behavior, growth and survival of benthic species causing shifts in taxonomic composition (Haselmair et al. 2010; Nerlović et al. 2011; Riedel et al. 2012; Stachowitsch 1984). Therefore, monitoring benthic community shifts in time can give further clues of strength and degree of anthropogenic and environmental impacts (Nerlović et al. 2011; Grotzinger et al. 2008; Hrs-Brenko 2006; Nerlović et al. 2011; Weber & Zuschin 2013).

The coast of the Adriatic Sea has been inhabited for a long time. Material remnants of hunter-fisher gatherers, can be dated back as far as 8000 BC (Kovačević 2002). Anthropogenic impact strongly increased with the onset of the industrialization at the 19th century and the concurrent intensification of fisheries including trawling and dredging (Tudela 2004; DeGroot 1984; Thrush & Dayton 2002). To be able to assess the effects of human impact on this ecosystem it is important to understand the prehumen state.

Environmental pollutants derive usually from infrastructural construction and development,

agriculture, urbanization, industrial development and tourism. Of major concern are contaminants including litters and debris, sediments, pathogens, heavy metals, radionuclides, oils and persistent organic pollutants (Williams 1996). Pollutants accumulate in marine sediments and desorb very slow when bound to particles. Therefore, high concentrations of contaminants can cause or contribute to long-term degradation of a benthic ecosystem (Burton 2002). In this study the content of heavy metals (Hg, Cu, Cr, Ni, Pb, As, Cd, Zn, Mn, Fe), persistent organic pollutants (PCBs, PAHs) and accumulation of nutrients (N, C, TOC) within the sediment was analysed.

Heavy metals enter the marine system through the atmosphere and effluent sources. They are by-products of industrial processes and discharged as wastes into the environment (Robson & Neal 1997). Heavy metals influence metabolic processes of organisms as they have a high affinity to sulphur and bind to sulfhydryl groups of proteins (Davies 1978). Intolerant species can suffer from strong reduction and even elimination by elevated heavy metal concentrations, thereby causing shifts in diversity and trophic structure of communities (Peterson 1986).

Persistent organic pollutants (POP) are usually lipophilic and hydrophobic and have long half lives in sediment, soil, air and biota (Jones & de Voogt 1999). These xenobiotic compounds enter many circles of volatilization and deposition, therefore being widely distributed from their source of introduction to the environment. POP have been found across the planet and strongly accumulate in food chains (GESAMP 1990; Islam & Tanaka 2004; Longwell et al. 1992; Rios et al. 2007). Polychlorinated biphenyls (PCBs) are not found naturally in the environment whereas Polycyclic aromatic hydrocarbons (PAHs) can originate from anthropogenic and natural processes (Creaser et al. 2007a). PAHs are a large group of different substances ranging from two ring Naphthalenes to complex ring structures. Many of these congeners are toxic to marine life and accumulate in the sediment and biota. They enter the marine environment by biogenic production from organisms, incineration, fossil fuels and diagenetic processes in the sediment. Although PAHs have also natural origin, levels in the environment are strongly elevated by anthropogenic activities of domestic combustion and fossil fuel burning (Bojes & Pope 2007; Hylland 2007; Neff 1979; Zeng & Vista 1997).

PCBs represent a group of 209 congeners differing in number and position of chlorine atoms. Because of their low inflammability and chemical stability PCBs are mainly used in electrical

equipment as dielectric fluid and coolant. In product manufactured before 1977 PCBs can also be found in numerous applications like surface coating, plasticizers, adhesives and flame retardants (Porta & Zumeta, 2002). Although the use and production of PCBs has been prohibited in most industrial countries since 1970, high levels of this compounds can still be found in various environments, both abiotic and biotic (Covaci et al. 2002; de Voogt et al. 1990; Voorspoels et al. 2002).

For this study sediment cores were taken close to the Brijuni islands and sliced in different section, to estimate sediment composition, environmental parameters such as pollutants and nutrients and taxonomic changes for respective layers. Sediment dating and time averaged death assemblages can give a glimpse into past conditions. Aim of this study is to identify composition of pre-impact benthic communities to test the degree of change and modification of benthic communities within the Holocene transgression.

MATERIAL AND METHODS

Study area

The Adriatic Sea extends northwest from its connection to the Mediterranean as a narrow landlocked sea, separating the Italian peninsula from the Balkans.

It is separated into three major regions. The southern and middle region are geographically divided by a line drawn from the Gargano through Pelagosa and Susac islands to the coast of Croatia. The boundary to the northern area is placed as a line between Ancona, Italy, and the north of Zadar in Croatia. Appreciably shallower than the southern regions, it has an average depth of 35m. Gently sloping towards the south its maximum depth does not exceed 100m (Buljan & Zore-Armanda 1976; Zavatarelli et al. 2000).

Water movement and circulation within the Northern Adriatic is both wind and density-driven and varies strongly between seasons. Circulation is primarily cyclonic. During fall and winter frequent bora storms generate profound circulation which decline during summer causing a strong isolation of Northern Adriatic waters from southern regions (Zore-Armanda & Gacic 1987).

Another major force driving surface water circulation is the fresh water inflow mainly by the Po river affecting the circulation through buoyancy input. Riverine input represents also the

main source of sediment and nutrients at the northern part of the Adriatic Sea. Therefor a strong west to east gradient of productivity forms. Western near-shore waters are considered to be mesotrophic to eutrophic whereas eastern regions vary from oligotrophic to meso-trophic (Zavatarelli et al. 1998, Harding et al. 1999).

The Northern Adriatic is a relatively young epeiric sea formed during the Holocene by rising sea level. The seafloor at the eastern part is manly covered by an accumulation of Pleistocene and Holocene sediment (McKinney 2007). It displays a pronounced west-to-east change of benthic communities. Infaunal dominated western regions typifying shelves of modern tem-perate and tropical oceans strongly differ from combined infauna-rich and epifauna-rich east-ern regions (Ott 1992), ecologically comparable to Paleozoic offshore environments (McKin-ney 2007).

Sampling was conducted south to Veliki Brijun, the main island of Brijuni Nationalpark located at the coordinates 44°53,146' North and 13°44,820' East at a depth of 44 m (Fig.1). Brijuni archipelago comprises of a group of 14 islands spreading over a total area of 7.48km^2 (Šoštarić & Küster, 2001; Fatovic-Ferencic, 2006). The islands were inhabited as early as prehistoric times. One of the first major anthropogenic impact was probably draining swamps at late 19th century (Bralic 1990; Šoštarić & Küster 2001). Brijuni island has been declared as national park in 1983 and was from this point onward excluded from strong public use (Bralic 1990). Located close to the southernmost tip off Istria it is strongly influenced by low nutrient water moving northward the eastern coast due to the Adriatic-wide cyclonic flow (McKinney 2007).
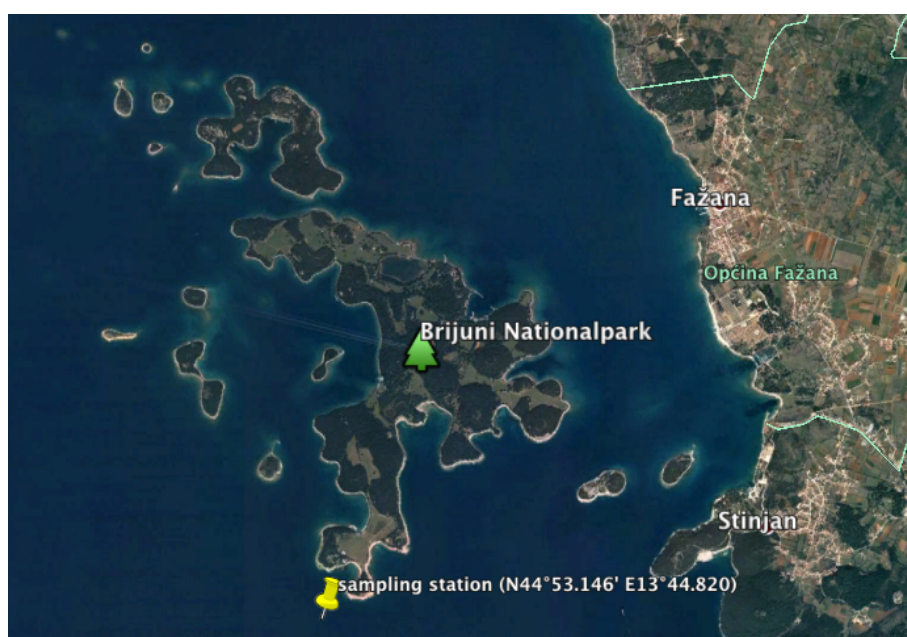

Fig. 1: Sampling station at Brijuni Nationalpark (Google Earth map).

Sampling

Samples were taken with a UWITEC™ piston corer. The device consists of the coring cylinder stabilized by a tripod. Mobile weights are mounted to the apex providing a so-called hammer action to drive the coring cylinder by lifting and release into the sediment. To retain the sediment, it is equipped with a closing mechanism working with hydraulic pressure once the final coring depth is reached. Cores with a length of 150cm and a diameter of 9cm were taken for sediment analysis and environmental pollutants. Another 150cm long core of 16cm diameter was taken to obtain sufficient material for analysis of hard part remains.

The uppermost 20 cm were sliced into 2 cm subsamples and into 5 cm for the remaining 130 cm. Samples were sieved under flowing water with 1mm mesh size and dried at 50°C. Material was sorted for biogenic material using a stereomicroscope and separated into the following taxonomic groups: Corallinaceae, Bryozoa, Brachiopoda, Ophiuroidea, Echinoidea, Bivalvia, Gastropoda, Polyplacophora, Scaphopoda, Polychaeta and Crustacea. All taxonomic groups were weighed separately for each layer. Due to the high number of hard part remains only every second layer was analysed. Corallinaceae were embedded and cut in thin sections for further determination. Literature used for identification of Corallinaceae were Harvey & Woelkerling (2007), Rasser & Piller (2000) and Falace et al. (2011). Bryozoa were determined to species level using specialist identification keys (Hayward & McKinney 2002; Hayward & Ryland 1998; Hayward & Ryland 1999; Zabala & Maluquer 1988) whereas molluscan specimens were only identified to family level (Bosch et al., 1995; Cossignani et al., 1992; 2011; Gofas et al., 2011; Huber, 2010). Bryozoa, Gastropoda, Bivalvia were both weighed and counted. Every colony fragment was counted to estimate Bryozoan abundance in terms of number. Bivalves were separated in left and right valves and double-valved specimens and counted as the sum of double-valved specimens and the higher number of right or left valves. Gastropods were counted if the apex was preserved. Crustacean hard part remains were identified to different taxonomic levels due to their preservation state. Specimen with a poor preservation state or where no characteristic trait was found were classified into 22 morphotypes. Literature used was Pessani et al. (2004), Costello et al. (2001), Garassino & De Angeli (2004a), Garassino & De Angeli (2004b) and Alvarez (1968). For all taxonomic groups topicality and correctness was checked at the Word Register of Marine Species

(http://www.marinespecies.org/14 January 2017). Mollusk species were categorized regarding their substrate relation (infaunal, semiinfaunal, host, borer, nestler, epifaunal mobile and epifaunal immobile) following Beesley et al. (1998), Borja et al. (2000), Gofas et al. (2011a), Gofas et al. (2011b), Huber (2010), Koulouri et al. (2006). Bryozoan species were categorized according to their growth type into several categories of encrusting and erect forms (See table 1).

Table1: Bryozoan growth-forms (modified after Nelson et al. 1988; Bone and James 1993).

Life habitat	Growth forms	
ERECT	cellariform	
	adeoniform	
	vinculariform	
	eschariform	
	reteporiform	
ENCRUSTING	membraniporiform	
	celleporiform	

Analysis of sediment and environmental pollutants

Grain size analysis was conducted with a sedigraph (SediGraph III 5120 Particle Size Analyzer) for the fraction <63μm and dry sieving for fraction 63μm grid size to >1mm grid size. Sediment was categorized into clay, silt, sand excluding particles >1mm and particles > 1mm.

Heavy metal content (Hg, Cu, Cr, Ni, Pb, As, Cd, Zn, Mn, Fe), organic pollutants (PCBs, PAHs) and nutrients (N, C, TOC) were determined at ISMAR Institute Venice. Total nitrogen (Ntot),

total carbon (Ctot) and total organic carbon (TOC) was estimated as percentage dry weight (% dw). Section to determine these parameters were chosen according to a preceding radiographic analysis of the core to find differences of structure and density to select depth intervals for subsampling. The following sections were analysed: 1 cm, 5 cm, 9 cm, 24 cm, 24 cm, 46 cm, 69 cm, 85 cm, 105 cm, 126 cm and 151 cm core depth.

The sediment was radiometric dated by ^{210}Pb dating at the Low Level Counting Label Arsenal, University of Natural Resources and Life Sciences, Vienna. Two natural origins of ^{210}Pb are known. ^{210}Pb formed at the atmosphere by decay of ^{222}Rn called unsupported ^{210}Pb and supported ^{210}Pb which is usually in an equilibrium with ^{226}Ra present in natural minerals and soil. ^{226}Ra is a decay product of the ^{238}U Series (Appleby & Oldfield 1978; Turekian & Graustein 2003). The third source is of anthropogenic origin including wastes enriched in radionuclide. ^{210}Pb dating is based on the determination of excess activity values (unsupported ^{210}Pb) in each layer of the core. Excess ^{210}Pb values are estimated by subtracting supported ^{210}Pb from the ^{210}Pb activities. Assuming a constant influx, unsupported ^{210}Pb should decline with increasing sediment as radioactive decay proceeds making it possible to estimate sedimentation rates (Pennington 1973; de Souza et al. 2012).

The core taken for analysis of hard part remains is only 100 cm long and therefore much shorter than the sediment core which was 160 cm long. To correlate differences in taxonomic composition to changes of abiotic parameters at the sediment core time averaging of respective layers was estimated by ^{14}C calibrated Amino acid racemisation (AAR) of shells. Layers of the same medium age in consideration of sediment composition were aligned to each other. The bivalve species *Timoclea ovata* was targeted for this dating method because of its high abundance throughout the core. Intra-crystalline proteins are targeted. This technique uses the chiral nature of amino acids. All protein amino acids except glycine can exist as either D- or L- enantiomer. AAR changes the relative frequency of D- or L- handed enantiomers during diagenesis. Racemisation rate depends highly on environmental factors, especially temperature. Therefor AAR yields only relative ages and has to be ^{14}C calibrated (Allen et al. 2013; Demarchi & Collins 2014; Kosnik & Kaufman 2008). Protein residues protected by skeletal hard parts survive in many environments for long time periods. Racemisation rate in fossils has a half-time of 10^4-10^5 yr making it suitable for Holocene to upper Pleistocene remains (Bada 1985).

Data assessment and statistical analysis

Statistical analysis was conducted in R (R core team, 2016) and PAST (Hammer et al. 2001). Cluster analysis and nonmetric-multidimensional scaling (nMDS) are based on Bray-Curtis similarity of square-root transformed data using the package vegan (Oksanen et al. 2015). Analysis was conducted for both, weight- and counting data. To find dominant taxa within the core, rank abundance distributions were done for the whole core and for each cluster. Dufrene-Legendre Indicator Species Analysis was conducted to test for statistical significance of the association of taxa to respective clusters by permutation. This function is part of the package labdv (Roberts 2016).

The function envfit() of the package vegan (Oksanen et al. 2015) was used to correlate shifts in community composition to the environmental parameters, nutrients (Ctot,TOC, Ntot), heavy metals (Hg, Cu, Cr, Ni, Pb, As, Cd, Zn, Mn, Fe) organic pollutants (PCBs, PAHs) and grain size. This function fits this environmental variable onto the ordination by associating site scores (nMDS scores of certain layers) to their concentration within the sediment.

Rarefaction of species richness and estimation of diversity was done with iNEXT (Hsieh 2016) and EstimateS (Colwell 2013). The Pearson correlation coefficient of estimated values of species richness and diversity and environmental parameters was calculated.
For graphical display and data organization Microsoft excel and the packages BiodiversityR (Kindt & Coe 2005), analogue (Simpson & Oksanen 2016) and ggplot2 (Wickham 2009) of R were used.

RESULTS

Hard part remains throughout the core consisted of Mollusca, Echinodermata, Crustacea, Bryozoa, Brachiopoda, Foraminifera and of non-geniculate Corallinaceae. Data analysis reveals a steep increase of total amount of hard part remains in the earlier stages of the Holocene transgression peaking at sediment depth of 50-55 cm. This layer is followed by a gradual decline towards the top. At the uppermost layers this trend weakens, showing even a minor increase in hard part remains at a depth 0-6cm (Fig. 2A). Relatively high amounts of hard part remains

in the 50-55 cm layer can be attributed to the high proportion of macroids, making up more than 80% of total weight in this layer, whereas it never exceeds 40% in the remaining layers. Dating by amino-acid racemisation (AAR) of molluscan shells showed a generally linear relation between sediment depth and the age of dated shells. The deepest layer has been dated with 5071 years (IQR= 1889 years) before present. The mean age of the layer comprising the highest proportion of macroids is 3921 years (IQR: 2150 years) (Fig. 2B).
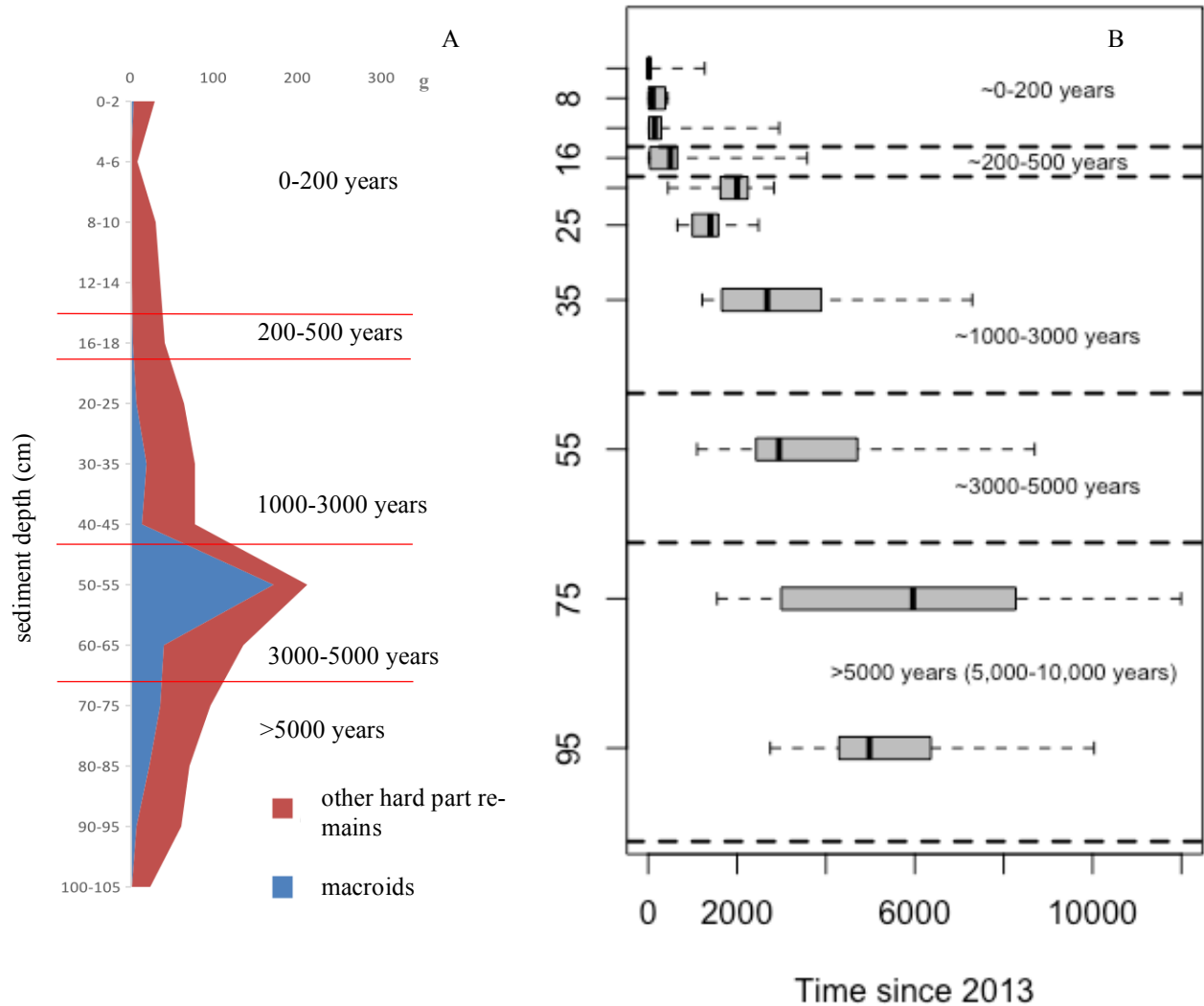
Figure 2: Total weight of hard part remains larger then 1mm (A). Age (time since 2013) of different sections was estimated by AAR-dating (B).

Abiotic parameters

Grainsize distribution along the core.

Relative clay content increases continuously from the lower parts, where it accounts for only about 6% towards the top, where it makes up more than 40% of sediment mass. Silt displays almost the same pattern, but contributes a high fraction to the sediment in the very lowest part of the core. It makes up nearly 70% before it strongly drops to a minimum of only 17% at a sediment depth of 70 cm. From that point upward it increases again and together with clay contributes 94% to sediment mass in the top layer. Fine and coarse sand decreases towards the top and has its maximum in the lower third of the core, where it accounts for up to 80% of sediment mass (Fig 3A). An age of ~112 years was estimated by radiometric dating of the sediment. This is roughly corresponding to a sedimentation rate of 1.2mm/year (Fig. 3B). At a depth of 105cm terrestrial sediment was reached.
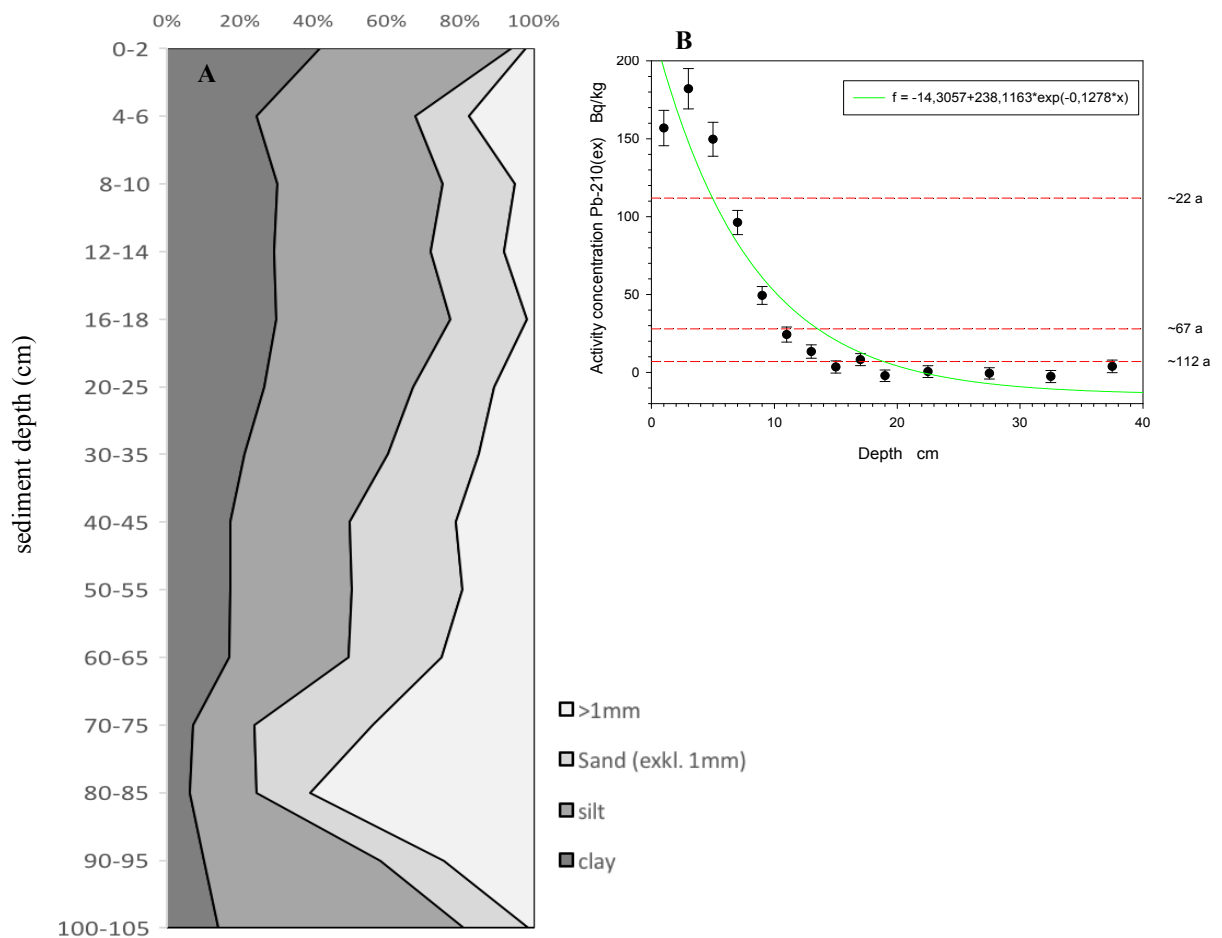
Figure 3: Sediment composition along a core taken at the same locality. Due to differences in core-length, the position of respective layers within the sediment core was adjusted to the shorter core by AAR-dating (A). Radiometric dating of the sediment (B).

Environmental pollutants

Heavy metals

Concentration of mercury at the lower part of the sediment core was low (0.02mg/kg), staying constant up to a sediment depth of 25 cm. From that point onward it increases nearly by two orders of magnitude reaching its maximum at layer 8-10cm (1.25 mg/kg). Towards the top concentration drops to 0.60 mg/kg. Lead displays a similar pattern with a concentration of 6.27 mg/kg at the bottom, peaking also at layer 8-10cm (23.85mg/kg) and a concentration of 21.31 mg/kg at the very top of the core. Distribution of Chromium, Copper, Nickel, Lithium, Zinc and Aluminium concentration values along the core are roughly opposite to the grain size distribution. Aforementioned heavy metals start at high concentrations at the bottom of the core (Cr: 40.82mg/kg, Cu: 16.29mg/kg, Ni: 33.57mg/kg, Li: 42.97, Zn: 43.0mg/kg, Al:12766mg/kg) and decrease rapidly toward a minimum concentration at layer 80-85cm (Cr: 17.49mg/kg, Cu: 4.11mg/kg, Ni: 14.91mg/kg, Li: 26.74, Zn: 20.60mg/kg, Al:7269mg/kg). Note that coarse sand <1mm makes up the highest proportion of sediment fractions in this part of the core. Iron displays the same pattern at the lower third with its minimum at 80-85cm depth (11572mg/kg) and highest values at the bottom of the core with a concentration of 19454 mg/kg. In contrast to that, the concentration of iron decreases from 70 cm upwards continuously towards the top. Arsenic peaks at a depth of 70-75 cm at a concentration of 19.67mg/kg and Cadmium reaches its maximum at layer 50-55cm with a concentration of 0.38 mg/kg. Phosphorous and Manganese decline from a high value toward the middle section of the core, where concentration drops to a minimum and increases from this point onward towards the top. Concentration of Phosphorus is 550.6 mg/kg at the bottom and has a second maximum with 307.5mg/kg in the 2-4cm layer. Minimum concentration of phosphorus in the midsection of the core is 2011.7mg/kg. Manganese has a concentration of 372.4 mg/kg at the bottom, 239.5 mg/kg in the middle of the core and 257.3mg/kg in the 2-4 cm layer.
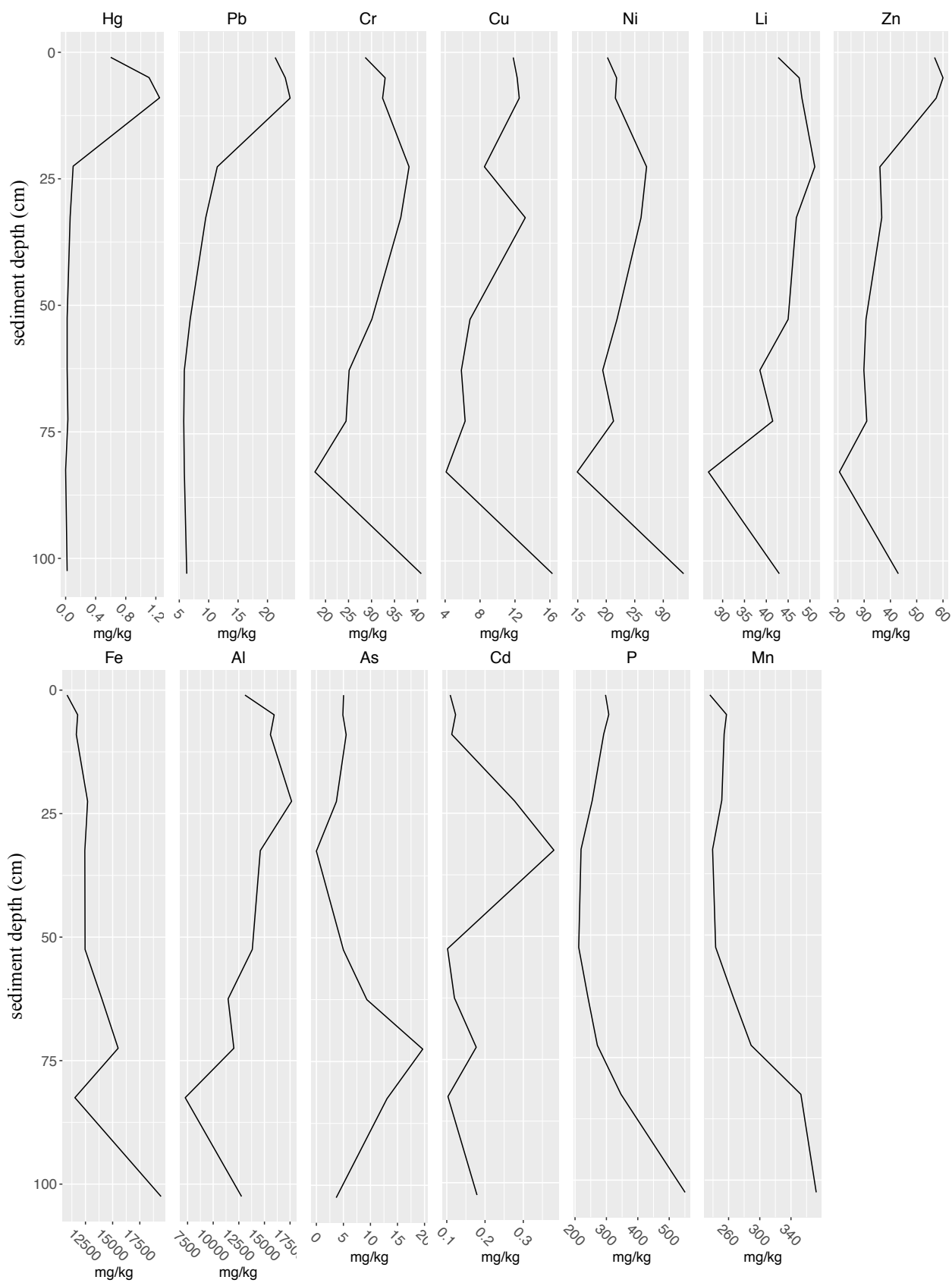
Figure 4: Heavy metal concentration along the core estimated from a separately taken sediment core.

Organic pollutants

Polycyclic aromatic hydrocarbons (PAH) and Polychlorinated biphenyl (PCB) have low concentrations in the sediment at the lower and middle part of the core. PAH, however, increases tremendously in the upper 30 cm of sediment. PCB reaches a concentration of 5.60ng/g and PAH up to 474.29 ng/g at layer 4-6cm. In deeper sediment layers, concentrations of PCB stay below 3 ng/g and PAH blow 15 ng/g.

Nutrients

Total Carbon (Ctot) and total organic carbon (TOC) increases towards the top. Ctot increases from 4.19% dw at the lowest layer to 6.04% dw at the top. Accumulation of TOC ranges from 0.99% dw at the bottom of the sediment core to 1.59 % dw. Total Nitrogen (Ntot) slightly decreases from the bottom to the midsection from 0.09 % dw to 0.08% dw and accumulates comparably stronger at the upper third to 0.13 % dw.
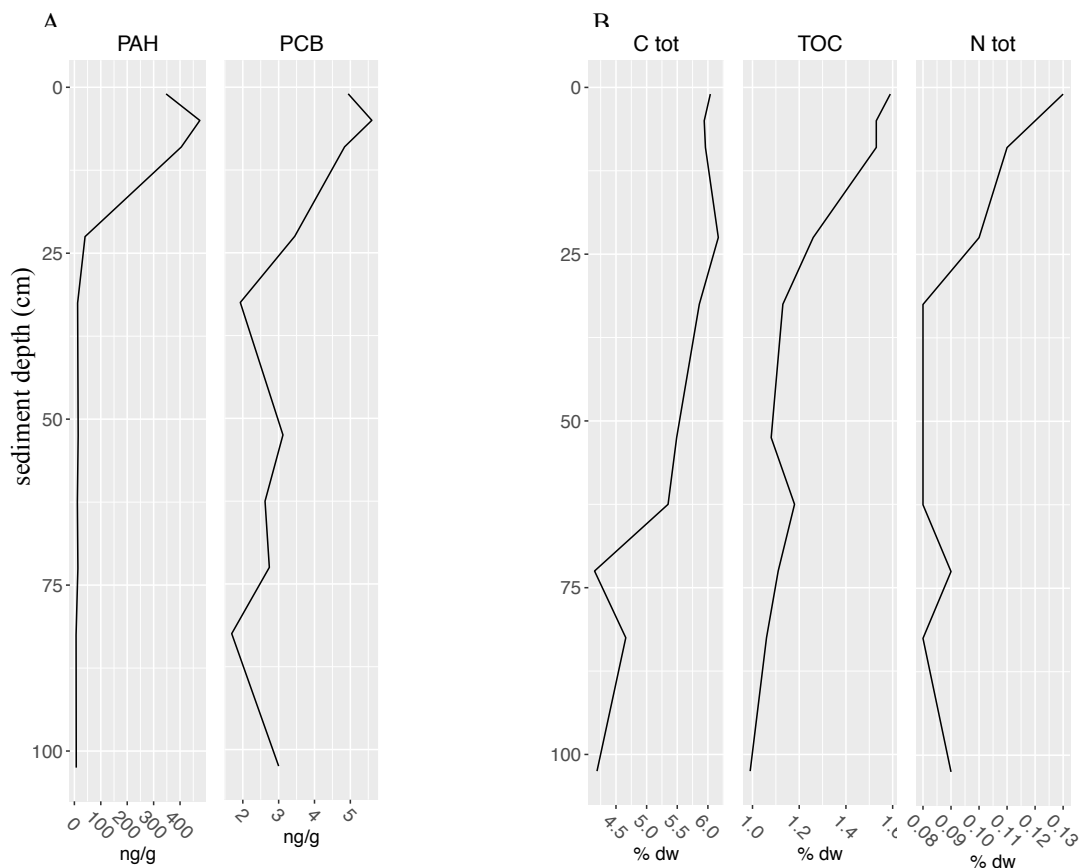
Figure 5: (A) Environmental organic pollutants along the core. (B) Nutrient concentration along the core. Concentration values are estimated from a separately taken core.

Taxonomic distribution and shifts along the core of major taxonomic groups

Cluster analysis (UPGMA) of all surveyed taxonomical groups revealed two significant clusters at a dissimilarity of 0.26 (PERMANOVA: R^2=0.74, F=9.41, p<0.001, 9999 permutations) separating the core into a lower (50-95cm depth) and upper section (0-45 cm depth). The layer 2-4cm and the very lowest layer 100-105cm are outliers (Fig. 6A). At a lower dissimilarity of 0.17 both clusters are divided into two further groups. The resulting clusters reach from 8 cm to 18 cm, from 20 cm to 45 cm, from 50 cm to 65 cm and from 70 cm to 95 cm sediment depth. Two layers at the top (0-2cm, 4-6cm) and the layer at the very bottom of the core (100-105cm) are outliers (Fig. 6A).

Ordination of taxonomic composition based on Bray-Curtis dissimilarity reveals a rather gradual shift in composition along the core, placing respective sections of the core along the first nMDS axis (Fig.6B).
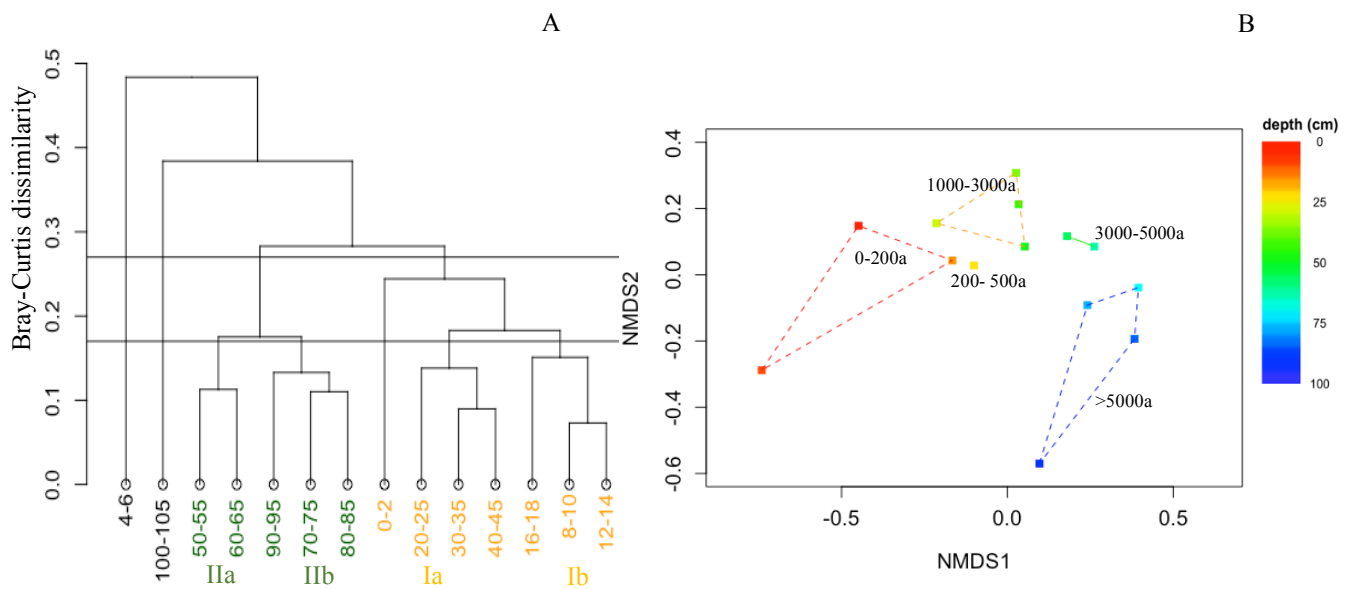
Figure 6: (A) Cluster analysis (UPGMA) of square root transformed total weight of taxonomic groups along the core, showing two significant clusters at Bray-Curtis dissimilarity of 0.26 and two outliers (layer: 4-6; 100-105) separating the core into a lower (cluster II) and an upper section (cluster I; PERMANOVA: R^2: 0.74, F:9.41, p<0.001, 9999 permutations). At 0.17 Bray-Curtis dissimilarity the core splits in 4 clusters (PERMANOVA: R^2:0.91, F:11.28, p<0.001, 9999 permutations) with three outliers (0-2,4-6,100-105cm depth). (B) nMDS based on square-root transformed weight of taxa based on Bray Curtis dissimilarity. Points display individual layers along the core. Colour gradient respective to sediment depth. Grouping of layers according to age-groups.

In terms of total weight Corallinaceae (95.36g) make up the largest fraction of hard part remains, followed by bivalves (52.09g), bryozoans (41.99) and gastropods (31.07g) (Fig. 7A). To a large extent the upper cluster resembles this pattern. This section is also dominated by Corallinaceae (78.35g). However, bivalves (23.73g) are replaced by bryozoans (30.81g) as the second most abundant taxon (Fig. 7B). The second cluster, comprising layers at the lower part of the core, was dominated by bivalves (26.62g) and gastropods (18.64g). Hard part remains of crustaceans (14.55g) were also found more frequently (Fig. 7C).
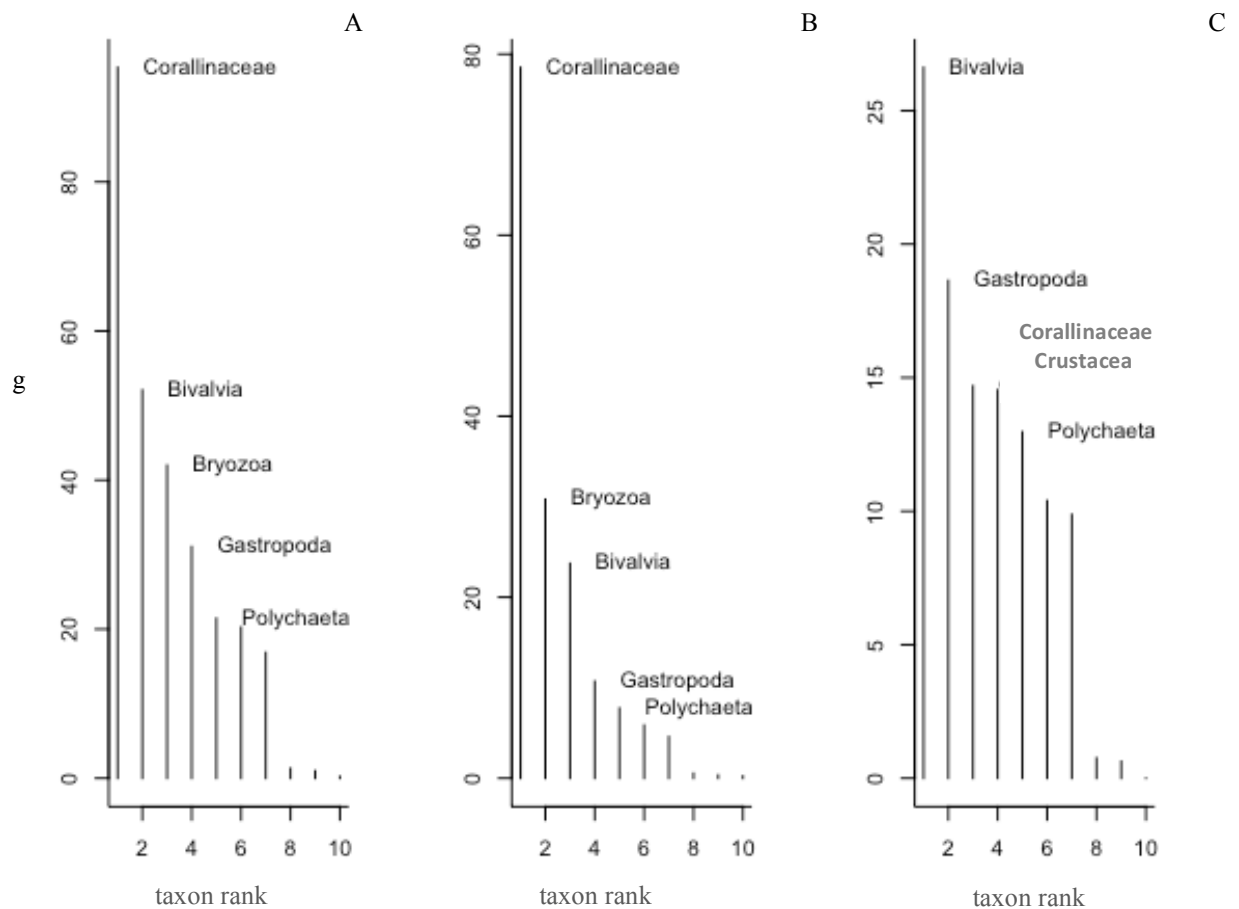
Figure 7: Rank abundance distribution of all taxonomic groups of the whole core (A), and distribution within cluster I (B) and cluster II (C) (see Figure 6 A).

A significant relation of the taxa Brachiopoda (iv= 0.85, p<0.01), Corallinaceae (iv=0.74, p<0.01) and Bryozoa (iv=0.63, p<0.05) to the upper cluster was found by Dufrene-Legendre Indicator Species Analysis. Scaphopoda (iv= 0.69, p<0.05), Echinoidea (iv= 0.65, p<0.01), Polychaeta (iv= 0.64, p<0.01), Polyplacophora (iv 0.63, p<0.01) and Gastropoda (iv= 0.61, p<0.01) could be assigned as indicators for the lower cluster. With increasing depth, the amount of

terrestrial organic material, mainly consisting of woody and reed like plant remains increase. (Tab. 2, Figure 8).

Table 2: Dufrene-Legendre Indicator Species Analysis according to cluster analysis (see Figure 6A).

	CLUSTER	INDICATOR VALUE	PROBABILITY
BRACHIOPODA	I	0.85	0.002
CORALLINACEAE	I	0.74	0.001
BRYOZOA	I	0.63	0.018
CRUSTACEA	II	0.70	0.008
SCAPHOPODA	II	0.69	0.012
ECHINOIDEA	II	0.64	0.003
POLYCHAETA	II	0.64	0.005
POLYPLACOPHORA	II	0.62	0.004
GASTROPODA	II	0.61	0.002
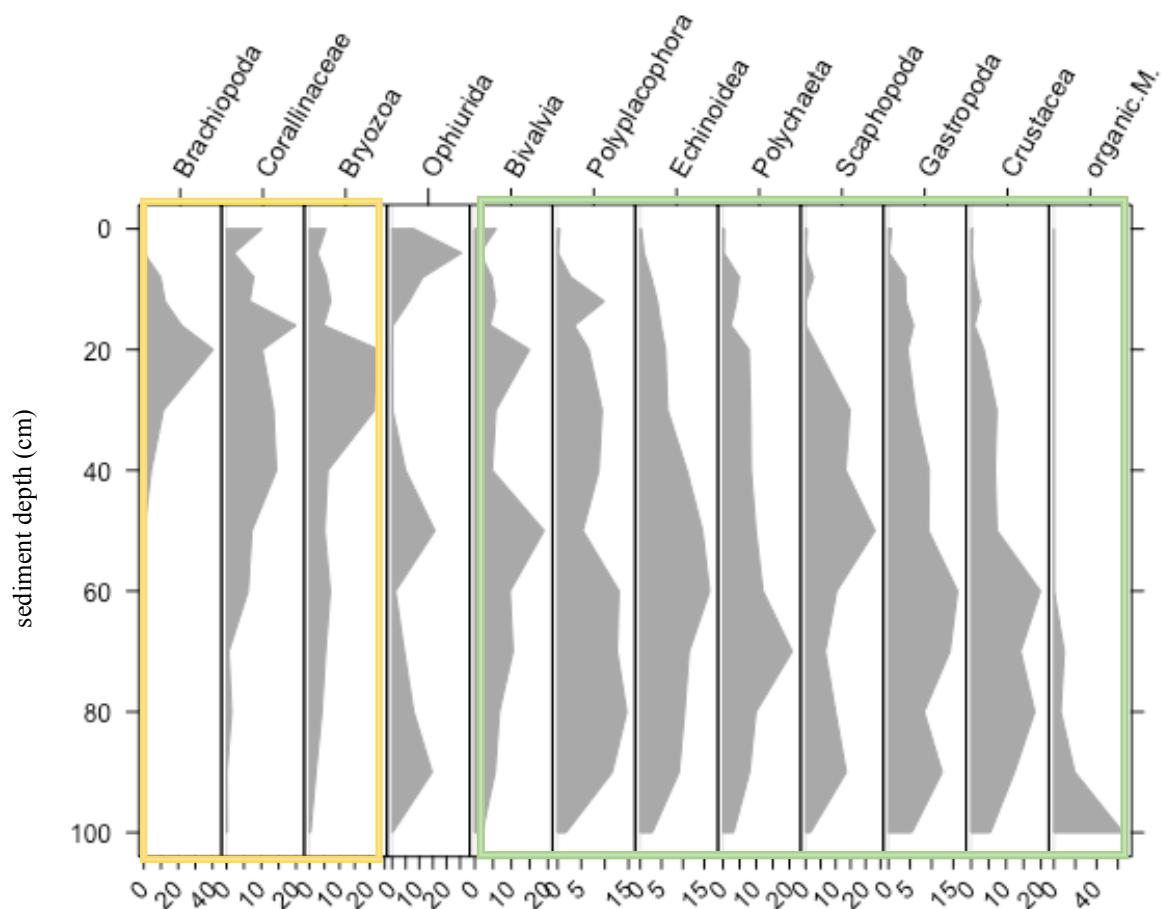
Figure 8: Relative abundances of taxa along the core. Species on the left are more prone to be found in the upper part of the core whereas taxa to the right at the bottom. Note that abundances are relative values based on the total abundance of each taxon in the core. Hard part remains served as proxy for abundance.

Impact of pollutants on taxonomic changes

Position of respective layer within the ordination plot (Fig. 6B) can be explained to a certain degree with the concentration of heavy metals and organic pollutants. Site scores (nMDS scores of respective layers) and concentration of Hg (R^2=0.64, p<0.05), Pb (R^2=0.82, p<0.01), Zn (R^2=0.78, p<0.01), Mn (R^2=0.79, p<0.05), Fe (R^2=0.69, p<0.05) and P (R^2=0.74, p<0.05) displayed a significant association (Tab. 3). Furthermore, association of organic environmental pollutants (PAH: R^2=0.80, p<0.01; PCB: R^2=0.74, p<0.01) and shifts in taxonomic composition could be shown (Tab 4). Composition was also influenced by nutrient content (C-tot: R^2=0.89; p<0.01, TOC: R^2=0.80, p<0.01; N.tot: R^2=0.74, p<0.05) (Tab. 5). Another important factor appears to be grain size of sediment as the content of clay also influences composition in the respective layers (R^2=0.59, p<0.05) (Tab. 6).

Table 3: Regression analysis of heavy metal concentration and compositional changes along the first and second nMDS axis (see Figure 6A).

	NMDS1	NMDS2	R^2	P	
Hg	-1.00	0.00	0.64	0.039	*
Cr	-0.91	-0.42	0.11	0.656	
Cu	-0.74	-0.67	0.41	0.166	
Ni	0.07	-1.00	0.11	0.663	
Pb	-0.97	0.25	0.82	0.003	**
As	0.91	-0.42	0.27	0.319	
Cd	0.26	0.97	0.11	0.667	
Li	-0.76	0.65	0.26	0.333	
Zn	-0.99	-0.12	0.78	0.003	**
Mn	0.40	-0.91	0.79	0.016	*
P	0.06	-1.00	0.74	0.019	*
Fe	0.48	-0.88	0.69	0.042	*
Al	-0.77	0.64	0.35	0.228	

Table 4: Regression analysis of organic environmental pollutants concentration and compositional changes along the first and second nMDS axis (see Figure 6A).

	NMDS1	NMDS2	R^2	P	
PAH	-0.99	0.02	0.80	0.006	**
PCB	-0.99	0.01	0.74	0.010	**

Table 5: Regression analysis of organic nutrient concentration and compositional changes along the first and second nMDS axis. (see Figure 6A).

	NMDS1	NMDS2	R^2	P	
CTOT	-0.60	0.80	0.89	0.001	***
TOC	-0.90	0.44	0.80	0.004	**
NTOT	-0.99	0.12	0.74	0.014	*

Table 6: Regression analysis of grains size distribution and compositional changes along the first and second nMDS axis. (see Figure 6A).

	NMDS1	NMDS2	R^2	P	
CLAY	-0.81	0.59	0.72	0.014	*
SILT	-0.60	-0.80	0.30	0.288	
SAND	0.83	0.56	0.46	0.121	
>1 mm	1.00	0.01	0.19	0.466	

Bryozoa

Taxonomic distribution and shifts along the core of Bryozoan species (count data)

Bryozoan species found belonged exclusively to the two orders Cheilostomatida and Cyclosto-matida. Within these two orders 79 species belonging to 37 families were found.
Individual based rarefaction-curve of the total assemblage shows a steep increase for the first thousand individuals, displaying no saturation (Fig. 9A). Species accumulation curve along the core displays a similar pattern, not reaching asymptotic behaviour (Fig. 9B).
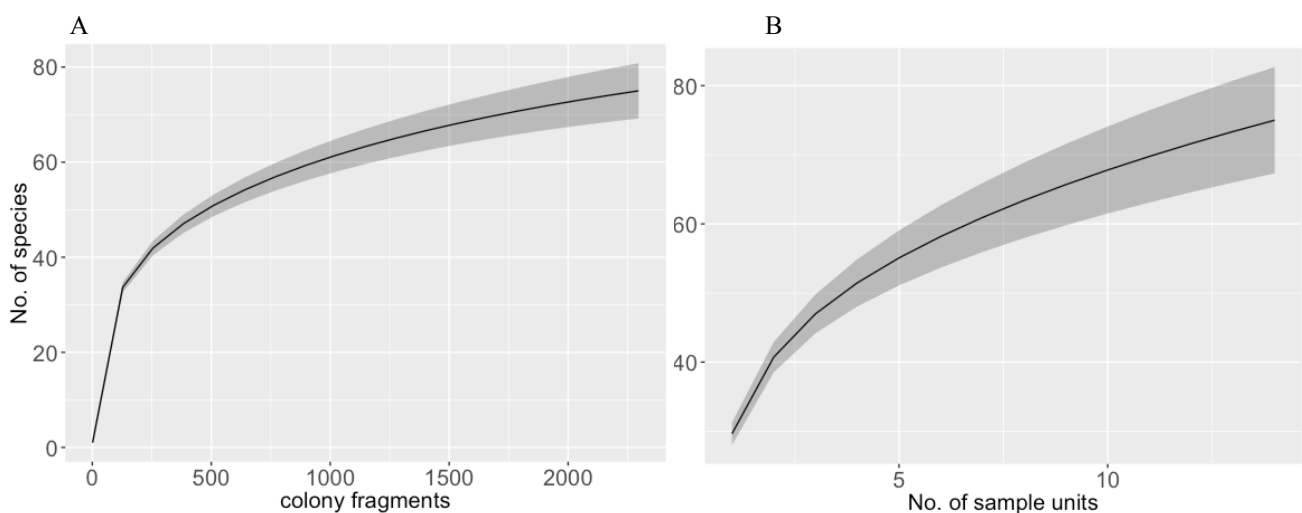
Figure 9: Individual based rarefaction curve (A) and sample based species accumulation curve (B) of bryozoan species with 95% confidence interval.

UPGMA cluster analysis on bryozoan data separates the samples along the core into two distinctive clusters at a Bray-Curtis dissimilarity of 0.5 (PERMANOVA: R^2=0.56, F=4.19, p<0.001, 9999 permutations). The upper cluster comprises layers from 0 cm to 45 cm sediment depth and layer 60-65cm. The lower cluster consists of the layers 50-55cm and the layer between a depth of 70-95 cm (Fig. 10A). Ordination indicates also higher dissimilarities between different agegroups (Fig. 10B).

A   B
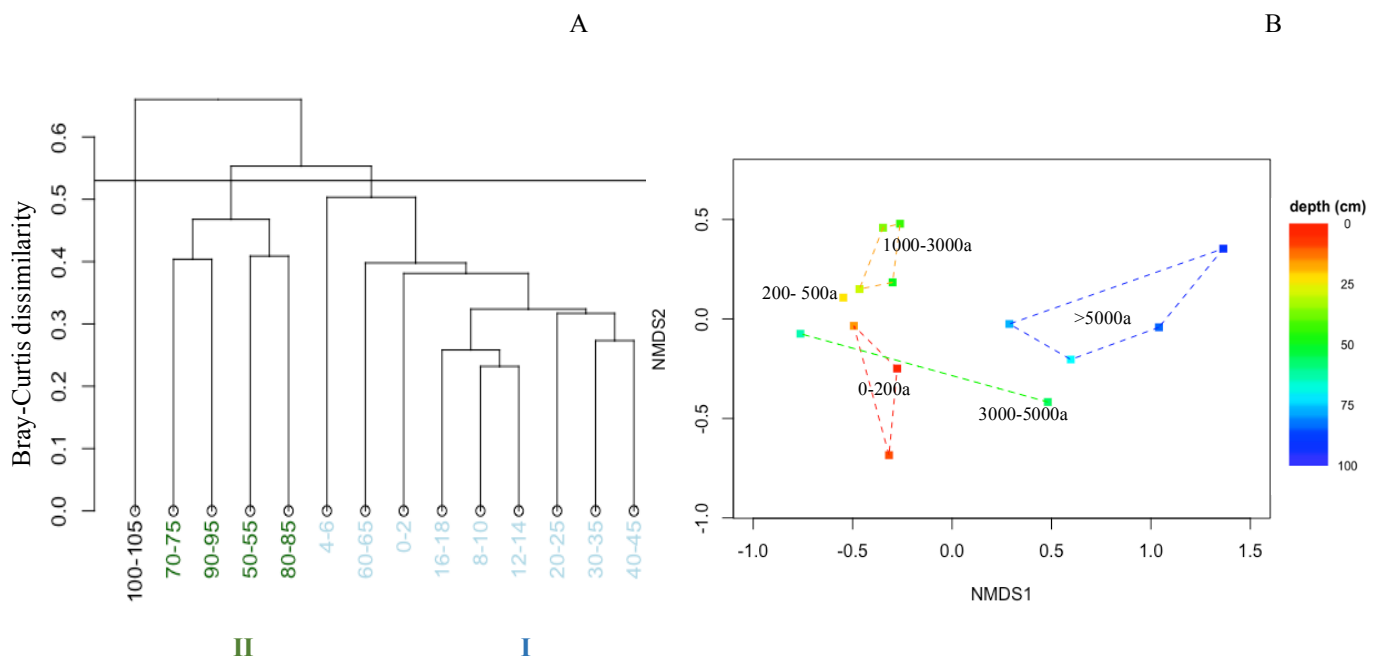
Figure 10: (A) Cluster analysis (UPGMA) of square root transformed abundance of bryozoan species along the core showing two significant clusters at Bray-Curtis dissimilarity of 0.5 and one outlier (100-105) separating the core in two a lower section (II) and an upper section (I) (PERMANOVA: R^2: 0.56, F:4.18, p<0.001, 9999 permutations) (B) nMDS based on square-root transformed abundance based on Bray Curtis dissimilarity. Points display individual layers along the core. Colour gradient respective to sediment depth. Grouping of layers according to age-groups.

Rank abundance distribution of bryozoan species and distribution of different growth-types (count data)

Cellaria salicornioides (872 fragments) was the most abundant species in terms of total number of colony fragments found, followed by *Adeonella pallasii (566), Cellaria fistulosa (404), Smittina cervicornis (352) and Schizotheca serratimargo (348).* The membraniporiform growth form makes up the highest proportion of bryozoa growth forms (27.94 %). Celleporiform Bry-

ozoa (7.65%) together with membraniporiforms can be ascribed to encrusting bryozoans. Together they account for 35.59 % of bryozoan hard part remains. Erect species make up the remaining 64.41 %, and consist of cellariform (24.49%), adeoniform (18.12%), vinculariform (12.72%), eschariform (5.64%) and reteporiform (3.41%) species (Fig. 11A).

Rank abundance distribution reveals also a steep slope and is dominated by *Cellaria salicornioides* (871). *Adeonella pallasii (565)* is the second most abundant species, followed by C*ellaria fistulosa (*404), *Smittina cervicornis (352)* and *Schizotheca serratimargo* (348).

Cluster I is strongly dominated by erect species (67.25 %). Cellariform Bryozoa are the most abundant growth-type (27.43 %), followed by adeoniform (19.27%), vinculariform (13.31%), eschariform (4.46%) and reteporiform (2.79%) species. Encrusting species account for only 32.75% and are composed of membraniporiform (25.07%) and celleporiform (7.68%) species (Fig 11B). The slope of the rank abundance curve of cluster II is flatter and dominated by the membraniporiform species *Copidozoum tenuirostre* (160). The difference to the subsequent most abundant species *Smittina cervicornis* (120), *Pentapora fascialis* (112*), Cellaria salicornioides (*92) and *Reteporella grimaldii* (80) is not as pronounced as in the upper cluster.

Species composition shifts towards higher proportion of membraniporiform (46.23%) bryozoans, which together with celleporiform species (7.23%) contribute more than half the number of found species. This results in a higher dominance of encrusting species in this cluster (53.46%). Hence cellariiform (7.86%), adeoniform (13.21%), vinculariform (9.43%), eschariform (8.81%) and reteporiform (7.23%) bryozoans together make up only 46.54% (Fig. 11C).
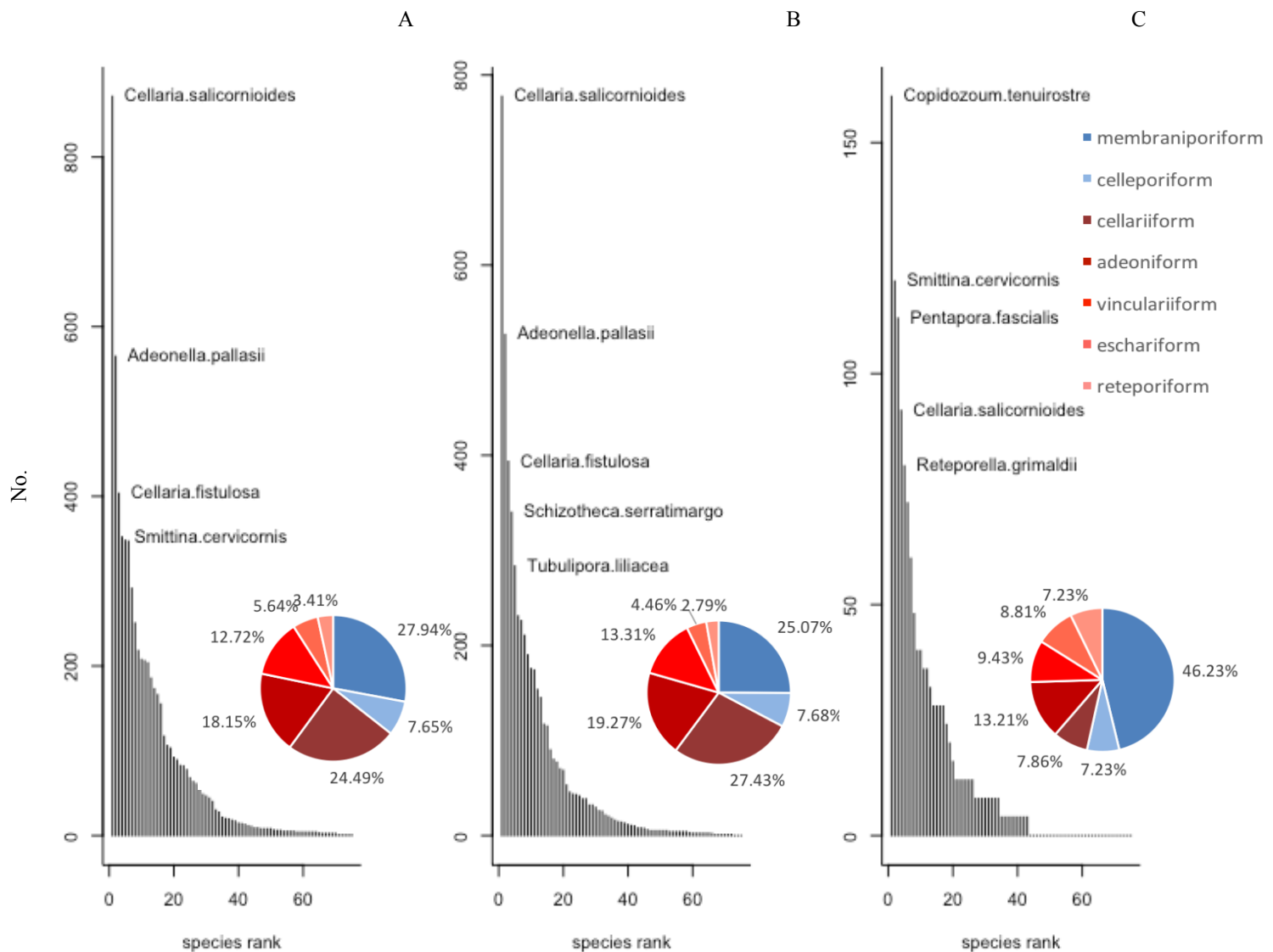
Figure 11: Rank abundance distribution of bryozoan species and relative abundance of different growth forms of the whole core (A), and distribution within cluster I (B) and cluster II (C) (see Figure 10). Erect growth forms are coded in red. Incrusting growth forms in blue.

Dufrene-Legendre Indicator Species Analysis revealed 10 bryozoan species to be significant related to the upper cluster (*Exidmonea coerulea*: iv=1, $p<0.001$; *Schizotheca serratimargo*: iv=0.95, $p<0.01$; *Tubulipora liliacea*: iv=0.94, $p<0.01$; *Adeonella pallasii*: iv=0.84, $p<0.01$; *Cellaria fistulosa*: iv=0.81, $p<0.01$; *Cellaria salicornioides*: iv=0.78; $p<0.01$; *Annectocyma major*: iv=0.75, $p<0.01$, *Schizomavella cornuta*: iv=o.71, $p<0.5$; *Myriapora truncata*: iv=0.70, $p<0.05$; *Phoceana tubulifera*: iv= 0.70, $p<0.01$). Only two species could be assigned to the lower cluster (*Copidozoum tenuirostre*: iv= 0.86, $p<0.01$; *Microporella ciliata*: iv=0.72, $p<0.05$) (Tab. 7).

Table 7: Dufrene-Legendre Indicator Species Analysis according to cluster analysis (see Figure 10).

SPECIES	CLUSTER	INDICATOR VALUE	PROBABILITY
EXIDMONEA COERULEA	I	0.99	0.001
SCHIZOTHECA SERRATIMARGO	I	0.95	0.002
TUBULIPORA LILIACEA	I	0.94	0.002
ADEONELLA PALLASII	I	0.84	0.003
CELLARIA FISTULOSA	I	0.81	0.005
CELLARIA SALICORNIOIDES	I	0.77	0.005
ANNECTOCYMA MAJOR	I	0.75	0.001
SCHIZOMAVELLA CORNUTA	I	0.70	0.023
MYRIAPORA TRUNCATA	I	0.70	0.034
PHOCEANA TUBULIFERA	I	0.70	0.005
COPIDOZOUM TENUIROSTRE	II	0.86	0.007
MICROPORELLA CILIATA	II	0.72	0.015

Bryozoan species richness and diversity (count data)

Species richness is generally higher at the upper part of the core. Layer 50-55cm, where a high proportion of macroids was found, is the major exception and has the highest species richness (Fig. 12A). None of the layers reached asymptote for interpolated values(Fig. 12A).

At the very bottom of the core the Shannon-Wiener index is relatively low and increases during the first phase of the Holocene transgression to a maximum (mean 24.00 ± 1.55 SE) at a sediment depth of 40-45 cm. From this point onward diversity declines steadily, reaching a minimum at a depth of 4-6 cm. The uppermost 4 cm show a slight recovery towards the top of the core (15.12±1.43SE).
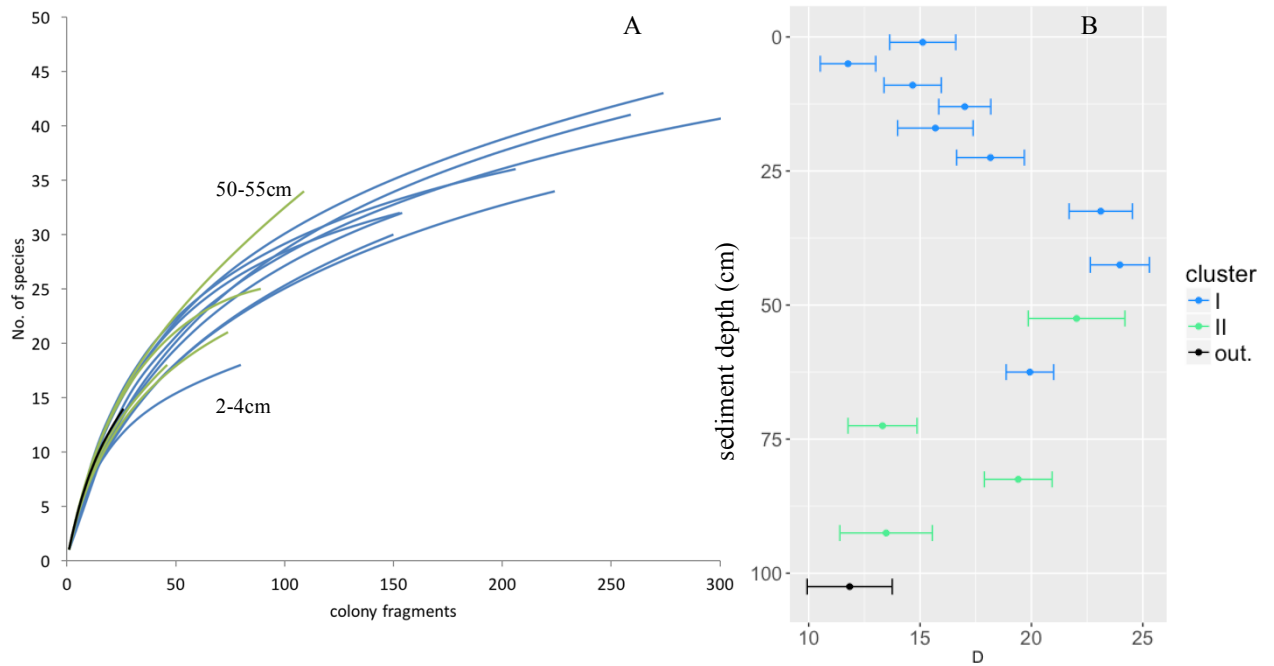
Figure 12: (A) Individual based rarefaction curve of bryozoan species in layers. Colony fragments served as proxy to estimated number of individuals. (B) Shannon Wiener diversity of bryozoan species along the core. Colour-coding according to cluster analysis (see Figure 10).

Impact of pollutants on compositional changes

Differences in species composition between layers can be described along a gradient of nutrients and grain size distribution. Location of individual layers in the NMDS plot corresponds to concentrations of Phosphorous (R^2=0.83, p<0.01) Iron (R^2=069, p<0.05) and Manganese (R^2=0.61, p<0.05) in the sediment (Tab. 8). No relation between compositional changes and concentration of organic pollutants was found. Total carbon accumulation shows a strong relation to arrangement of respective layers at Bray-Curtis based ordination (R^2=0.87, p>0.001) (Tab.10). Grain size is related to species composition because the content of sand correlates with distribution of layers in the ordination plot (R^2=0.68, p<0.05) (Tab. 11).

Table 8: Regression analysis of heavy metal concentration and changes of bryozoan species composition along the first and second nMDS axis.

	NMDS1	NMDS2	R^2	P	
Hg	-0.63	-0.78	0.46	0.096	.
Cr	-0.83	-0.55	0.16	0.548	
Cu	-0.98	-0.22	0.46	0.123	
Ni	-0.86	0.51	0.16	0.523	
Pb	-0.52	-0.85	0.56	0.054	.

27

As	0.26	0.96	0.41	0.131	
Cd	0.33	-0.94	0.06	0.809	
Li	-0.10	-1.00	0.15	0.548	
Zn	-0.80	-0.60	0.51	0.089	.
Mn	-0.53	0.85	0.61	0.046	*
P	-0.81	0.59	0.83	0.002	**
Fe	-0.31	0.95	0.69	0.025	*
Al	-0.13	-0.99	0.26	0.339	

Table 9: Regression analysis of organic environmental pollutants concentration and changes of bryozoan species composition along first and second nMDS axis.

	NMDS1	NMDS2	R^2	P	
PAH	-0.65	-0.76	0.49	0.086	.
PCB	-0.70	-0.71	0.35	0.217	

Table 10: Regression analysis of organic nutrient concentration and changes of bryozoan species composition along the first and second nMDS axis.

	NMDS1	NMDS2	R^2	P	
C.TOT	0.11	-0.99	0.87	0.001	***
TOC	-0.39	-0.92	0.46	0.130	
N.TOT	-0.76	-0.65	0.41	0.159	

Table 11: Regression analysis of grains size distribution and changes of bryozoan species composition along the first and second nMDS axis.

	NMDS1	NMDS2	R^2	P	
CLAY	-0.20	-0.98	0.64	0.028	*
SILT	-0.98	-0.17	0.36	0.216	
SAND	0.87	0.49	0.68	0.019	*
>1 mm	0.66	0.76	0.17	0.537	

No significant correlation between rarefied species richness and environmental pollutants could be found. Neither impact of nutrient concentration and sediment composition on diversity was detected (Tab. 12A).

Environmental parameters and the Shannon-Wiener diversity index, however, showed significant correlations. The heavy metals mercury (t_8=-3.11, $p<0.05$), lead (t_8=-2.86, $p<0.05$) and zinc (t_8=-2.75, $p<0.05$) are negatively correlated with diversity (Tab. 12B). The same holds true for the organic pollutants PAH (t_8=-3.29, $p<0.05$), PCB (t_8=-3.00, $p<0.05$) (Tab. 13B) and the

concentration of nutrients (N.tot: $t_8=-3.39$, $p<0.01$; TOC: $t_8=3.31$, $p<0.05$) (Tab. 14B). No correlation of diversity with grain size was found.

Table 12: Correlation (Pearson's r) of heavy metal concentration to rarefied species richness **(A)** and Shannon-Wiener diversity **(B)** in sediment layers.

A	T	DF	P		B	T	DF	P	
Hg	-1.064	8	0.319		Hg	-3.114	8	0.014	*
Cr	0.313	8	0.762		Cr	0.012	8	0.991	
Cu	-0.302	8	0.77		Cu	-0.695	8	0.507	
Ni	0.178	8	0.863		Ni	0.395	8	0.703	
Pb	-0.821	8	0.436		Pb	-2.861	8	0.021	*
As	-1.07	8	0.316		As	-0.591	8	0.571	
Cd	0.437	8	0.673		Cd	0.693	8	0.508	
Li	0.578	8	0.579		Li	-0.76	8	0.469	
Zn	-0.784	8	0.456		Zn	-2.75	8	0.025	*
Mn	-1.473	8	0.179		Mn	0.566	8	0.587	
P	-1.569	8	0.155		P	-0.16	8	0.877	
Fe	-0.341	8	0.742		Fe	0.409	8	0.693	
Al	0.315	8	0.761		Al	-0.89	8	0.399	

Table 13: Correlation (Pearson's r) of organic environmental pollutants concentration to rarefied species richness **(A)** and Shannon-Wiener diversity **(B)** in sediment layers.

A	T	DF	P		B	T	DF	P	
PAH	-1.128	8	0.292		PAH	-3.295	8	0.011	*
PCB	-0.825	8	0.433		PCB	-3.000	8	0.017	*

Table 14: Correlation (Pearson's r) of nutrient concentration to rarefied species richness **(A)** to Shannon-Wiener diversity **(B)** in sediment layers.

A	T	DF	P		B	T	DF	P	
C.TOT	0.741	8	0.480		C.tot	-0.601	8	0.564	
TOC	-0.709	8	0.498		TOC	-3.309	8	0.011	*
N.TOT	-1.232	8	0.253		N.tot	-3.391	8	0.009	**

.

Table 15: Correlation (Pearson's r) of grain size distribution to rarefied species richness **(A)** and to Shannon-Wiener diversity **(B)** in sediment layers.

A	T	DF	P	B	T	DF	P
CLAY	0.649	12	0.529	**CLAY**	-1.753	12	0.105
SILT	-0.070	12	0.945	**SILT**	-0.759	12	0.463
SAND	1.633	12	0.129	**SAND**	1.613	12	0.133
>1 mm	-1.008	12	0.333	**>1 mm**	0.896	12	0.388

Influence of bryozoan growth-forms on data analysis

Comparison of average fragment weight revealed a significant difference between growth-types (χ^2=20.44, df=5, p<0.01; Kruskal-Wallis H-test) (Fig. 13A). Celleporiforms were found to have the highest average fragment weight, displaying also the highest variance (11.13mg± 9.31SD). Breakage of adeoniform species results in the second heaviest category of fragments (7.64mg±4.43SD), followed by vinculariform (4.89mg±6.20SD) and reteporiform (4.19mg±2.95SD) growth-forms.

Membraniporiform (2.67mg±2.70SD) and cellariiform species (1.81mg±1.48SD) represent the lightweights of Bryozoan growth-forms in terms of fragmented hard part remains.

No significant difference exists between the mean weight of erect and incrusting species (W=378, p=0.28; Mann-Whitney U-test) (Fig. 13B).
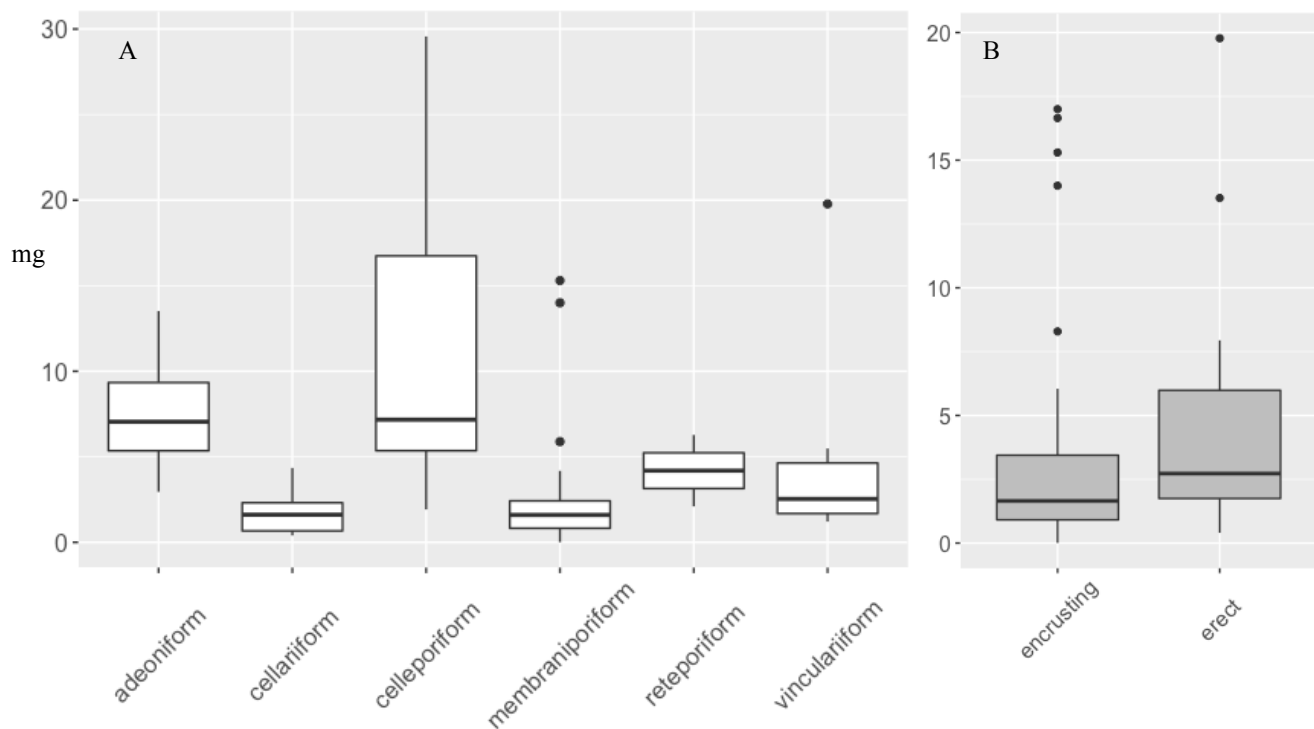
Figure 13: (A) Average fragment weight of different growth types (Kruskal-Wallis: $\chi^2 = 20.443$, df = 5, p<0.01). (B) Average fragment weight of erect and encrusting Bryozoan specimens. (Wilcoxon rank sum test: W = 378, p = 0.2794)

Taxonomic distribution and shifts along the core of Bryozoan species (weight)

Cluster analysis (UPGMA) of square-root transformed total weight of bryozoan species separates the core also in two cluster clusters at a Bray-Curtis dissimilarity of 0.5 (PERMANOVA: R^2=0.40, F=3.65, p<0.001, 9999 permutations) (Fig. 14A). Clustering total weight resembles roughly the previous analysis of counted fragments part remains, with the exception, that layer 80-85 cm is located in the upper cluster. Separation into an upper and a lower part of the core is therefore not as distinctive. The upper age-groups are more densely clumped, whereas layers older then 5000 are grouped more loosely (Fig. 14B).
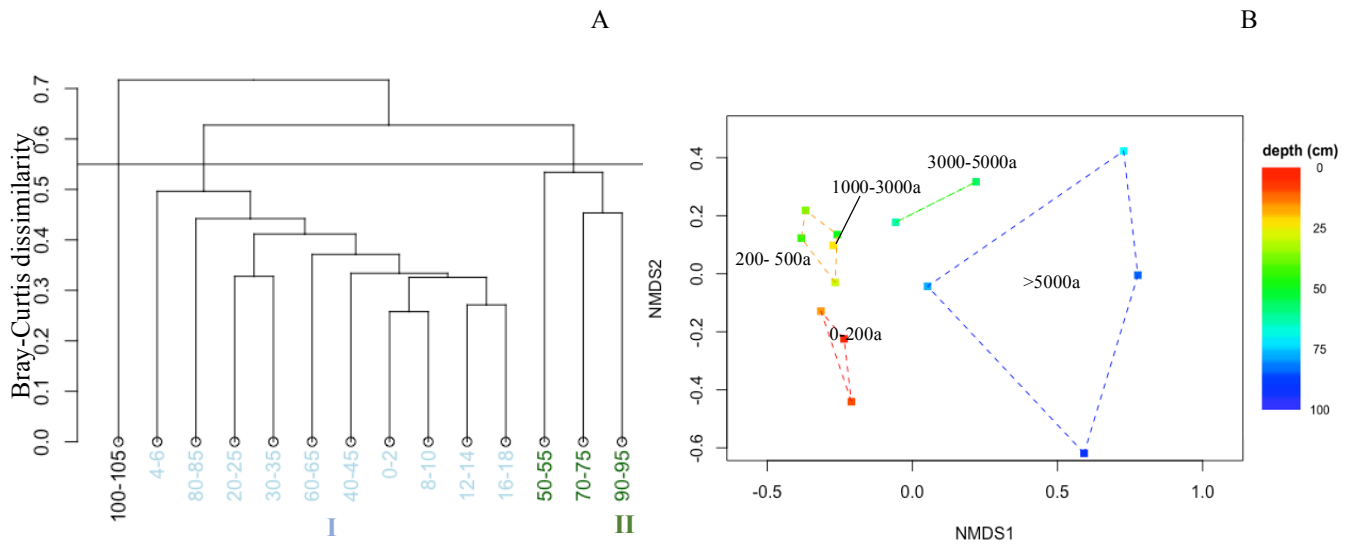
Figure 14: (A) Cluster analysis (UPGMA)of square root transformed weight of bryozoan species along the core showing two clusters at Bray-Curtis dissimilarity of 0.55 and one outlier (100-105cm) (PERMANOVA: R^2: 0.40, F:3.65, p<0.001, 9999 permutations). (B) nMDS based of square-root transformed weight data based on Bray Curtis dissimilarity. Points are layers along the core. Colour gradient respective to sediment depth. Grouping of layers according to age-groups.

Rank abundance distribution of Bryozoan species and distribution of different growth-types (weight)

Rank abundance curve of total weight is not as steep as that of count data. *Myriapora truncata* was the most dominant species in terms of total weight (18.64g), closely followed by *Schizotheka serratimargo* (17.51g). Another abundant species were *Schizotheca serratimargo* (17.51g), *Dentiporella sardonica* (15.65g), *Pentapora fascialis* (14.63g) and *Adeonella pallasii* (12.00g) (Fig. 15A).

Erect species strongly dominated the samples, making up 71.58% of bryozoans found. In contrast to the distribution of growth-forms according to count data, cellariiform species (7.03%) are replaced by adeoniform species (30.76%) as the most dominate form. Vinculariform (20.18%) and eschariform (11.52%) also surpass cellariiform species. Only the reteporiform growth-type (2.09%) was less frequent than the previously dominant growth from.

The remaining 28.42% of incrusting species is split up into 8.42% of membraniporiforms and 20% celleporiforms. Membraniporiform species, in terms of number the dominant group within the encrusting species is now replaced by celleporiforms.

The upper cluster displays again a roughly similar pattern as the whole core, dominated by *Myriapora truncata* (18.59g), *Schizotheca serratimargo* (17.50g), *Dentiporella sardonica* (15.39g), *Adeonella pallasii* (11.62g) and *Pentapora fascialis* (10.30g) (Fig 15B).

Erect species again make up more than two thirds of the species found (71.25%). Adeoniform (31.61%) and vinculariform species (21.73%) are even more abundant in this part of the core. Within the group of encrusting species (28.75%) the picture changes scarcely compared to the whole core (membraniporiform 8.31%, membraniporiform 20.14%).

The lower cluster is strongly dominated by the species *Pentapora fascialis (4.29g),* followed at some distance by *Smittina cervicornis* (2.09g), *Turbicellepora camera* (0.94g), *Rhynchozoon neapolitanum* (0.63g) and *Reteporella grimaldii* (0.51g). Percentage of encrusting species is even smaller in this cluster accounting for 26.05% of found species. Relative abundance of membraniporiform species stays roughly the same compared to the other parts of the core (8.75%), whereas celleporiform species decrease slightly (17.30%).

The picture within the group of erect species (73.95%), however, changes profoundly. Cellariforms make up only 1.96%. Adeonifom (22.40%) and vinculariform species (5.45%) decrease in their relative abundance. Species with eschariform growth become dominant in this cluster (38.81%). Reteporiform bryozoa make up 5.32% of bryozoan hard part remains.

Dufrene-Legendre Indicator Species Analysis revealed 9 bryozoan species to be significant in relation to the upper cluster (*Schizotheca serratimargo*: iv=0.99, p<0.01; *Myriapora truncata*: iv=0.99, p<0.01; *Exidmonea coerulea*: iv=0.90, p<0.01; *Adeonella pallasii*: iv=0.88, p<0.01; *Cellaria salicornioides*: iv=0.87, p<0.01; Cellaria fistulosa: iv=0.86; p<0.01; *Tubulipora cf. liliacea*: iv=0.83, p<0.01, *Annectocyma cf. major*: iv=o.78, p<0.01; *Phoceana tubulifera:* iv=0.73, p<0.05). No species was found to be significantly related to the lower cluster.
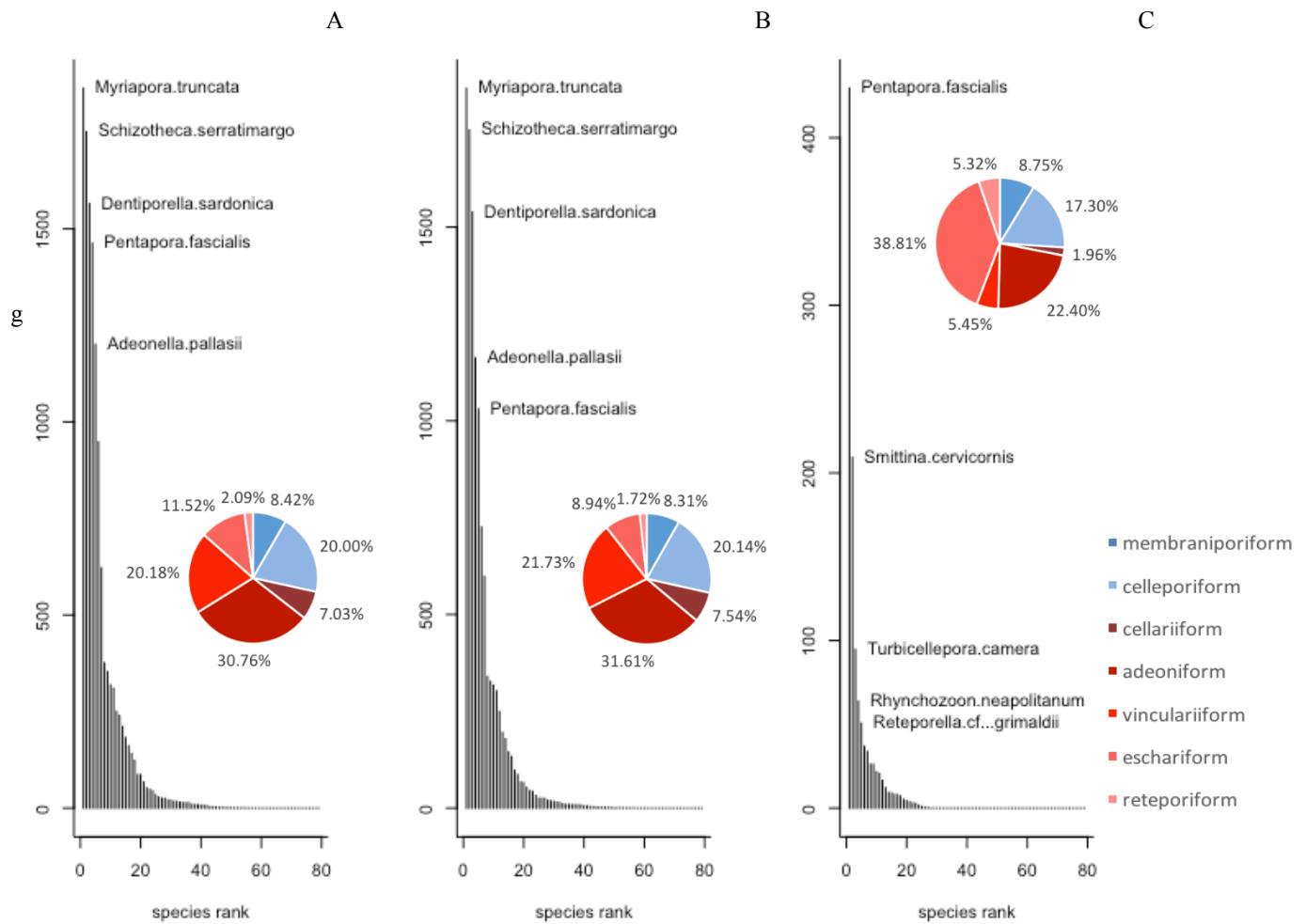
Figure 15: Rank abundance distribution of bryozoan species and relative abundance of different growth forms of the whole core (A) and distribution within cluster I (B) and cluster II (C) (see Figure 14). Erect growth-forms are coded in red, encrusting growth-forms in blue. Abundances are from weight data.

Table 16: Dufrene-Legendre Indicator Species Analysis according to cluster analysis (see Figure 14).

SPECIES	CLUSTER	INDICATOR VALUE	PROBABILITY
SCHIZOTHECA SER-RATIMARGO	I	0.99	0.003
MYRIAPORA TRUNCATA	I	0.99	0.001
EXIDMONEA COERULEA	I	0.90	0.004
ADEONELLA PALLASII	I	0.88	0.003
CELLARIA SALICORNI-OIDES	I	0.87	0.002
CELLARIA FISTULOSA	I	0.86	0.009
TUBULIPORA CF. LILIACEA	I	0.83	0.002
ANNECTOCYMA CF. MA-JOR	I	0.78	0.001
PHOCEANA TUBULIFERA	I	0.73	0.032

34

Bryozoan diversity estimated from weight displays stronger fluctuations along the core compared to count data, having its highest values at sediment depth of 12-14cm and 40-45cm.
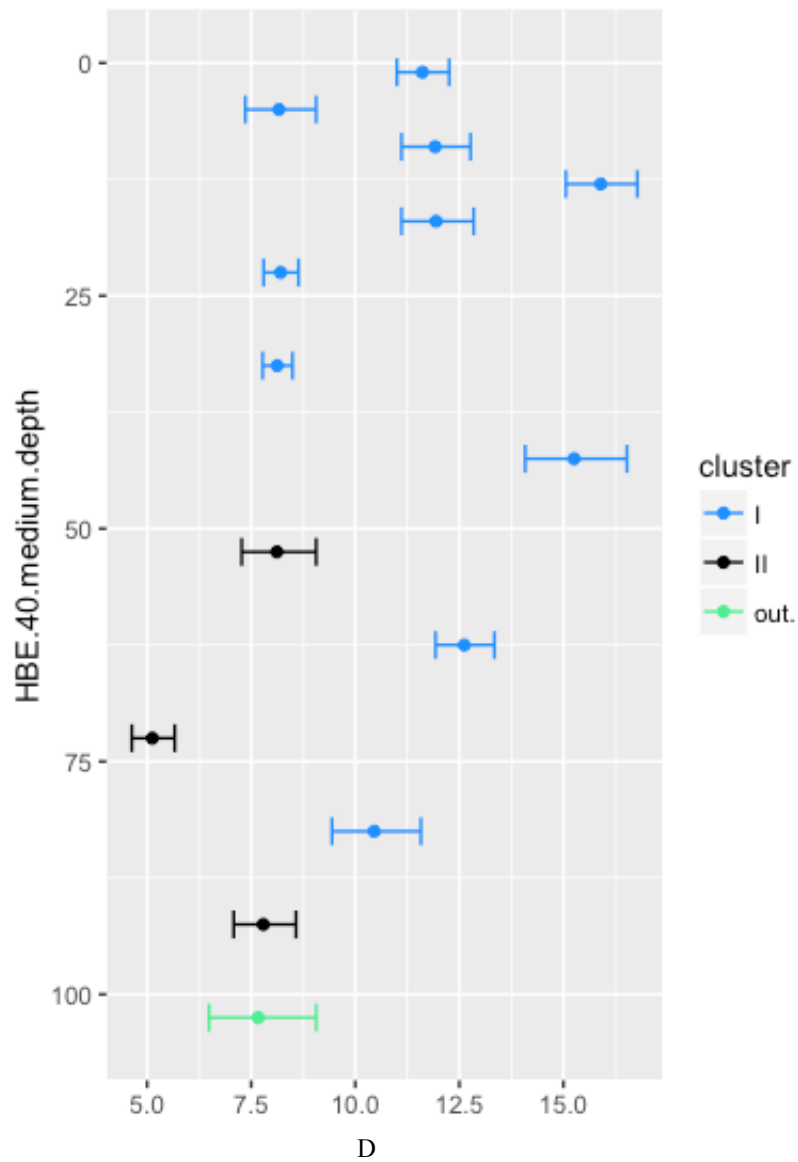
Figure 16: Shannon Wiener diversity of bryozoan species along the core base on weight. Colour-coding according to cluster analysis (see Figure 14)

Impact of pollutants on compositional changes (weight)

Distribution of individual layers in the nMDS plot reflects concentration of environmental parameters and accumulation of nutrients. This comprises the heavy metal copper (R^2=0.72, p<0.01), phosphorous (R^2=0.71, p<0.05) (Tab.17) and total carbon (R^2= 0.68, p<0.05) (Tab. 18). Silt content showed a significant correlation with the second axis of the nMDS plot (R^2=0.58, p<0.05) (Tab. 20).

Table 17: Regression analysis of heavy metal concentration and changes of bryozoan species composition along first and second nMDS axis.

	NMDS1	NMDS2	R^2	P	
Hg	-0.31	-0.95	0.29	0.240	
Cr	0.08	-1.00	0.37	0.203	
Cu	0.16	-0.99	0.72	0.007	**
Ni	0.52	-0.85	0.36	0.227	
Pb	-0.46	-0.89	0.37	0.167	
As	0.45	0.89	0.64	0.059	.
Cd	-1.00	-0.09	0.08	0.733	
Li	-0.30	-0.95	0.08	0.655	
Zn	-0.03	-1.00	0.46	0.096	.
Mn	0.92	-0.38	0.33	0.205	
P	0.63	-0.78	0.72	0.048	*
Fe	0.98	-0.19	0.67	0.057	.
Al	-0.52	-0.85	0.14	0.531	

Table 18: Regression analysis of organic environmental pollutants concentration and changes of bryozoan species composition along first and second nMDS axis.

	NMDS1	NMDS2	R^2	P
PAH	-0.28	-0.96	0.29	0.247
PCB	-0.03	-1.00	0.22	0.407

Table 19: Regression analysis of organic nutrient concentration and changes of bryozoan species composition along the first and second nMDS axis.

	NMDS1	NMDS2	R^2	P	
C.TOT	-0.94	-0.35	0.67	0.021	*
TOC	-0.66	-0.75	0.26	0.330	
N.TOT	-0.17	-0.98	0.22	0.418	

Table 20: Regression analysis of grains size distribution and changes of bryozoan species composition along the first and second nMDS axis.

	NMDS1	NMDS2	R^2	P	
CLAY	-0.67	-0.75	0.38	0.173	
SILT	0.15	-0.99	0.74	0.008	**
SAND	0.29	0.96	0.44	0.119	
>1 mm	0.05	1.00	0.39	0.169	

In contrast to diversity estimated from count data, no correlation between concentration of environmental parameters and bryozoan diversity estimated from total weight was found (Tab. 21-24).

Table 21: Correlation (Pearson's r) of heavy metal concentration to the Shannon-Winer diversity index of sediment layers.

	T	DF	P
Hg	0.995	8	0.349
Cr	-0.811	8	0.441
Cu	-0.195	8	0.850
Ni	-1.382	8	0.204
Pb	1.073	8	0.314
As	-0.595	8	0.568
Cd	-1.289	8	0.234
Li	-0.709	8	0.499
Zn	0.581	8	0.577
Mn	-0.498	8	0.632
P	-0.306	8	0.767
Fe	-1.442	8	0.187
Al	-0.524	8	0.615

Table 22: Correlation (Pearson's r) of organic environmental pollutants concentration to the Shannon-Winer diversity index of sediment layers.

	T	DF	P
PAH	0.998	8	0.348
PCB	0.588	8	0.573

Table 23: Correlation (Pearson's r) of nutrient concentration to the Shannon-Winer diversity index of sediment layers.

	T	DF	P
C.TOT	1.335	8	0.218
TOC	1.401	8	0.199
N.TOT	0.631	8	0.546

Table 24: Correlation (Pearson's r) of grain size distribution to the Shannon-Winer diversity index of sediment layers.

	T	DF	P
CLAY	1.684	12	0.118
SILT	0.203	12	0.843
SAND	-0.459	12	0.655
>1 mm	-0.889	12	0.391

Crustacea

Crustacean hard part remains consisted mainly of carapace, propodus and dactylus. The state of preservation differed strongly between specimens. Identification of species proved difficult and specimens where often classified at very different taxonomic levels. Only specimens of *Upogebia cf. deltaura* where distinctive enough to be identified to species level. *Eriphia, Ebalia* and *Callianassa* could be identified to genus level, whereas Parthenopidae, Pilumnidae and Paguroidea only to family- or superfamily level. Other specimens where assigned to 22 different morphotypes. Crustacean abundance is highest in the lower third of the core, reaching its maximum at layer 60-65cm with a total weight of 4.01g. In the uppermost 20 cm crustacean abundance is generally low. *Upogebia cf. deltaura* contributes up to 80% of crustacean hard part remains (Fig. 17).
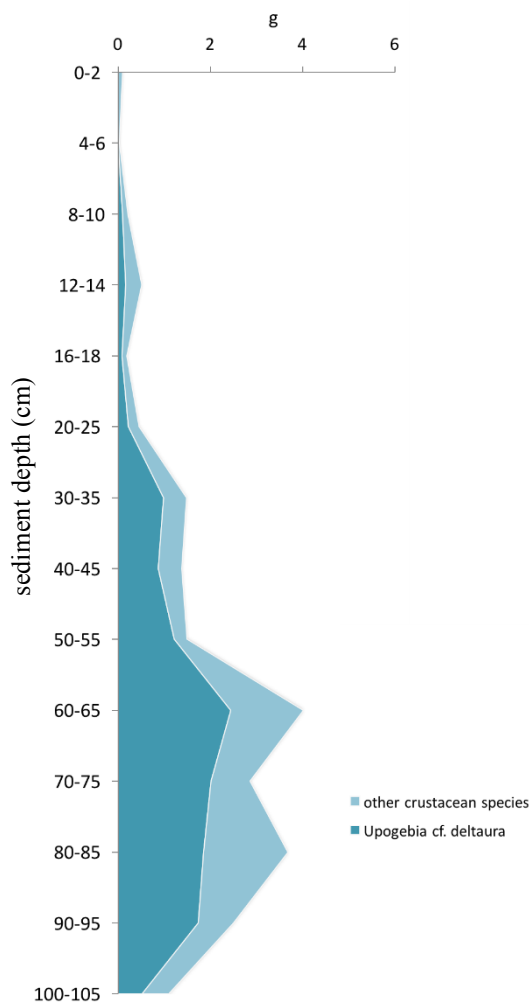
Figure 17: Abundance of crustaceans along the core. Due to its frequent occurrence *Upogebia cf. deltaura* was denoted separately.

Cluster analysis (UPGMA) of crustacean separates the core again in two distinctive clusters (PERMANOVA: R^2=0.51, F=4.71, p<0.01, 9999 permutations). The upper cluster comprises layers from 0 to 25 cm sediment depth. The lower cluster consists of layers between 30-105 cm (Fig. 18A).Bray-Curtis dissimilarity based nMDS analysis, displays a dense clustering of the lower layers older than 5000 years (Fig 18B).
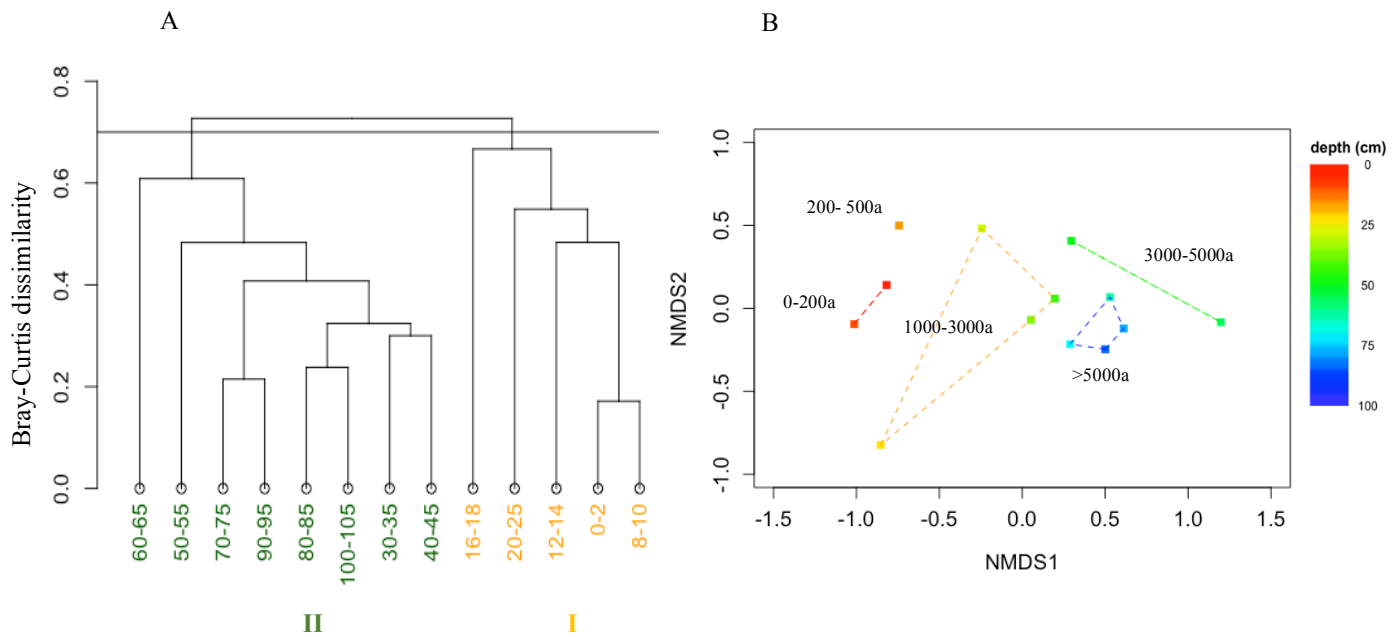
Figure 18: (A) Cluster analysis (UPGMA) of square root transformed abundance of Crustacea along the core showing two significant clusters at Bray-Curtis dissimilarity of 0.7 separating the core into lower section and an upper section (PERMANOVA: R^2: 0.41, F:7.6, p<0.001, 9999 permutations).
(B) nMDS based on square-root transformed weight based on Bray Curtis dissimilarity. Points display individual layers along the core. Colour gradient respective to sediment depth. Grouping of layers according to age-groups.

Impact of pollutants on compositional changes

Correlation of environmental parameters to site scores of individual layers in the nMDS ordination displayed a significant relation of environmental pollutants and nutrient levels to shifts in species composition. Concentration of mercury (R^2=0.72, p<0.01) and lead (R^2=0.85, p<0.01) are significantly correlated to shifts in composition (Tab. 25). Polycyclic aromatic hydrocarbons can also be related to distribution of individual layers in the ordination plot (R^2=0.75, p<0.05) (Tab.26). Composition shift also seems to be nutrient driven as total organic

carbon ($R^2=0.64$, $p<0.05$) and total nitrogen ($R^2=0.64$, $p<0.05$) correlate to site scores of respective layers (Tab. 27). Sediment grain size has no influence on crustacean composition (Tab. 28).

Table 25: Regression analysis of heavy metal concentration and changes of crustacean species composition along the first and second nMDS axis.

	NMDS1	NMDS2	R^2	P	
Hg	-0.77	-0.64	0.73	0.008	**
Cr	-0.48	0.87	0.08	0.782	
Cu	-0.45	-0.89	0.30	0.343	
Ni	0.18	0.98	0.00	0.998	
Pb	-0.96	-0.29	0.85	0.005	**
As	0.85	-0.53	0.15	0.63	
Cd	0.07	1.00	0.01	0.956	
Li	-0.25	0.97	0.40	0.216	
Zn	-0.86	-0.52	0.62	0.054	.
Mn	0.18	-0.98	0.47	0.139	
P	-0.03	-1.00	0.32	0.327	
Fe	0.63	-0.78	0.35	0.266	
Al	-0.27	0.96	0.48	0.134	

Table 26: Regression analysis of organic environmental pollutants concentration and changes of crustacean species composition along first and second nMDS axis.

	NMDS1	NMDS2	R^2	P	
PAH	-0.85	-0.52	0.75	0.03	*
PCB	-0.89	0.46	0.58	0.078	.

Table 27: Regression analysis of organic nutrient concentration and changes of crustacean species composition along first and second nMDS axis.

	NMDS1	NMDS2	R^2	P	
C.TOT	-0.46	0.89	0.52	0.11	
TOC	-1.00	0.06	0.65	0.041	*
N.TOT	-1.00	0.08	0.64	0.044	*

Table 28: Regression analysis of grains size distribution and changes of crustacean species composition along first and second nMDS axis.

	NMDS1	NMDS2	R^2	P	
CLAY	-0.83	0.56	0.61	0.056	.
SILT	-0.61	-0.80	0.15	0.61	
SAND	0.53	0.85	0.41	0.206	
>1 mm	0.83	-0.56	0.23	0.469	

Bivalvia

Taxonomic distribution and shifts of bivalves along the core (count data)

Throughout the core 7189 individuals accounting for 31 families were found. Cluster analysis (UPGMA) separates the core at a dissimilarity of 0.33 in a smaller upper cluster and a larger lower cluster (PERMANOVA: R^2=0.71, F=13.25, p<0.001, 9999 permutations). The upper cluster (cluster I) reaches from the top toward a depth of 18 cm. Layer 4-6 cm is an outlier, differing most from the remaining layers. The second cluster comprises all layers from 20 cm downwards (cluster II). At a dissimilarity of 0.23 this cluster is again separated into two, from 20cm to 45cm depth (cluster IIa) and from 50 cm to 95 cm sediment depth (IIb) (PERMANOVA: R^2=0.87, F=10.96, p<0.001, 9999 permutations) (Fig. 19A). Ordination showed a high dissimilarity between layer 4-6cm and the remaining layers (Fig. 19B).

A   B
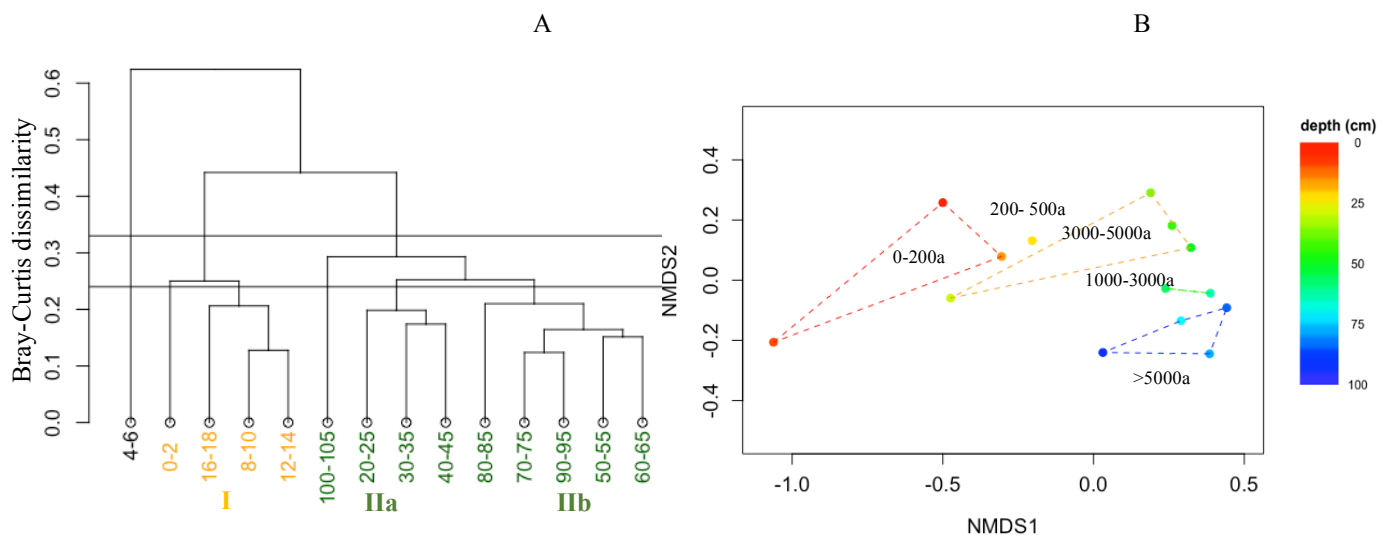
Figure 19: Cluster analysis (UPGMA) of square root transformed abundance of bivalves along the core, showing two significant clusters at Bray-Curtis dissimilarity of 0.33 and one outlier (4-6cm) separating the core in a lower and an upper section (PERMANOVA: R^2: 0.71, F:13.26, p<0.001, 9999 permutations). At a Bray-Curtis dissimilarity of 0.24 the lower cluster is separated into two additional clusters (PERMANOVA: R^2:0.87, F:10.69, p<0.001, 9999 permutations) with one outlier (100-105cm depth).
(B) nMDS based on square-root transformed Bray Curtis dissimilarity. Points display individual layers along the core. Grouping of layers according to age-groups.

Rank abundance distribution of bivalves and distribution of different sediment relation-types (count data)

Veneridae are clearly the dominant family within the core, with 1710 individuals, followed by Cardiidae (1106), Anomiidae (951), Noetiidae (499) and Corbulidae (439). Most of the specimens found were infaunal (57.13%). Shells from epifaunal families made up little more than 30% (epifaunal mobile and facultative mobile: 7.11%, epifaunal immobile: 23.37%, nestler 2.83%). Semiinfaunal species were less abundant, accounting for 5.61%. Parasitic species using other species as substrate contributed 2.99% and boring bivalves less than 1% to the total number of found specimens (Fig. 20A).

Cluster I is also dominated by Veneridae followed by Cardiidae, Nuculidae, Anomiidae and Corbulidae. Generally, the slope of the rank abundance distribution is much flatter at this part of the core compared to the whole core. Infaunal species make up 63.83% at this cluster, whereas epifaunal species account for 24.92%. Immobile epifauna decreases to 15.92%. Shells of host species made up 4.02 % and boring bivalves were completely absent from this section of the core (Fig. 20B).

Cluster II resembles to a large extent the composition of the whole core, displaying also a steep slope of the RAD with an even higher dominance of Veneridae compared to cluster I (Fig. 20C). Splitting this group into the two clusters IIa and IIb showed that only the lower part of the core is strongly dominated by Veneridae, whereas in the upper part of cluster II (cluster IIa) Veneridae are closely followed by Cardiidae. Semiinfaunal species reached their highest relative abundance in this middle section of the core (9.66%). Occurrence of boring bivalves was restricted to cluster IIb. Relative abundance of epifaunal immobile bivalves was also highest at the deepest part of the core (26.89%) (Fig. 20E).
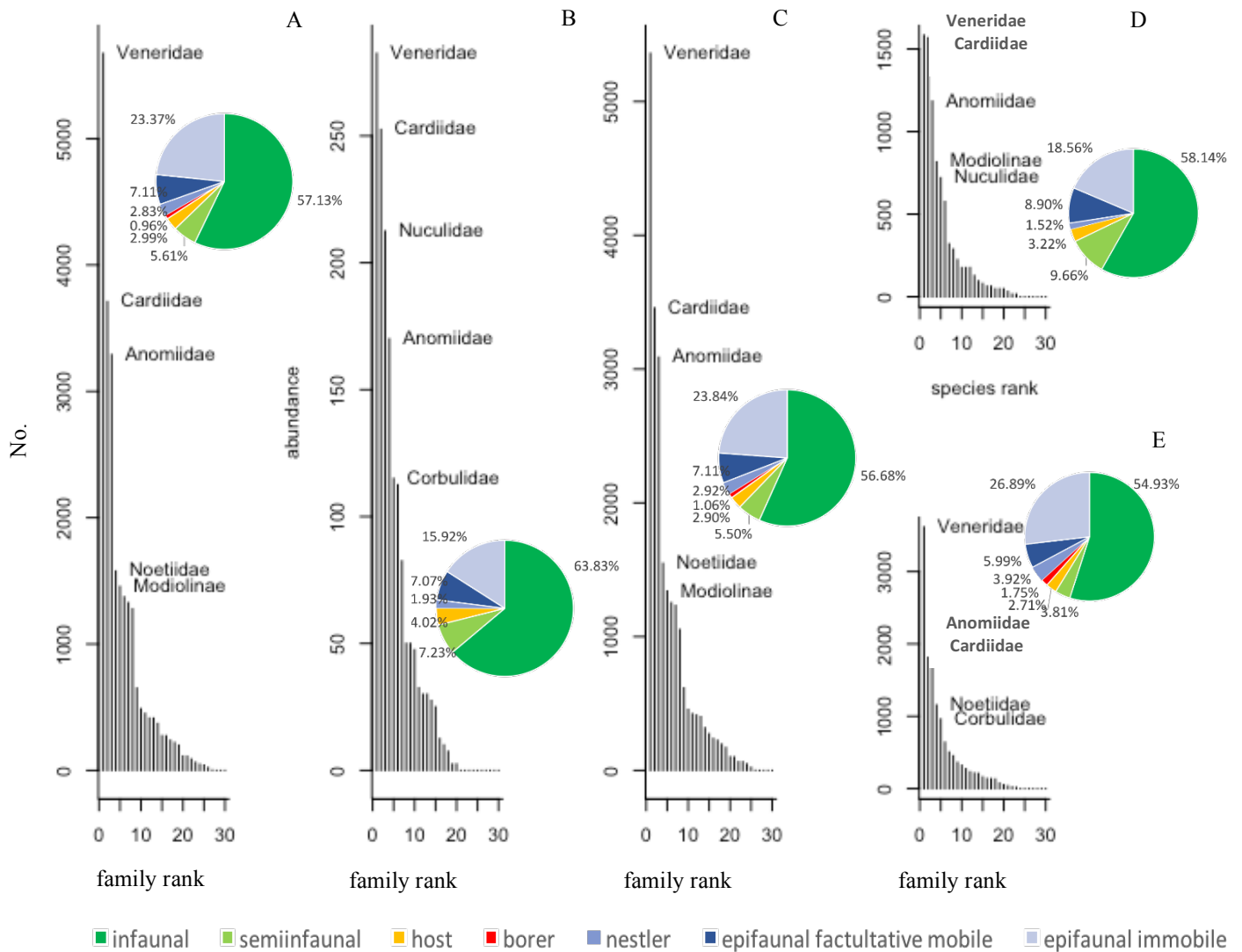
Figure 20: Rank abundance distribution of bivalve families and relative abundance of different sediment relation types of the whole core (A), and distribution within cluster I (B) and cluster II (C). Cluster II is additionally split into cluster IIa (D) and IIb (E) (see Figure 19).

Dufrene-Legendre Indicator Species Analysis revealed 8 families to be significantly related to cluster IIa (Semelidae: iv=0.75, p<0.01; Modiolinae: iv=0.66, p<0.01; Nuculidae: iv=0.65, p<0.001; Kellidae: iv=0.78, p<0.01; Lucinidae: iv=0.54, p<0.01; Pectinidae: iv=0.54, p<0.01; Cardiidae: iv=0.53, p<0.01; Tellinidae: iv=0.52, p<0.05). Four families could be assigned to the lower cluster IIb (Glycymerididae: iv=0.821, p<0.01; Ostreidae: iv=0.76, p<0.05; Noetiidae: iv=0.60, p<0.01; Hiatellidae: iv=0.56, p<0.05). No family was found to be significantly related to the upper part of the core of cluster I (Tab. 29).

Table 29: Dufrene-Legendre Indicator Species Analysis according to cluster analysis of Bivalve species (see Figure 19).

FAMILY	CLUSTER	INDICATOR VALUE	PROBABILITY
SEMELIDAE	IIa	0.75	0.006
MODIOLINAE	IIa	0.66	0.003
NUCULIDAE	IIa	0.65	0.001
KELLIDAE	IIa	0.58	0.002
LUCINIDAE	IIa	0.54	0.006
PECTINIDAE	IIa	0.54	0.005
CARDIIDAE	IIa	0.53	0.007
TELLINIDAE	IIa	0.52	0.019
GLYCYMERIDIDAE	IIb	0.82	0.005
OSTREIDAE	IIb	0.76	0.024
NOETIIDAE	IIb	0.60	0.01
HIATELLIDAE	IIb	0.56	0.037

Impact of pollutants on compositional changes (count data)

Location of individual layers within the ordination plot based on compositional dissimilarity can be correlated to concentration of the heavy metals mercury (R^2=0.74, p<0.01), lead ((R^2=0.88, p<0.01), zinc (R^2=0.88, p<0.01), manganese (R^2=0.61, p<0.05) and the environmental pollutants PAH (R^2=0.88, p<0.01) and PCB (R^2=0.88, p<0.001) (Tab. 30 & 31). Grouping seemed also to be influenced by nutrient content, as total carbon (R^2=0.75, p<0.05), total organic carbon (R^2=0.84, p<0.01) and total nitrogen (R^2=0.86, p<0.01) concentration correlate with the position within the nMDS plot (Tab.32). Clay content could be another parameter influencing compositional differences between layers (R^2=0.92, p<0.001) (Tab.33).

Table 30: Regression analysis of heavy metal concentration and changes of bivalve family composition along the first and second nMDS axis.

	NMDS1	NMDS2	R^2	P	
Hg	-0.97	0.25	0.74	0.008	**
Cr	-0.33	0.94	0.18	0.483	
Cu	-0.85	0.53	0.31	0.256	
Ni	-0.06	1.00	0.01	0.953	
Pb	-0.75	0.66	0.88	0.002	**
As	0.28	-0.96	0.32	0.255	

Cd	0.27	0.96	0.28	0.292	
Li	-0.30	0.95	0.46	0.138	
Zn	-0.86	0.52	0.88	0.001	***
Mn	0.16	-0.99	0.61	0.043	*
P	-0.12	-0.99	0.29	0.259	
Fe	0.27	-0.96	0.30	0.277	
Al	-0.33	0.94	0.52	0.093	.

Table 31: Regression analysis of organic environmental pollutants concentration and changes of bivalve family composition along first and second nMDS axis.

	nMDS1	*nMDS2*	R^2	*p*	
PAH	-0.95	0.30	0.88	0.003	**
PCB	-0.90	0.43	0.88	0.001	***

Table 32: Regression analysis of organic nutrient concentration and changes of bivalve family composition along the first and second nMDS axis.

	NMDS1	NMDS2	R^2	P	
C.TOT	-0.26	0.97	0.75	0.012	*
TOC	-0.64	0.77	0.84	0.004	**
N.TOT	-0.77	0.64	0.86	0.003	**

Table 33: Regression analysis of grains size distribution and changes of bivalve family composition along the first and second nMDS axis.

	NMDS1	NMDS2	R^2	P	
CLAY	-0.34	0.94	0.92	0.001	***
SILT	-0.72	0.69	0.26	0.34	
SAND	0.90	-0.43	0.37	0.188	
>1 mm	0.36	-0.93	0.47	0.106	

Taxonomic distribution and shifts of bivalves along the core (weight)

Cluster analysis of (UPGMA) according to weight, separates the core at a dissimilarity of 0.45 also into two distinctive clusters (PERMANOVA: R^2=0.49, F=5.25, p<0.001, 9999 permutations). The lower cluster II reaches also from 20-95 cm, however, layer 100-105cm is placed within the upper cluster I. Like in the previous analysis of abundances, layer 4-6 cm differs strongly from the other layers. Position of individual layers within the core is less reflected by dissimilarity between different layers compared to abundance data (Fig. 21B).
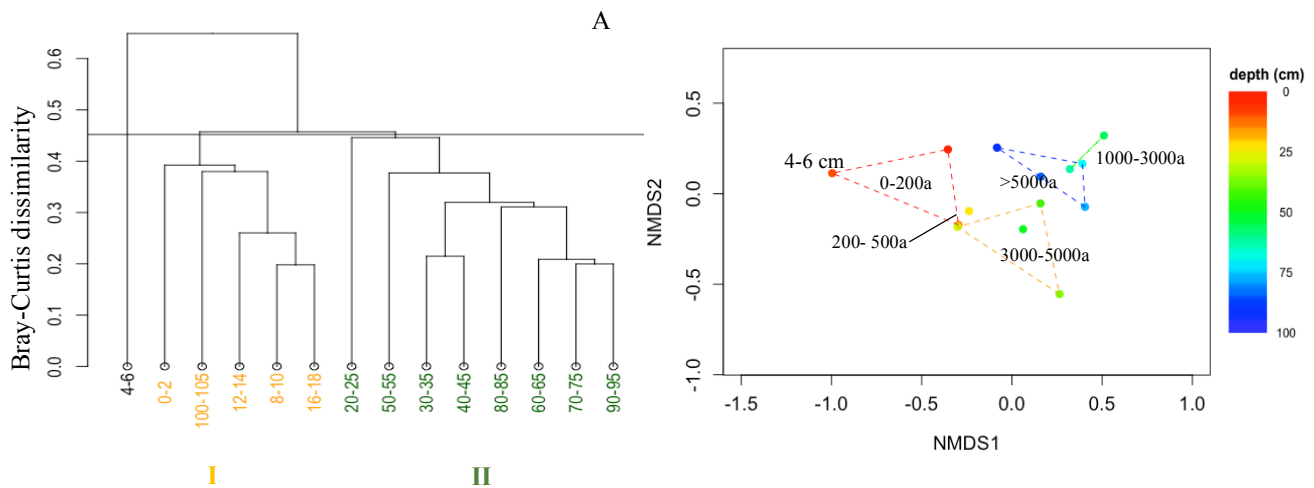
Figure 21: (A) Cluster analysis (UPGMA) of square-root transformed weight data of bivalve families along the core showing two clusters at Bray-Curtis dissimilarity of 0.45 and one outlier (4-6 cm) (PERMANOVA: R^2: 0.48, F:5.25, p<0.001, 9999 permutations).
(B) nMDS based on square-root transformed weight data based on Bray Curtis dissimilarity. Points display individual layers along the core. Colour gradient respective to sediment depth. Grouping of layers according to age-groups.

Rank abundance distribution of bivalves and distribution of different sediment relation-types (weight)

Veneridae contribute most in terms of total weight of bivalves' shell remains (10.33g). The second most abundant family are Nuculidae (5.94g) followed by Pectinidae (5.55g), Ostreidae (5.29g) and Arcidae (3.73g).

Infaunal bivalves make up more than 50% of total weight in the core (53.12%). Semiinfaunal species make up only 2.73%. Epifaunal taxa accounted for 42.95% (epifaunal immobile: 28.75%, epifaunal mobile and fakultative mobile: 13.13%, nestler 1.07%). Boring bivalves contribute only 0.19% to the total weight of bivalves and families using another species as substrate made up 1.00% (Fig. 22A).

The upper cluster is strongly dominated by infaunal taxa, contributing 65.95% to total mass, whereas epifaunals contribute only 30.36% at this part of the core (epifaunal immobile: 25.41%, epifaunal mobile and fakultative mobile: 4.95%, nestler 1.41%). Seminfaunal taxa make up 1.77%, host species 0.51% and boring bivalves are completely absent at this cluster

(Fig 22B). The lower cluster again resembles to a large extent the overall distribution of the whole core (Fig. 22C).

Only for cluster II a relation to bivalve families was found. Abundance of Pectinidae (iv=0.92, p<0.001), Limidae (iv=0.90, p<0.001), Modiolidae (iv=0.88, p<0.001), Cardiidae (iv=0.85, p<0.001), Anomiidae (iv=0.79, p<0.01), Tellinidae (iv=0.71, p<0.05) and the subfamily Noetiinae (iv=0.64, p<0.05) was significantly higher at this part of the core.
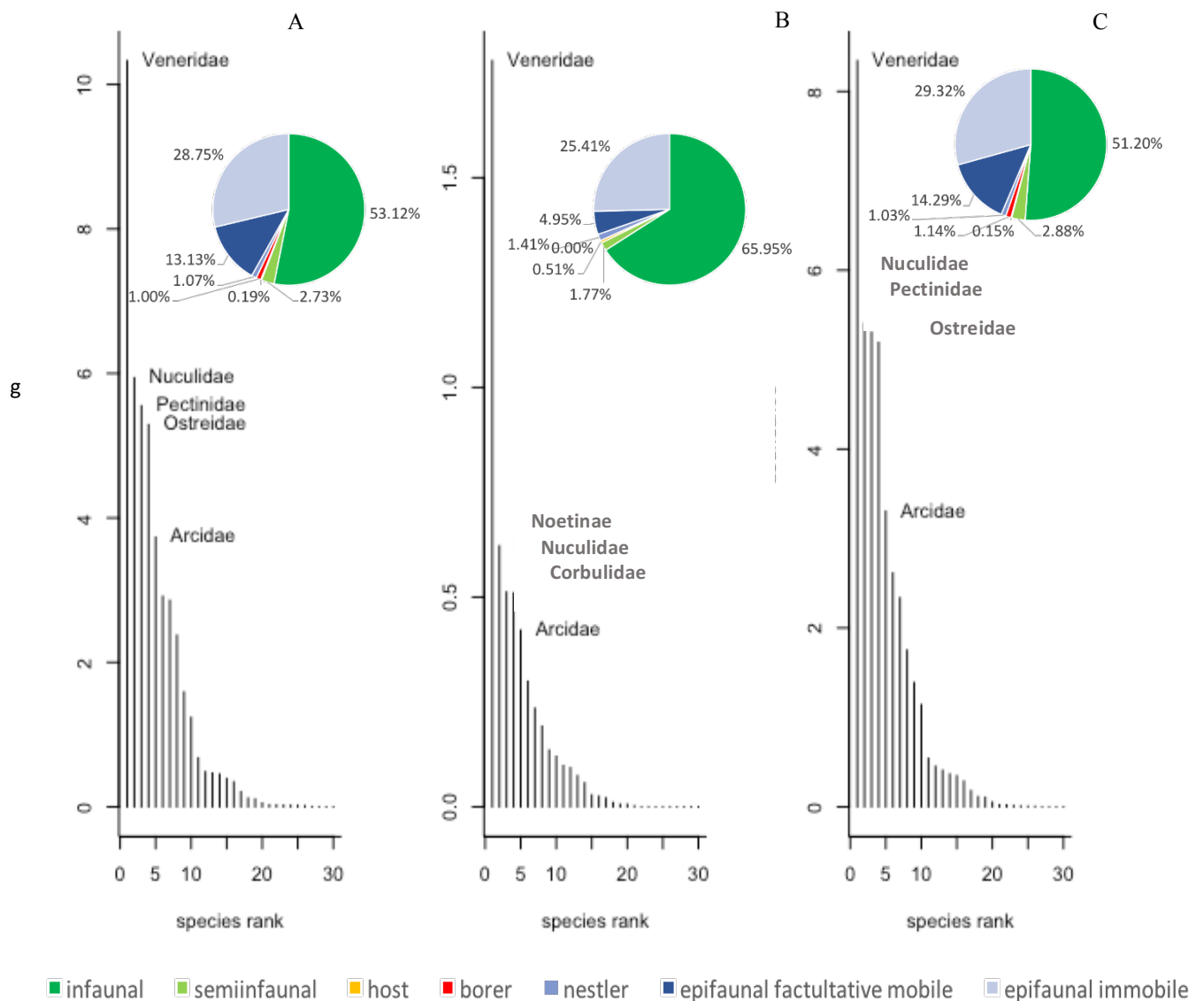

Figure 22: Rank abundance distribution of bivalve species and relative abundance of different sediment relation types of the whole core (A), and distribution within cluster I (B) and cluster II (C).

Table 34: Dufrene-Legendre Indicator Species Analysis according to cluster analysis of bivalve families (see Figure 21).

FAMILY	CLUSTER	INDICATOR VALUE	PROBABILITY
PECTINIDAE	II	0.92	0.001
LIMIDAE	II	0.90	0.001
MODIOLINAE	II	0.88	0.002
CARDIIDAE	II	0.85	0.001
ANOMIIDEA	II	0.79	0.002
TELLINIDAE	II	0.71	0.038
NOETINAE	II	0.64	0.034

Impact of pollutants on compositional changes (weight)

Correlation of heavy metals to site scores of the nMDS (see Figure 21B) showed that mercury (R^2=0.73, p<0.05), lead (R^2=0.76, p<0.01) and zinc concentration (R^2=0.83, p<0.01) could be related to shifts in community composition along the core (Tab. 35). The same holds true for the organic environmental pollutants PAH (R^2=0.81, p<0.01) and PCB (R^2=0.71, p<0.01) (Tab. 36). Another environmental parameter driving this shift was nutrient content (TOC: R^2=0.63, p<0.05, N.tot: R^2=0.68, p<0.05) (Tab. 37). No significant correlation of grainsize distribution and community shifts was found (Tab. 38).

Table 35: Regression analysis of heavy metal concentration and changes of bivalve species composition along first and second nMDS axis.

	NMDS1	NMDS2	R^2	P	
Hg	-0.94584	-0.32464	0.7327	0.014	*
Cr	-0.63579	-0.77187	0.1668	0.545	
Cu	-0.99472	0.10259	0.413	0.174	
Ni	-0.65143	-0.7587	0.0176	0.939	
Pb	-0.91181	-0.41061	0.7636	0.01	**
As	0.7293	0.68419	0.1718	0.519	
Cd	0.1772	-0.98417	0.2367	0.38	
Li	-0.60226	-0.7983	0.2295	0.408	
Zn	-0.99957	-0.02939	0.8301	0.003	**
Mn	0.54097	0.84104	0.0559	0.841	
P	-0.55969	0.82871	0.1047	0.622	

Fe	0.35767	0.93385	0.1337	0.583
Al	-0.51302	-0.85838	0.3652	0.199

Table 36: Regression analysis of organic environmental pollutants concentration and changes of bivalve species composition along first and second nMDS axis.

	NMDS1	NMDS2	R^2	P	
PAH	-0.99	-0.13	0.80	0.003	**
PCB	-1.00	-0.05	0.71	0.009	**

Table 37: Regression analysis of organic nutrient concentration and changes of bivalve species composition along first and second nMDS axis.

	NMDS1	NMDS2	R^2	P	
C.TOT	-0.48	-0.88	0.36	0.201	
TOC	-0.91	-0.42	0.63	0.034	*
N.TOT	-0.98	-0.22	0.68	0.022	*

Table 38: Regression analysis of grains size distribution and changes of bivalve species composition along first and second nMDS axis.

	NMDS1	NMDS2	R^2	P
CLAY	-0.86	-0.51	0.36	0.231
SILT	-0.98	0.22	0.31	0.314
SAND	1.00	0.10	0.38	0.18
>1 mm	0.99	0.15	0.23	0.433

Gastropoda

Taxonomic distribution and shifts of gastropods along the core (abundances)

Within the whole core 2577 specimens were found, accounting for 44 families. Cluster analysis (UPGMA) of gastropod families displayed significant clustering, but a less clear separation of the core into different sections. The lower cluster reaches from 50cm sediment depth downwards, however the very deepest layer from 100-105 cm is placed closer to layer 12-14cm. The other cluster comprises layers from a sediment depth of 8-25cm, layer 12-14 cm being the only exception. These two clusters are separated at a dissimilarity of 0.36 (PERMANOVA: R^2=0.79, F=6.18, p<0.05, 9999 permutations). The upper two layers 0-2 cm and 4-6cm differ greatly from all other layers at a dissimilarity of 0.6 (PERMANOVA: R^2=0.38, F=7.48, p<0.05, 9999 permutations) (Fig. 23A).

The nMDS plot displays strong differences in composition within the age-group ranging from 0 to 200 years BP (Fig. 23B).
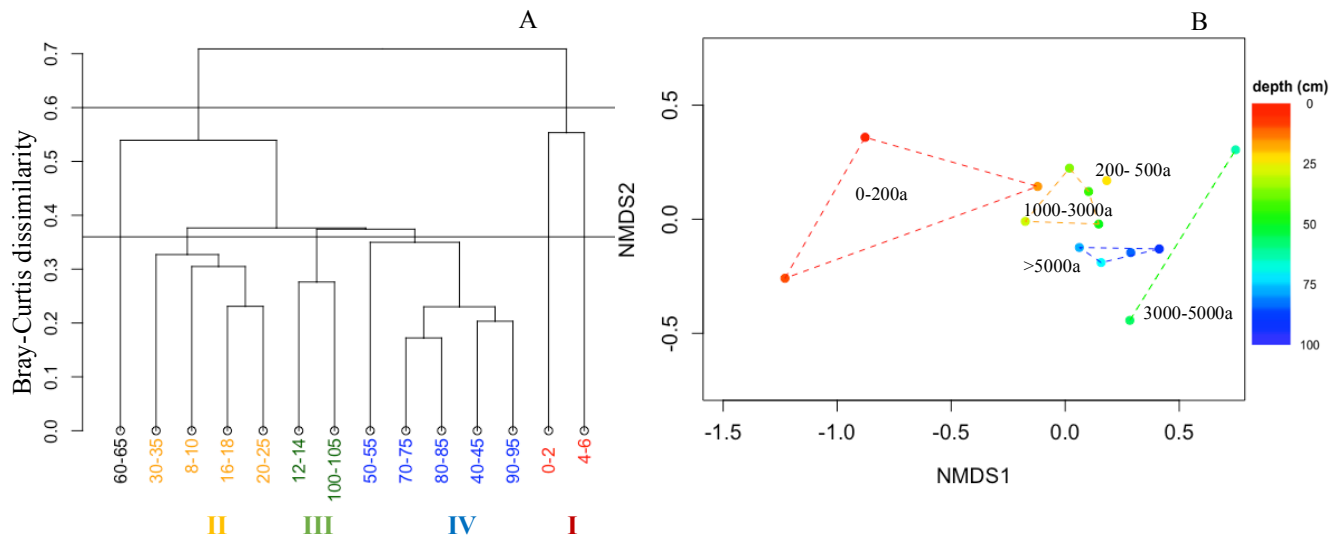

Figure 23: (A) Cluster analysis (UPGMA)of square root transformed abundance of gastropod families along the core, separates the upper layers (0-2cm, 4-6cm) from the remaining layers at a dissimilarity of 0.7 (PERMANOVA: R^2: 0.38, F:7.47, p<0.01, 9999 permutations). At a dissimilarity of 0.36 the remaining layers are grouped into a cluster from 8-35 cm, with layer 12- 14 cm being the exception and a cluster from 40-95cm sediment depth. Layer 12-14 and 100-105 cm depth are placed in a separated group (PERMANOVA: R^2: 0.79, F:6.18, p<0.001, 9999 permutations). (B) nMDS based on square-root transformed abundance based on Bray Curtis dissimilarity. Points display individual layers along the core. Colour gradient respective to sediment depth. Grouping of layers according to age-groups.

Rank abundance distribution of gastropods and distribution of different sediment relation-types (count data)

The most abundant gastropod family were the Rissoidae with 819 individuals. Cerithiidae were the second most abundant family within the core making up 607 specimens, followed at some distance by Trochidae (218), Nassariidae (138) and Cerithiopsidae (92).

Infaunal gastropods make up more than 80% of shells found (86.46%). Host families account for 8.69%, whereas all other sediment-relation types never exceeded 5% (infaunal: 1.13%; semiinfaunal: 1.20%. To a relative small proportion also limnic (2.41%) and terrestrial gastropods (0.12%) were found.

51

The three clusters differ only little. The main difference between the upper and the lower cluster is the absence of terrestrial and the smaller number of limnic gastropods in the upper part of the core. The uppermost 6 cm (cluster I), which differ the most from all remaining layers do so, because of the relatively lower number of rissoid gastropods at this section of the core (Fig. 24).

A significant relation of the gastropod families Hydrobiidae (iv=0.81, p<0.05), Fissurellidae (iv=0.81, p<0.05), Conoidea (iv=0.79, p<0.001), Muricidae (iv=0.79, p<0.01), Trochidae (iv=0.78, p<0.001), Naticidae (iv=0.77, p<0.05), Cerithidae (iv=0.77, p<0.05), Nassariidae (iv=0.72, p<0.05), Aclididae (iv=0.70, p<0.05), Rissoidae (iv=0.65, p<0.01), Epitoniidae (iv=0.63, p<0.05) and Eulimidae(iv= 0.60, p<0.05) to cluster II was found. The abundance of the two families Tornidae (iv=1, p<0.05) and Columbellidae (iv=0.80, p<0.05) is significantly related to the cluster IV (Tab. 39).
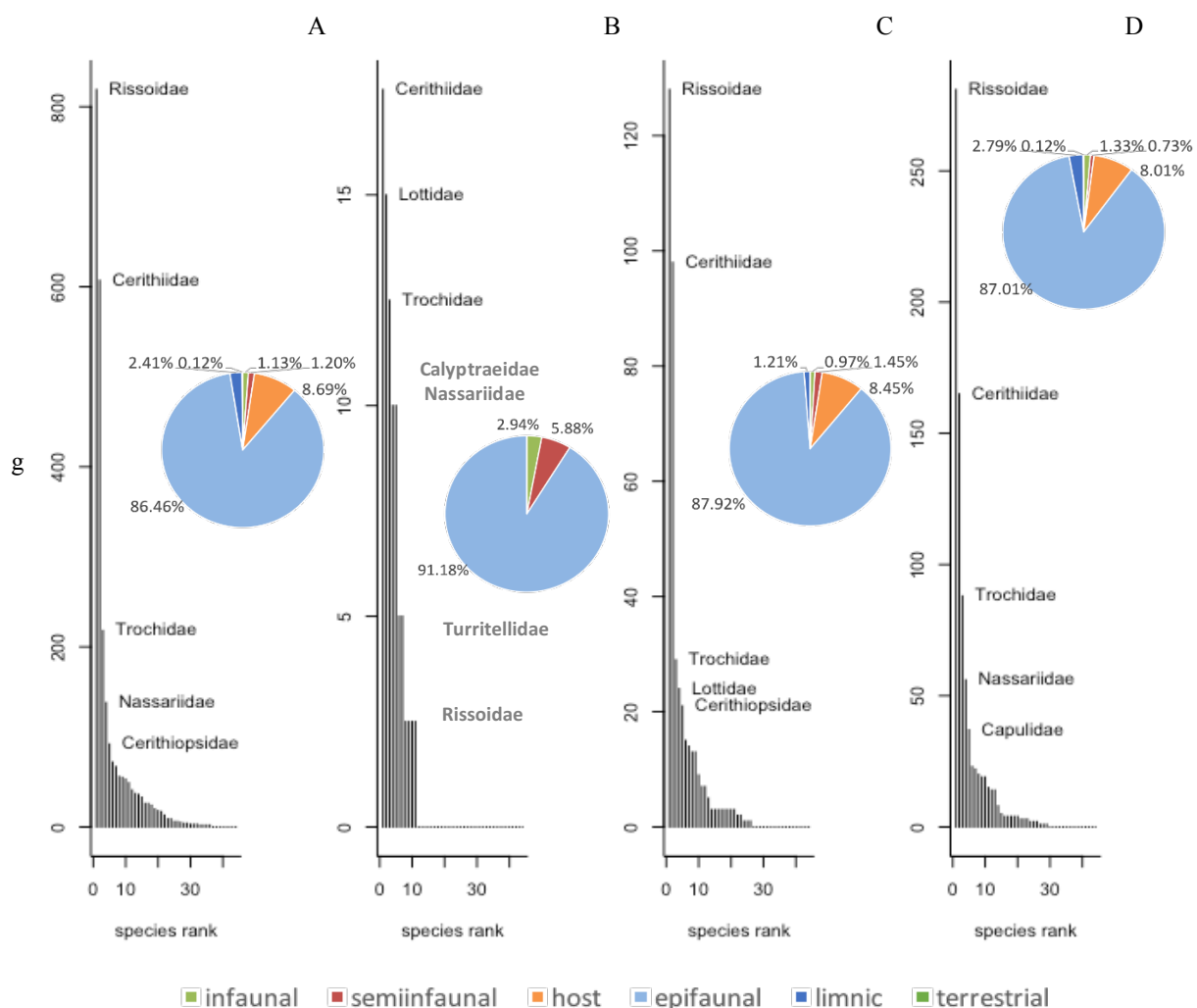

Figure 24: Rank abundance distribution of gastropod families and relative abundance of different sediment relation types of the whole core (A), and distribution within cluster I (B), cluster II (C) and cluster IV (D) (see Figure 23).

Table 39: Dufrene-Legendre Indicator Species Analysis according to cluster analysis of gastropod families (see Figure 23).

FAMILY	CLUSTER	INDICATOR VALUE	PROBABILITY
HYDROBIIDAE	II	0.83	0.002
FISSURELLIDAE	II	0.81	0.023
CONOIDEA	II	0.79	0.001
MURICIDAE	II	0.79	0.002
TROCHIDAE	II	0.78	0.001
NATICIDAE	II	0.77	0.012
CERITHIIDAE	II	0.73	0.022
NASSARIIDAE	II	0.72	0.018
ACLIDIDAE	II	0.70	0.014
RISSOIDAE	II	0.65	0.007
EPITONIIDAE	II	0.63	0.038
EULIMIDAE	II	0.60	0.032
TORNIDAE	IV	0.99	0.023
COLUMBELLIDAE	IV	0.80	0.037

Impact of pollutants on compositional changes (count data)

Location of individual layers within the ordination plot based on compositional dissimilarity between them, can be correlated to concentration of the heavy metals lead (R^2=0.74, p<0.001), zinc (R^2=0.59, p<0.05) and the organic pollutants PAH (R^2=0.73, p<0.001) and PCB (R^2=0.61, p<0.05) (Tab. 40-41). Total organic carbon (R^2=0.80, p<0.001) and total Nitrogen (R^2=0.83, p<0.001) could also be a potential driver of gastropod community shifts (Tab.42). Content of clay showed a significant correlation with the second axis of the nMDS plot (R^2=0.69, p<0.05) (Tab. 43).

Table 40: Regression analysis of heavy metal concentration and changes of gastropod family composition along the first and second nMDS axis.

	NMDS1	NMDS2	R^2	P	
Hg	-0.94	0.33	0.53	0.062	.
Cr	-0.35	0.94	0.01	0.961	
Cu	-0.75	0.66	0.12	0.649	
Ni	0.96	-0.28	0.03	0.88	
Pb	-0.81	0.59	0.74	0.005	**
As	0.36	-0.93	0.09	0.723	
Cd	0.31	0.95	0.09	0.712	

Li	-0.72	0.69	0.08	0.739	
Zn	-0.84	0.54	0.59	0.037	*
Mn	0.44	-0.90	0.21	0.461	
P	0.10	-1.00	0.03	0.888	
Fe	0.72	-0.69	0.33	0.26	
Al	-0.73	0.68	0.13	0.611	

Table 41: Regression analysis of organic environmental pollutants concentration and changes of gastropod family composition along the first and second nMDS axis.

	NMDS1	NMDS2	R^2	P	
PAH	-0.94	0.35	0.73	0.005	**
PCB	-0.96	0.28	0.61	0.035	*

Table 42: Regression analysis of organic nutrient concentration and changes of gastropod family composition along first and second nMDS axis.

	NMDS1	NMDS2	R^2	P	
C.TOT	-0.44	0.90	0.44	0.135	
TOC	-0.66	0.75	0.80	0.003	**
N.TOT	-0.79	0.62	0.83	0.002	**

Table 43: Regression analysis of grains size distribution and changes of gastropod family composition along first and second nMDS axis.

	NMDS1	NMDS2	R^2	P	
CLAY	-0.42	0.91	0.69	0.022	*
SILT	-0.39	0.92	0.11	0.704	
SAND	0.61	-0.79	0.57	0.064	.
>1 mm	0.28	-0.96	0.17	0.525	

Taxonomic distribution and shifts of gastropods along the core (weight)

Cluster analysis (UPGMA) of square-root transformed total weight of gastropod hard part remains show that the upper most layers 0-2cm and 4-6cm differ most from the other layers like in the previous analysis of count data (PERMANOVA: R^2=0.37, F=7.12, p<0.05, 9999 permutations). However, the boundary between the two clusters at a dissimilarity of 0.53 is drawn at a different depth than in the analyses on abundances. Cluster I comprises layers 8-10cm, 16-18cm and the two layers 14-16cm and 100-105cm, which were previously placed in a separate group. Layer 20-25cm and 30-35cm which belonged to this cluster are placed on cluster II,

reaching now from 20 to 95 cm depth (PERMANOVA: R^2=0.63, F=5.73, p<0.001, 9999 permutations)(Fig. 25A). Dissimilaity between the 0-200 year old layers is great within this groups but also compared to the remaining layers (Fig. 25B).
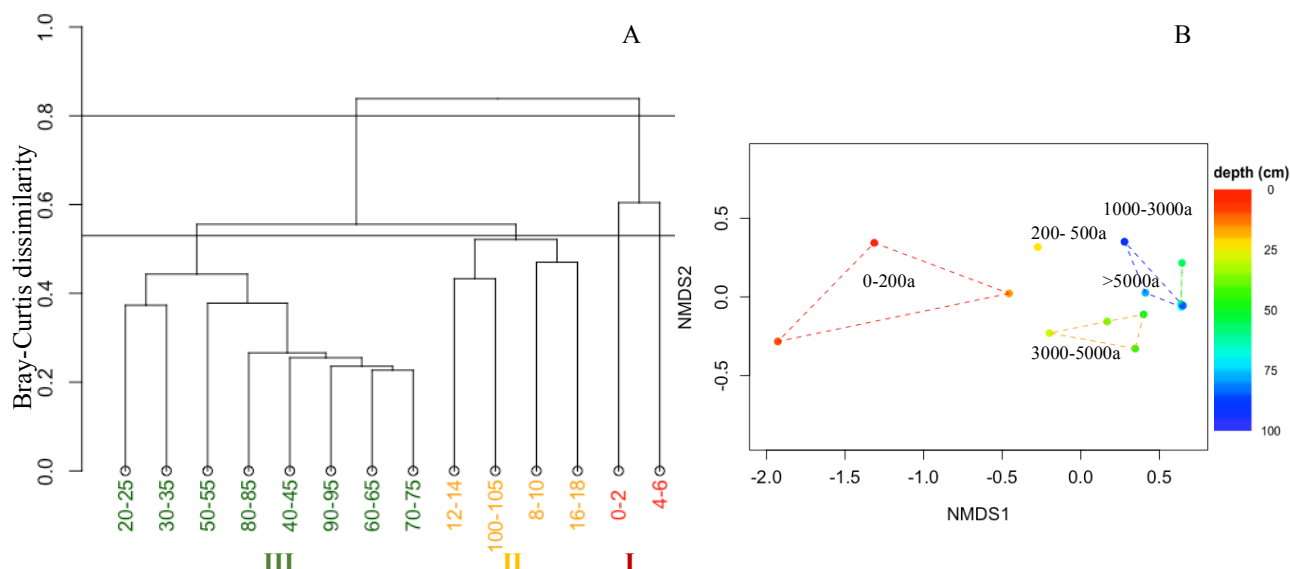

Figure 25: (A) Cluster analysis (UPGMA) of square-root transformed weight of gastropod species along the core, separates the upper layers (0-2cm, 4-6cm) from the remaining layers at a dissimilarity of 0.8 (PERMANOVA: R^2: 0.37, F:7.12, p<0.01, 9999 permutations). At a dissimilarity of 0.53 the remaining layers are grouped into a cluster from 8-18 cm, with layer 100-105 cm being placed within this group. Layers from 20 cm to 95 cm depth are placed in a separated group (PERMANOVA: R^2: 0.63, F:5.73, p<0.001, 9999 permutations). (B) nMDS of square-root transformed abundance estimated from weight data based on Bray Curtis dissimilarity. Points display individual layers along the core. Colour gradient respective to sediment depth. Grouping of layers according to age-groups.

Rank abundance distribution of gastropods and distribution of different sediment relation-types (weight)

Rissoidae were the most abundant family also in terms of total weight, being the dominant family throughout the core. In general, gastropod distribution differs not much between the two methods of quantification. Infaunal species dominate the assemblage making up more than 80% of total weight. Other sediment relation types show also a similar distribution pattern as revealed with abundance data (Fig. 26A). The most striking difference between the two clusters is a higher proportion of semiinfaunal individuals in the upper (3.55%) compared to the lower cluster (0.99%) and the difference in relative abundance of host species (cluster I: 5.23%; cluster II: 9.02%). Infaunal species abundance is also slightly higher in the upper part

of the core (88.13%) (Fig. 26C). However, abundance of infaunal species in the lower part remains still high (83.92%) (Fig. 26 D). In the uppermost 6 cm rissoid abundance is relatively low compared to the other parts of the core. In terms of total weight Nassariidae dominate these layers (Fig. 26B).
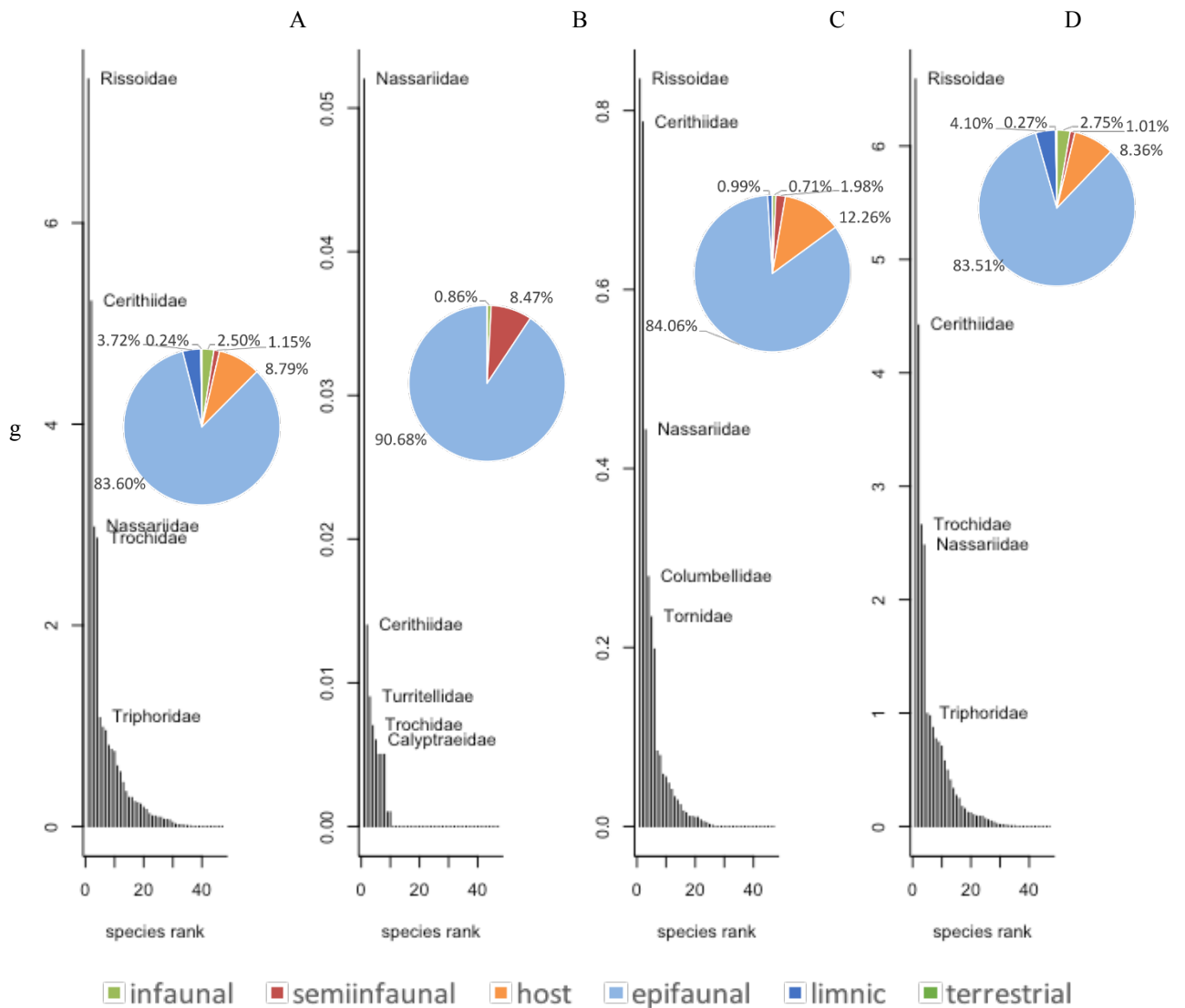

Figure 26: Rank abundance distribution of gastropod families and relative abundance of different sediment relation types of the whole core (A), and distribution within cluster I (B) cluster II (C) and III (D) (see Figure 25).

Table 44: Dufrene-Legendre Indicator Species Analysis according to cluster analysis of gastropod families (see Figure 25).

FAMILY	CLUSTER	INDICATOR VALUE	PROBABILITY
COLUMBELLIDAE	I	0.742	0.039
MURICIDAE	II	0.9799	0.001
TROCHIDAE	II	0.862	0.003
CONOIDAE	II	0.8604	0.002
RISSOIDAE	II	0.7958	0.001
HYDROBIIDAE	II	0.7898	0.003
CERITHIIDAE	II	0.6394	0.047

Impact of pollutants on compositional changes (weight)

Compositional differences estimated from weight measurement also correlate with the concentration of lead (R^2=0.80, p<0.01), zinc (R^2=0.77, p<0.01) but also mercury (R^2=0.68, p<0.05) (Tab. 45). Organic pollutants PAH (R^2=0.85, p<0.01) and PCB (R^2=0.79, p<0.01) are another factor driving ecological shifts (Tab. 46). Nutrient concentration displayed no impact of gastropod community changes (Tab.47). The same holds true for grain size, as sand smaller than 1mm shows a significant correlation to compositional differences within the ordination plot (R^2=0.66, p<0.05) (Tab. 48).

Table 45: Regression analysis of heavy metal concentration and changes of gastropod family composition along the first and second nMDS axis.

	NMDS1	NMDS2	R^2	P	
Hg	-0.95	-0.32	0.68	0.03	*
Cr	-0.84	-0.54	0.03	0.906	
Cu	-0.63	0.78	0.24	0.392	
Ni	0.20	0.98	0.02	0.913	
Pb	-1.00	-0.09	0.80	0.005	**
As	1.00	0.07	0.10	0.676	
Cd	0.14	-0.99	0.37	0.188	
Li	-0.34	-0.94	0.15	0.539	
Zn	-0.89	0.46	0.77	0.004	**
Mn	0.23	0.97	0.20	0.463	

P	-0.06	1.00	0.27	0.347
Fe	0.37	0.93	0.26	0.316
Al	-0.32	-0.95	0.23	0.413

Table 46: Regression analysis of organic environmental pollutants concentration and changes of gastropod family composition along the first and second nMDS axis.

	NMDS1	NMDS2	R^2	P	
IPA	-1.00	0.02	0.85	0.004	**
PCB	-0.85	0.53	0.79	0.006	**

Table 47: Regression analysis of organic nutrient concentration and changes of gastropod family composition along first and second nMDS axis.

	NMDS1	NMDS2	R^2	P	
C.TOT	-0.43	-0.90	0.36	0.208	
TOC	-1.00	-0.10	0.75	0.012	*
N.TOT	-0.79	0.61	0.86	0.005	**

Table 48: Regression analysis of grains size distribution and changes of gastropod family composition along the first and second nMDS axis.

	NMDS1	NMDS2	R^2	P	
CLAY	-0.72	0.69	0.50	0.086	.
SILT	-0.27	0.96	0.37	0.203	
SAND	0.46	-0.89	0.66	0.035	*
>1 mm	0.38	-0.93	0.24	0.379	

Echinoidea

Main occurrence of Echinoidea is restricted to the lower half of the core. Total weight in-creases from the lowest part at 105 cm (0.46g) towards its maximum at 60 cm sediment depth (2.74g). From this point onward, weight steadily declines to a minimum at the top layer (0.04g). Irregularia make up the largest part of echinoid remains contributing to 80% ±0.10SD of echinoid total weight within the core (Fig. 27). Irregular Echinoids consist almost exclusively of one species, *Echinocyamus pusillus.* Hard part remains belonging to another species were found only sporadically and were strongly fragmented.
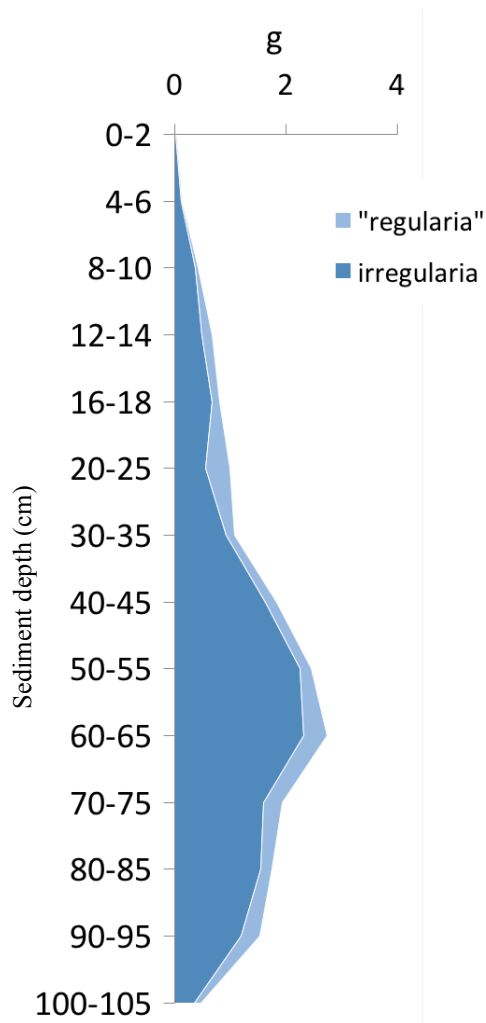
Figure 27: Weight of regular and irregular Echinoidea along the core estimated from total weight of found hard part remains. *Echinocyamus pusillus* makes up the main part of total irregular echinoids weight.

Corallinaceae

The biggest fraction of hart part remains within the core can be attributed to Corallinaceae (Figure 7A & 28). Weight of Corallinaceae is low in the deepest 30 cm of the core. It is much higher in the middle to upper section of the core, having its maximum at layer 16-18cm depth (18.94g). At a sediment depth between 4-6 cm total weight drops to 1.97g before it increases again towards the top (9.62g). *Titanoderma pustulatum* (Lamouroux) Nägeli was found at a layer depth of 20-25cm. Frequently found fragments most likely belong to the genus *Phymato-lithon* and belong according to the classification of Steneck (1986) to the maerl and nodular growth-type.
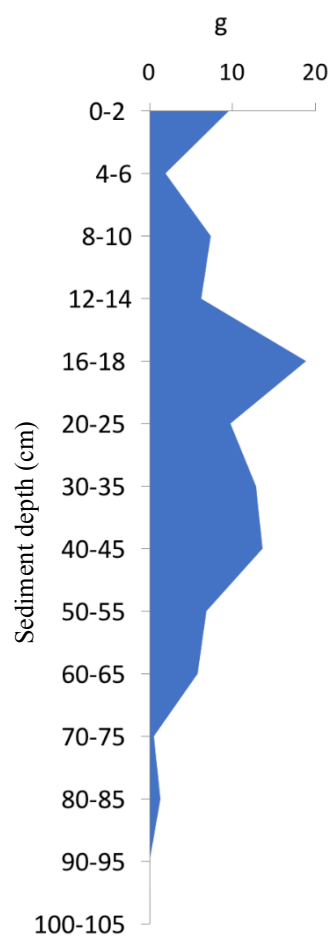
Figure 28: Weight of Corallinaceae along the core estimated from total weight of found hard part remains.

DISCUSSION

Taking all taxa found into account pronounced differences in taxonomic composition between the upper part of the core and the lower part were visible, indicating profound ecological changes in time. Cluster analysis separated the core in a lower section from a sediment depth of 50-95cm and a upper section from 0-45 cm (Fig. 6). The lower cluster therefore would range from 3000 years to more than 5000 years before present with its oldest specimens found dating as far back as 10 000 years (BP). This two clusters are further divided into clusters from 70-95 cm, 65-50cm, 45-20cm and 18-6cm sediment depth. Time averaging from AAR dated specimens place the lowermost cluster at an age of more than 5000 years. The second lowest cluster between 3000-5000 years (Fig.2). Clustering was clearly related to depth with layers from similar depths being more prone to be found in the same cluster (Fig. 6). These results suggest that ecological conditions changed in time. Ordination showed that most layers were located along the first nMDS axis according to the depth in which they were found in the sediment and consequently according to age (Fig. 6 B). This would rather hint to a gradual shift in species composition. Considering grain-size distribution - with coarse material at the lower parts of the core becoming considerably finer towards the top - sea-level rise could be interpreted as major driver of compositional differences (Fig 3A).

Frequently found terrestrial material such as woody and reed like plant remains at the very lower layers marks the onset of the Holocene transgression and an environment with strong terrestrial influence, suggesting a shallow water ecosystem (Fig. 8). According to a study estimating past transgression states at the Adriatic, sea-level reached already 6000 years ago -2m below present-day level. From this time point onward it increased much slower than it did at the timespan from 10 000 to 6000 BP (Antoniolo et al. 2007). Having that in mind, differences in sea-level can be excluded as sole driver of compositional changes, as for at least the upper part of the core sea-level stayed relatively constant.

The amount of hard part remains found at respective layer peeks at a depth of 50-55cm depth (Fig. 2). This increase in total weight can to a large extend be attributed to macroids at this part of the core. (Fig.2). This layer is placed at an age between 3000-5000 years BP, when todays sea-level was almost reached and transgression started to stagnate (Antoniolo et al. 2007). The core was retrieved at a depth of 44m, therefore it can be assumed that formation of these macroids took place at a depth at about 40m.

The high occurrence of macroids at the 50-55cm deep layer, initiated by large oysters overgrown mainly by calcareous algae, bryozoan and serpulid worms (own observation) could hint

to the presence of secondary hard bottom like conditions. Layers of similar characteristics were reported from a core taken in close proximity, dated to be slightly older ranging between 4500 to 5000 yrs BP (Schnedl, unpublished data). This layer is characterized by the highest bryozoan species richness throughout the core.

Titanoderma pustulatum found at a sediment depth between 20-25cm was the only calcareous algae identified to species level. This species is reported to form thin crusts having an important role in the early stages of biological constructions in the Mediterranean (Steneck 1986; Basso 2007). The majority of Corallinaceae found most likely belong to the genus *Phymatolithon* belonging to the maerl and nodular growth-type. *Phymatolithon calcareum* is the most common species of this genus forming large maerl beds of dead and living material and is included in the Annex V of the EC Habitats Directive (Council Directive 92/43/EEC). Lattice formed by interlocked thali of maerl species result in complex structures providing suitable habitats for a variety of invertebrate species (Keegan 1974; Bosence 1976; Foster 2001; Steller et al. 2003). Although calcareous algae have a well preserved extensive record, identification of calcareous red algae has proven to be difficult and needs specialist expertise. However, only few genera show predominant morphological states and are phylogenetically constrained. Convergent anatomic and morphological evolution within this group, reveals adaptation to environmental condition (Paine & Suchanek 1983, Steneck 1986). Therefor functional ecological detail, independent of taxonomy can help to shed light on past environmental conditions. The maerl and nodular type found mostly belongs to the free-living morphology.

Free living coralline encrust unstable substrate such as other corallines, cobbles and small biogenic material or live unattached as individual branches. They live in environments with reduced sedimentation, moderate wave action and currents (Adey & McKibbin 1970; Adey & Spearapani 1971; Bosellini 1971; Adey 1973; Doty 1959; Littler 1972; Littler 1973; South & Hooper 1980; Birkett et al. 1998 Basso et al. 2007). They rely on periodically overturning from either water flow or organisms. Without this periodically disturbances they may not prevail being overgrown by more competitive species (Adey 1970; Bosellini 1971; Adey 1973; Bosence 1976). Anthropogenic pollution and exploitation is reported to have harmful effects on calcareous algae (Björk et al. 1995, Hall-Spencer & Moore 2000, Grall & Hall-Spencer 2003, Wilson et al. 2004). Industrialization and intensification of fisheries including bottom trawling and dredging (DeGroot 1984; Thrush & Dayton 2002) could be one possible explanation for the sudden decline in abundance towards the 4-6cm layer (Fig. 28). Burial with fine sediment that can be caused by resuspension due to dredging leads to detrimental effects. This

effect rather occurs due to the physio-chemical properties of the sediment and increase of hydrogen sulphide than the lack of light (Chapman and Fletcher 2002, Wilson et al. 2004). The same applies to sewage outfalls and eutrophication being particularly harmful due to smothering and increased oxygen demand (Grall & Hall-Spencer 2003, Wilson et al. 2004). Only a few studies investigating heavy metal pollution have been carried out so far. Wilson (2004) reported that even low concentrations of heavy metal harm the algae probably even stronger if pollution is cronical rather than a single event.

The total amount of Corallinaceae found at the uppermost layer (0-2cm) is again higher compared to the of 4-6cm layer. This pattern can also be seen at other taxa like Bryozoa, Bivalvia and at a more moderate form at Polychaeta and Gastropoda (Fig 8). According to AAR dating 4-6 cm sediment depth would correspond to an age placed sometime near the year 1907 and the uppermost part close to the year 2000 (Fig 2B). This increase in hard-part remains towards the top could be interpreted as a partial recovery on the benthic community due to the establishment of the Brijuni National park in the year 1983 (Bralic 1990). At similar study focusing solely on molluscs however, such a recovery at the uppermost part was not observed (Schnedl 2014).

A general increase in pollutants and nutrients toward the top of the core has been found originating at the shallower sediment layers at least to a certain degree form anthropogenic sources (Pempkowiak et al. 1999; Wang et al. 2007; Duysak & Ersoy 2014). Especially the heavy metals mercury, lead and organic pollutants (PCB, PAH) display distinctive peaks at relatively young sediment layers strongly emphasising anthropogenic origin (Fig. 4 & Fig. 5A).

Community changes of major taxonomic groups show a significant relation to concentration of mercury and lead in the sediment (Tab. 3). This holds also true for shifts in composition within the taxonomic groups of crustaceans and bivalves (Tab. 26, Tab.30 & Tab.35). Changes within gastropods estimated from weight was also significant to changes on lead concentration, but mercury was only marginally significant to (p=0.062) for count data (Tab.40 & Tab. 45). These findings are supported by the study of Schnedl (2014) which reported negative effects of mercury and lead on molluscan species richness at a close by sampling station. Significant correlations between this two heavy metals and bryozoan diversity of respective layers, could also been shown (Tab. 12B). Mercury concentrations exceeded threshold-values proposed by National Oceanic and Atmospheric Administration (NOAA) for screening of marine sediment in the uppermost 10 cm of the core, whereas lead did not.

Cadmium and arsenic also surpass these specified values, however having their highest values

in the lower and middle part of the core (Fig. 4). This makes human activity as primary source highly unlikely. Neither was found to have an effect on observed taxonomical shifts (Tab. 3).

Zinc and manganese display a roughly similar pattern to mercury and lead having peaks in the upper part of the core, but starting at already high values at 105cm depth (Fig.4). Zinc and manganese concentration correlate with shifts in a community composition on higher taxonomic level but also changes within the Bivalvia (Tab 3, Tab. 30 & Tab. 35). In addition, changes in zinc concentration was related to changes in bryozoa diversity and gastropods (Tab.13B, Tab. 40 & Tab 45). A similar study at the vicinity of Piran focusing on molluscs, reported zinc and the heavy metals iron and mercury to be negatively correlated with species richness (Mautner 2014). Iron was the only heavy metal displaying a continuous decrease towards the top. A relation to changes within bryozoans and the total assemblage was found (Tab. 3 & Tab. 8)

Organic pollutants displaying similar concentration patterns like mercury and lead are therefore also significantly related to community shifts in total assemblage, within crustaceans, bivalves, gastropods, diversity and rarefied species richness of bryozoans (Tab. 4, Tab.13, Tab. 24, Tab.31, Tab.36, Tab. 41 & Tab. 46). The strong peak of PAH, which can have both anthropogenic and natural origin suggest an elevation due to urbanization and industrialisation (Bojes & Pope 2007; Hylland 2007; Neff 1979; Zeng & Vista 1997). PCB, which can only originate from anthropogenic sources (Creaser et al. 2007) was found in older sediment layers than its time of origin. This indicates penetration of this organic pollutant into deeper sediment layers after accumulation within the sediment, probably due to downward mixing because of bioturbation(Fig 5A).

Collinearity of pollutants concentration along the core makes it difficult to differentiate between the influence of respective pollutant on benthic communities. The overall community shifts in the upper part of the core and the general increase of contaminants in the more recent layers may be interpreted as community changes as response to increased anthropogenic discharge of pollutants. However only mercury exceeds threshold-values proposed by NOAA.

The steady increase of total Carbon in the sediment (Ctot) correlates with changes in the total assemblage and bryozoan species (Fig 5B & Tab. 6). TOC and Ntot, which in addition display a pronounced increase within the upper 30 cm, correlate to changes within crustaceans, bivalves and gastropods (Fig.5, Tab. 27, Tab. 32, Tab. 37, Tab. 42 & Tab. 47). This part of the core

corresponds to the timespan from about 2000 years to present day (Fig. 2). High levels of nutrients make an ecosystem sensible to hypoxic and anoxic events. Prolonged oxygen depletion can severely impact benthic communities triggering mass mortalities of macroepifaunal organisms (Haselmair et al. 2010; Jackson et al. 2001; Riedel et al. 2008, Riedel et al. 2012). Benthic mortalities caused by eutrophication have occurred in the Northern Adriatic periodically and became more frequent since the year 1969 (Crema et al. 1991; Barmawidjaja et al. 1995; Degobbis et al. 2000; N'siala et al. 2008; Nerlović et al. 2011).

Observed compositional changes can also be influenced by the sediments properties. Relation of taxonomic shifts and composition of clay, silt and sand showed significant correlations in all analysed taxa, however results from weight and count data differed (Tab. 16, Tab. 20, Tab. 33, Tab. 38, Tab. 43 & Tab. 48). Correlation of grainsize distribution and compositional changes can to some degree also be influenced by concentration of pollutants and nutrient in the sediment and vice versa. Heavy metal concentration and the content of fine particles in the sediment have been reported to show strong correlation (Zonta et al. 1994).

Data of bryozoan hard part remains differed the most between the count and weight approach. *Cellaria salicornioides* was clearly the most dominant species in terms of numbers (Fig. 11). This is not the case for estimates based on weight. *Myriapora truncata* a more robustly built species makes up the highest total weight of all species found in the core and the slope of the species rank abundance curve is not as steep compared to count data (Fig. 15). Analysis of different growth-types could show a significant difference in the average weight of bryozoan fragments (Fig 13). *C. salicornioides* is an erect diffuse and delicate branching species typical for the cellariform growth-type and therefore prone to break into many small lightweight fragments. Estimating abundance only from count data, therefore most likely leads to an overestimation of the abundance of delicate branching species and an underestimation of robust growth forms. Data assessment based solely on weight data, on the other hand leads to an overestimate of species of rather robust growth forms.

The cellariform growth-type makes up more than 30 % in the upper part of the core based on count data (Fig. 11B). Cellariform species commonly live in moderate depth on solid and loose substrate with low to moderate currents (Stach 1936; Stach 1937; Gautier 1962; Lagaaij & Gautier 1965; Labracherie and Prud'homme 1966; Schopf 1969; Caulet 1972; Harmelin 1988; McKinney & Jackson 1989; Nelson et al. 1988; Smith 1995). Compared to other bryozoan growth-types it can withstand relatively high sedimentation rates (Lagaaij & Gautier 1965; Schopf 1969; Reguant et al. 1985). At the lower part of the core abundances of cellariform

bryozoa stay well below 10% and are replaced by membraniporiforms as the most dominate growth-type (Fig. 11C). Species belonging to this group are adapted to littoral and sublittoral zones (Stach 1936). Therefore, they are rather found in places with higher water energy attached to solid or to some extend on flexible substratum (Stach 1936; Stach 1937; Gautier 1962; Lagaaij & Gautier 1965; Labracherie and Prud'homme 1966; Schopf 1969; Caulet 1972; Harmelin 1988; McKinney & Jackson 1989; Nelson et al. 1988; Smith 1995). The lower part is characterized by encrusting species shifting to more erect species towards the top (Fig. 11). Although no significant difference between the average weight of erect and encrusting species was found, this change is not visible from weight data (Fig. 15). The high proportion of eschariiform species undermines the dominance of encrusting species. This growth-type is adapted to sublittoral zones (Zahra et al. 2004). This would contradict other finding suggesting a shallow environment with strong terrestrial influence. However, fragments found in the samples exclusively belong to the one species, *Pentapora fascialis* (see species list appendix). This species was found by Novosel et al. (2004) as shallow as 1m depth at a submarine freshwater spring, being able to tolerate even brackish conditions.

Bryozoan diversity increased from 105cm sediment-depth towards the layer of 40-45 cm and declines again from that point onward to the top. This pattern is visible from both approaches, count and weight data. Weight data values, however fluctuate stronger along the core (Fig. 12B & Fig. 16). This may be explained by larger fragments, resulting in a high dominance of certain species in terms of weight. Species richness stays relatively constant throughout the core with two exceptions. One is the high number of species at the macroid layer (50-55cm), the other the low species richness at the 2-4 cm layer (Fig. 12 A). The latter may be interpreted as the previously described anthropogenic impact before the establishment of the Brijuni Nationalpark.

Cluster analysis of molluscan shell remains display distinctive clusters along the core for both gastropods and bivalves (Fig. 19, Fig. 21, Fig 23, Fig. 25). Ecological groups, however, differ only little between individual clusters (Fig. 20, Fig. 22, Fig. 24, Fig 26). The reason for that could be the identification to family level only, as Schnedel (2014) could show major changes along the core for species level data. Bivalves are dominated by venerids throughout the core (Fig. 20). Only in terms of total weight a change to a higher proportion of infaunal species at the upper part is observable, hinting to changes in size of individuals, rather than changes in numbers. Most striking is the strong dissimilarity of layer 4-6 cm and the remaining layers of bivalve samples (Fig. 21 & Fig 23). This layer represents a period when anthropogenic pressure

is suggested to be at a maximum before the declaration of this region as a protected area (Bralic 1990) (Fig. 2B). This may be also the case for dissimilarity analysis based on gastropod hard part remains as the upper 6cm differ in a similar manner from the other samples (Fig. 23 & Fig. 25). Occurrences of terrestrial and limnic snails at the lower part of the core again suggest string terrestrial influence. Only occasionally found limnic gastropods in the upper layers suggest that these shells have been transported there from the Brijuni islands, or were brought up to younger layers by reworking (Fig. 24 & Fig. 26).

Crustacean occurrence is almost entirely restricted to the lower half of the core, being practically absent from the upper 6cm. Hard part remains found belong for the most part to the species *Upogebia cf. deltaura* (Fig. 17). Compared to other species of the genus *Upogebia* this species is associated with coarser sediment like shell-sands, gravel and maerl beds (Gustavson 1934; Samuelsen 1974; Tunberg 1986; Swift 1993; Astall et al. 1997; Hughes & Atkinson 1997). Association to coarser grade muddy gravel results in a general occurrence of *Upogebia deltaura* in shallower habitats compared to species of the same genus (Hall-Spencer & Atkinson 1999). This mud shrimp can build burrows reaching up to 65cm into the sediment (Tunberg 1986). The high occurrence of *U. deltaura* in the lower parts and it strong burrowing activity, could be one reason for the broader range of age groups in this section probably caused by increased reworking in these layers (Fig. 2B). It should be considered that burrow-dwelling lifestyle can also lead to a displacement of hard part remains into deeper section of the core. The echinoid *Echinocyamus pusillus* has a similar distribution along the core (Fig. 27) as *U. deltaura* and meets the same requirements to its habitat. It is found most frequently at depth of 10-20m and is adapted to for nestling in the intestine of shelly-gravel (Nichols 1959; Malcom et al. 1983). Distribution of *U. deltaura* and *E. pusillus* strengthen the argument for the lower part of the core to have been a shallow water environment.

CONCLUSION

The down-core record of bryozoan, crustacean and molluscan hard parts reflects multiple ecological shifts. A transition from terrestrial to marine conditions at the bottom of the core as a signal of the Holocene transgression. The lower 30 cm of the core is characterized by coarse sediment, strong reworking and taxa adapted to moderate to high energy environments. These findings suggest shallow water conditions. A conspicuous peak of macroids occurrence, bryozoan species richness around 50-60 cm core depth hints to the development of secondary hard-bottom like state at 3000-5000 years BP, after rapid rise in sea-level had already stagnated and present time water depth was almost reached. At the younger part of the core a marked decrease

in total weight in the uppermost 20 cm, associated with a shift in community composition, possibly attributable to anthropogenic impact was observed.

ACKNOWLEDGMENTS

REFERENCES

Adey W.H. (1970). Some relationships between crustose corallines and their substrate. Sci. Island Anniv. 2:21-25

Adey W.H. (1973). Temperature control of reproductivity and productivity in a subarctic coralline alga. *Phycologia* 12:111-18

Adey W.H. & McKibbin D.L. (1970). Studies on the maerl species Phymatolithon calcareum (Pallas) nov. comb. and Lithothamnium coralloides Crouan in the Ria de Vigo. Bot. Mar. 12:100-6

Adey W.H. & Spearapani C. P. (1971). The biology of Kvaleya a new parasitic genus and species of Corallinaceae. Phycologia 10:29-42

Allen A.P., Kosnik A.M., Kosnik M.A. & Kaufman S.D. (2013). Characterizing the dynamics of amino acid racemization using time-dependent reaction kinetics: A Bayesian approach to fitting age-calibration models. *Quaternary Geochronology* 18: 63-77.

Alvarez Z. R. (1968). Crustáceos Decápodos Ibéricos. *Inv. Pesq* 32: 510.

Antonioli F., Anzidei M., Lambeck K., Auriemma R., Gaddi D, Furlani S., Orru P., Solinas E., Gaspari A, Karinja A., Kovacic V. & Surace L. (2007) Sea-level change during the Holocene in Sardinia and in the northeastern Adriatic (central Mediterranean Sea) from archaeological and geomorphological data. *Quaternary Science Reviews* 26 2463–2486.

Appleby P. & Oldfield F. (1978). The calculation of dates assuming a constant rate of supply of unsupported 210Pb to the sediment. CATENA, 5, 1–8.

Astall C.M., Taylor A.C. & Atkinson R.J.A. (1997). Behavioural and physiological implications of a burrow-dwelling lifestyle for two species of upogebiid mud-shrimp (Crustacea: Thalassinidea). *Estuarine, Coastal and Shelf Science,* 44,155^168.

Bada L.J. (1985). Amino acid racemization dating of fossil bones, University of California *Earth Planet. Sci.* 13: 241 8

Barmawidjaja D.M., van der Zwaan G.J., Jorissen F.J., & Puskaric S. (1995). 150 years of eutrophication in the northern Adriatic Sea: Evidence from a benthic foraminiferal record. *Marine Geology*, *122*(4), 367–384. doi:10.1016/0025-3227(94)00121-Z

Basso D., Nalin R., Padova, & Massari F., (2007). Genesis and composition of the Pleistocene *Coralligène de plateau* of the Cutro Terrace, Geol. Paläont. Abh. 244/2 173 – 182

Beesley P.L., Ross G.J., & Wells A. (Eds.). (1998). *Mollusca: The Southern Synthesis. Fauna of Australia, volume 5.* Melbourne: CISRO Publishing.

Begon M., Harper J.L. & Townsend C. R. (1986) Individuals, populations and communities. *Ecology*. – 854 pp.,

Oxford (Blackwell Scientific Publications).

Bellan-Santini, D., Lacaze, J.-C. & Poizat, C. (1994). Les biocénoses marines et littorales de Méditerranée, synthèse, menaces et perspectives. 246 pp., Paris (Muséum National d'Histoire Naturelle).

Birkett, D.A., Maggs, C., Dring, M.J., 1998. Maerl, vol. V. An overview of dynamic and sensitivity characteristics for conservation and management of marine SACs. *Scottish Association for Marine Science*. (UK Marine SACs Project), 116 pp.

Birks HJB. 1996. Contributions of Quaternary palaeoecology to nature conservation. *J. Veg. Sci*. 7:89–98

Björk M., Mohammed M.S., Björklund M. & Semesi A. (1995). Coralline Algae, Important Coral-Reef Builders Threatened by Pollution. *Research and Capacity Building for Sustainable Coastal Management*. 24, No. 7/8: 502-505.

Bojes H.K., & Pope P.G. (2007). Characterization of EPA's 16 priority pollutant polycyclic aromatic hydrocarbons (PAHs) in tank bottom solids and associated contaminated soils at oil exploration and production sites in Texas. *Regulatory Toxicology and Pharmacology : RTP*, *47*(3), 288–95. doi:10.1016/j.yrtph.2006.11.007

Bone Y., James N.P., (1993). Bryozoans as carbonate sediment producers on the cool-water Lacepede Shelf, Southern Australia. *Sediment. Geol*. 85, 247–271.

Bordeaux Y.L. & Brett C.E. (1990) Substrate specific associations of epibionts on Middle Devonian brachiopods: implications for paleoecology. *Historical Biology* 4, 203-220.

Borja A., Franco J., & Perez V. (2000). A Marine Biotic Index to Establish the Ecological Quality of Soft-Bottom Benthos Within European Estuarine and Coastal Environments. *Marine Pollution Bulletin*, *40*(12).

Bosch D.T., Dance S.P., Moolenbeek R.G., & Oliver P.G. (1995). *Seashells of Eastern Arabia*. (S.P. Dance, Ed.). Motivate Publishing.

Bosellini A., Ginsburg R.M. (1971). Form and internal structure of recent algal nodules (rhodolites) from Bermuda. J. Geol. 79:669-82

Bosence D.W.J. (1976). Ecological studies on two unattached coralline algae from western Ireland. *Palaeontology* 19:365-95

Burton Jr. G.A. (2002). Sediment quality criteria in use around the world. *Limnology*, *3*(2), 65–76. doi:10.1007/s102010200008

Bralic I. (1990). *Nacionalni parkovi Hrvatske, Nacionalni park Brijuni (The National Parks of Croatia, The National Park of Brioni Islands)* (pp. 103–117). Zagreb: Skolska knjiga.

Buljan M. & Zore-Armanda M. (1976) Oceanographic properties of the Adriatic Sea. *Oceanography and Marine Biology Annual Review* 14: 11-98

Caulet M.J. (1972). Les sediments organogenes du precontinent algerien. Mem. Mus. Natl. Hist. Nat., Paris, 25, 289 pp.

Chapman A.S., Fletcher R.L., (2002). Differential effects of sediments on survival and growth of Fucus serratus embryos (Fucales, Phaeophyceae). Journal of Phycology 38, 894–903.

Corriero G. & Pronzato R. (1987) Epibiontic sponges on the bivalve *Pinna nobilis*. *Marine Ecology Progress Series* 35, 75-82.

CPW (Conserv. Paleobiol. Worksh.). 2012. *Conservation Paleobiology: Opportunities for the Earth Sciences. Report to the Division of Earth Sciences, National Science Foundation*. Ithaca, NY: Paleontol. Res. Inst.

Creaser C.S., Wood M.D., Alcock R., Copplestone D., Crook P.J., (2007). UK Soil and Herbage Pollutant Survey: UKSHS Report No. 8 Environmental Concentrations of Polychlorinated Biphenyls (PCBs) in UK Soil and Herbage. Environment Agency, Bristol England.

Crema R., Castelli A., & Prevedelli D. (1991). Long Term Eutrophication Effects on Macrofaunal Communities in Northern Adriatic Sea. *Marine Pollution Bulletin*, *22*(10), 503–508.

Cossignani T., Cossignani V., Di Nisio A., & Passamonti M. (1992). *Atlante delle conchiglie del Medio Adriatico (Atlas of shells from the Central Adriatic Sea)*. Piceno, Ancona: L'informatore.

Costello M.J., Emblow C.S. & White R. (2001). European Register of Marine Species. A check-list of the marine species in Europe and a bibliography of guides to their identification. *Patrimoines naturels*. 50: 243 p.

Davies A.G. (1978). Pollution studies with marine plankton; Part II. Heavy metals. Advances in Marine Biology 15, 381–508.

Degobbis D., Precali R., Ivancic I., Smodlaka N., Fuks D. & Kveder S. (2000). Long-term changes in the northern Adriatic ecosystem related to anthropogenic eutrophication. *International Jaouranal of Environment and Pollution* 13: 495-533.

DeGroot S.J. (1984). The impact of bottom trawling on benthic fauna of the North Sea. *Ocean Management*, 9, 177–190.

Delcourt PA, Delcourt HR. 1998. Paleoecological insights on conservation of biodiversity: a focus on species, ecosystems, and landscapes. *Ecol. Appl.* 8:921–34

Demarchi B. & Collins M. (2014) Amino Acid Racemization Dating. *Encyclopedia of Scientific Dating Methods* 13-26

DeSouza V.L.B., Rodrigues K.R.G., Pedroza E.H., Melo R.T., De Lima V.L. De, Hazin C. a., Nascimento R.K. Do. (2012). Sedimentation Rate and 210Pb Sediment Dating at Apipucos Reservoir, Recife, Brazil. *Sustainability*, *4*(12), 2419–2429. doi:10.3390/su4102419

Dietl P.G., Kidwell M.S., Brenner M, Burney A.D., Flessa W.K., Jackson S.T. & Koch L.P. (2015) Conservation paleobiology: Leaving Knowledge of the past to Inform Conservation and Restoration. *Annual Review of Earth and Planetary Science* 43:79-103

Dietl P.G., & Flessa K. (2011). Conservation paleobiology: putting the dead to work. *Trends in Ecology & Evolution*, *26*(1), 30–37. doi:10.1016/j.tree.2010.09.010

Dietl GP. 2009. Paleobiology and the conservation of the evolving web of life. See Dietl & Flessa 2009, pp. 221–44

Doty M. (1959). An enumeration of the hypothetical roles of algae in coral atolls. 8th *Pac. Sci. Cong.*, Manila. 923-8

Duysak Ö., & Ersoy B. (2014). A Biomonitoring Study: Heavy Metals in Monodonta turbinata (Mollusca: Gastropoda) From Iskenderun Bay, North-Eastern Mediterranean. *Pakistan J. Zool.*, *46*(5), 1317–1322.

Falace A., Kaleb S., Orlando-Bonaca M., Marvic B. & Lioej L. (2011) First contribution to the knowledge of coralline algae distribution in the Slovenian circalittoral zone (Northern Adriatic) ANNALES Ser. Hist. nat. 21

Fatovic-Ferencic. (2006). Brijuni Archipelago: Story of Kupelwieser, Koch , and Cultivation of 14 Islands. *Croatian Media Journal*, *47*, 369–371.

Flessa KW. 2002. Conservation paleobiology. *Am. Paleontol.* 10:2–5

Forester A.J. (1979) The association between the sponge *Halichondria panicea* (Pallas) and scallop *Chlamys varia* (L.) a commensal-protective mutualism. *Journal* of *Experimental Marine Biology and Ecology* 36, 1-10.

Foster M.S. (2001). Rhodoliths: Between rocks and soft places – Minireview. *Journal of Phycology* 37, 659–667.

Froyd CA, Willis KJ. 2008. Emerging issues in biodiversity and conservation management: the need for a palaeoecological perspective. *Quat. Sci. Rev.* 27:1723–32

Gautier Y.V., (1962). Recherches ecologiques sur les Bryozoaires Cheilostomes en Mediterranee occidentale. Rec. Trav. Sta. Mar. Endoume, 24 (38), 434 pp.

Garassion A. & De Angeli A. (2004a). Pantherope angulifrons Latereile, 1825, and Atelecyclus rotundatus (Olivi, 1782) from the Sicilian (upper Pleistocene) of Favignana Island (Egadi Islands, Sicily, S Italy), *Atti soc. it. Sci. nat. Museo civ. Stor. nat.* Milano, 145 (I): 19-28

Garassion A. & De Angeli A. (2004b), Decapoda crustacea fauna from the Pliocene and Pleistocene of Adra, Stirone and Enza River (Piacenza, Parma and Regio Emilia Province, N Italy), Atti soc. it. Sci. nat. Museo civ. Stor. nat. Milano, 145 (I): 29-57

GESAMP (1990). Joint Group of Experts on the Scientific Aspect of Marine Pollution: The State of the Marine

Environment UNEP Regional Seas Report and Studies No. 115, UNEP.

Gillson L, Ekblom A, Willis KJ, Froyd C. 2008. Holocene palaeo-invasions: the link between pattern, process and scale in invasion ecology? *Landsc. Ecol.* 23:757–69

Gillson L, Marchant R. 2014. From myopia to clarity: sharpening the focus of ecosystem management through the lens of palaeoecology. *Trends Ecol. Evol.* 29:317–25

Gofas S., Moreno D., & Salas C. (2011a). *Moluscos marinos de Andalucia, volume 1*. Malaga: Servicio de Publicaciones e initercambio Cientifico, Universidad de Malaga.

Gofas S., Moreno D., & Salas C. (2011b). *Moluscos marinos de Andalucia, volume 2*. Malaga: Servicio de Publicaciones e initercambio Cientifico, Universidad de Malaga.

Goff J.A., Jenkins C., & Calder B. (2006) Maximum a posteriori resampling of noisy, spatially correlated data: Geochemistry, Geophysics, Geosystems, v. 7, doi: 10.1029/2006GC001297.

Gorham E, Brush GS, Graumlich LJ, Rosenzweig ML, Johnson AH. 2001. The value of palaeoecology as an aid to monitoring ecosystems and landscapes, chiefly with references to North America. *Environ. Rev.* 9:99–126

Grall J. & Hall-Spencer J.M. (2003). Problems facing maerl conservation in Brittany. *Aquatic Conservation: Marine and Freshwater Ecosystems* 13, 55–S64.

Grotzinger J., Siever R., Jordan T. H., & Press F. (2008). *Press/Siever - Allgemeine Geologie* (5th ed.). Berlin: Spektrum Akademischer Verl.

Gustavson G. (1934). On the Thalassinidea of the Swedish west coast. *Arkiv för Zoologi*, 28, 1-19.

Hall-Spencer J.M. & Moore P.G. (2000). Scallop dredging has profound, long-term impacts on maerl habitats. *Journal of Marine Science* 57, 1407–1415.

Harding L.W., Debobbis Jr. D., & Precali R. (1999). Production and fate of phytoplankton: Annual cycels and interannual variability. In Malone T.C., Malej A., Harding Jr. L.W., Smodlaka N., & R.E. Turner, eds., Ecosystems at the Land-Sea Margin, 131-172. Washington: American Geophysical Union.

Harmelin J.-G. (1988). Les Bryozoaires, de bons indicateurs bathymetriques en paleoecologie? Geol. Mediterr. 15 (1), 49– 63.

Hrs-Brenko M. (2006). The basket shell, *Corbula gibba* Olivi, 1792 (Bivalve Mollusks) as a species resistant to environmental disturbances : A review. *Acta Adriatica*, *47*(1), 49–64.

Harvey A.S. & Woelkerling W.J (2007). A guide to nongeniculate coralline red algal (Corallinales, Rhodophyta) rhodolith identification, *Ciencias Marinas* 33(4): 411-426

Haselmair A, Stachowitsch M., Zuschin M. & Riedel B. (2010). Behaviour and mortality of benthic crustaceans

in response to experimentally induced hypoxia and anoxia in situ. *Marine Ecology Progress Series*, *414*, 195–208. doi:10.3354/meps08657

Hayward J.P. & McKinney F.K. (2002) Northern Adriatic Bryozoa from the vicinity of Rovinj, Croatia, *Bulletin of the American museum of natural history* No 270, 139.

Hayward J.P. & Ryland J.S. (1998) Synopsis of the British fauna, Cheilostomatous Bryozoa Part I   Aeteoidea – Cribilinoidea, No. 10 (Second edition). The Linnean Society of London.

Hayward J. P. & Ryland J. S. (1999) Synopsis of the British fauna, Cheilostomatous Bryozoa Part II   Hippothooidea – Celleporoidea, No. 14 (Second edition). The Linnean Society of London.

Huber, M. (2010). *Compendium of Bivalves*. ConchBook.

Hughes D.J. & Atkinson R.J.A. (1997). A towed video survey of megafaunal bioturbation in the north-eastern Irish Sea. Journal of the Marine Biological Association of the United Kingdom, 77, 635^653.

Hurst J.M. (1974) Selective epizoan encrustation of some Silurian brachiopods from Gotland. *Palaeontology 17*, 423-429.

Hylland K. (2007). Polycyclic Aromatic Hydrocarbon (PAH) Ecotoxicology in Marine Ecosystems *Journal of Toxicology and Environmental Health*, Volume 69: 109-123.

Islam Md. S. & Tanaka M. (2004) Impacts of pollution on coastal and marine ecosystems including coastal and marine fisheries and approach for management: a review and synthesis *Marine Pollution Bulletin* 48 624–649

Jackson J.B., Kirby M.X., Berger W.H., Bjorndal K.A., Botsford L.W., Bourque B. J., Warner R. R. (2001). Historical overfishing and the recent collapse of coastal ecosystems. *Science (New York, N.Y.)*, *293*(5530), 629–37. doi:10.1126/science.1059199

Jackson ST, Hobbs RJ. 2009. Ecological restoration in the light of ecological history. *Science* 325:567–69

Jones K.C. & De Voogt P. (1999). Persistent organic pollutants (POPs): state of the science. *Environmental Pollution*. Volume 100, 1–3: 209–221

Keegan B.F. (1974). The macrofauna of maerl substrates on the west coast of Ireland. *Cahiers de Biologie Marine* 15, 513–530.

Kidwell, S.M. & Jablonski, D. 1983: Taphonomic feedback. Ecolo- gical consequences of shell accumulation. *In* Tevesz, M.J.S. & McCall, P.L. (eds.): *Biotic Interactions in Recent and Fossil Benthic Communities,* 195-248. Plenum Press, New York.

Kosnik M.A. & Kaufman S.D. (2008). Identifying outliers and assessing the accuracy of amino acid racemization measurements for geochronology: I. Age calibration curves. Quaternary Geochronology 3: 308-327.

Koulouri P., Dounas C., Arvanitidis C., Koutsoubas D., & Eleftheriou A. (2006). Molluscan diversity along a Mediterranean soft bottom sublittoral ecotone. *Scientia Marina*, *70*(December), 573–583.

Kovačević Z. (2002). History and political ecology of the Adriatic Sea. Religion, Science and the Environment: Adriatic Sea Symposium, (pp. 8 pp.). http://www.rsesymposia.org/themedia/ File/1151678043-Kovacevic.pdf.

McKinney F. K. (2007). The Northern Adriatic Ecosystem: Deep Time in a Shallow Sea. (p. 299). New York: Columbia University Press.

Laborel J. (1961). Le concrétionnement algal "coralligène" et son importance geomorphologique en Méditerranée. – Recueil des traveaux de la Station marine, Endoume, 23: 37-60.

Laborel J. (1987). Marine biogenic constructions in the Mediterranean, A review. Scientific Reports of the Port-Cros national Park, 13: 97-126.

Labracherie M. & Prud'homme J., (1966). Essai d'interpretation de paleomilieux grace a`la methode de distribution des formes zoariales chez les Bryozoaires. *Bull. Soc. Geol.* Fr. 8, 102– 106.

Lagaaij R. & Gautier Y.V. (1965). Bryozoan assemblages from marine sediments of the Rhone delta, France. *Micropaleontology* 11 (1), 39–58.

Lee D.E., Scholz J. & Gordon D.P. (1997) Paleoecology of a late Eocene mobile rockground biota from North Otago, New Zealand. *Palaios 12,* 568-581.

Lescinsky H.L. (1993) Taphonomy and Paleoecology of Epibionts on the Scallops *Chlarnys hastata* (Sowerby 1843) and *Chlamys rubida* (Hinds 1845). *Palaios 8,* 267-277.

Littler M.M. (1972). The crustose Corallinaceae. Ann. Rev. Oceanog. Mar. Biol. 10:311-47

Littler M.M. (1973). The population and community structure of Hawaiian fringing reef crustose Corallinaceae (Rhodophyta, Cryptonemiales). J. Exp. Mar. Biol. Ecol. 11:103-20

Longwell, A.C., Chang, S., Hebert, A., Hughes, J.B., Perry, D., 1992. Pollution and developmental abnormalities of Atlantic fisheries. Environmental Biology of Fishes 35 (1), 1–21.

Lotze H. K., Lenihan H. S., Bourque B. J., Bradbury R. H., Cooke R. G., Kay M. C. & Bay M. (2006). Depletion, Degradation, and Recovery Potential of Estuaries and Coastal Seas. *Science*, *312*(June), 1806–1809.

Louys J. ed. 2012. *Paleontology in Ecology and Conservation*. Berlin: Springer-Verlag

Lyman RL. (2012). Biodiversity, paleozoology, and conservation biology. See Louys 2012, pp. 147–69 Lyman RL. 2012b. A warrant for applied palaeozoology. *Biol. Rev.* 87:513–25

Malcom T., Harold A.S. & Mooi R. (1983). Feeding structures, behaviour and microhabitat of Echinocyamus pusillus (Echinoidea: Clypeastroidea). *Biol. Bull.* 165.:745-757.

Mautner A.K. (2014). Long-term environmental shifts as deduced from molluscan death assemblages in a sediment core (northern Adriatic Sea, Piran) Masterthesis, University of Vienna.

McKinney F.K. & Jackson J.B.C. (1989). Bryozoan Evolution. *Special Topics in Paleontology*, Hyman, Boston, 238 pp.

McKinney F.K. (2003) Preservation potential and paleoecological significance of epibenthic suspension feeder-dominated benthic communities (northern Adriatic Sea): PALAIOS, v. 18, p. 47–62.

McKinney F.K., (2007) The Northern Adriatic Ecosystem: Deep Time in a Shallow Sea: Columbia University Press, New York, p. 299.

McKinney F.K. & Hageman S.J. (2006) Paleozoic to modern marine ecological shift displayed in the northern Adriatic Sea: Geology, v. 34, p. 881–884.

McKinney F.K., Hageman S.J., & Jaklin A., (2007) Crossing the ecological divide: Paleozoic to modern marine ecosystem in the Adriatic Sea: Sedimentary Record, v. 5, p. 4–8.

Michael W.R. & Piller W.E. (2000) Designation of *Phymatolithon* (Corallinaceae, Rhodophyta) in Fossil Material and Its Paleoclimatological Indications *Micropaleontology* Vol. 46, No. 1 89-95

Nebelsick J.H., Schmid B. & Stachowitsch M. (1997) The encrustation of fossil and recent sea-urchin tests: eco-logical and taphonomic significance. *Lethaia 30,* 271-284.

Neff J.M. (1979). *Polycyclic aromatic hydrocarbons in the aquatic environment. Sources, fates and biological effects*, Barking, Essex, England: Applied Sciences.

Nelson C.S., Hyden F.M., Keane, S.L., Leask, W.L. & Gordon D.P., (1988). Application of bryozoan zoarial growth-form stud- ies in facies analysis of non-tropical carbonate deposits in New Zealand. *Sediment. Geol.* 60, 301–322.

Nerlović V., Doğan A., & Hrs-Brenko M. (2011). Response to oxygen deficiency (depletion): Bivalve assemblages as an indicator of ecosystem instability in the northern Adriatic Sea. *Biologia*, *66*(6), 1114–1126. doi:10.2478/s11756-011-0121-3

Nichols D. (1959). The histology and activities of the tube-feet of Echinocyamus pusillus. Q. J. *Microsc. Sci. 100: 539-555.*

Novosel M., Olujic G, Cocito S. & Pozar-Domac A. (2004) Submarine freshwater springs: a unique habitat for the bryozoan *Pentapora fascialis*. in Cancino M. & Jackson W. (eds) Bryozoan Studies 2004. Thirteenth International Bryolozoology Association Conference.

NRC (Natl. Res. Counc.). 2005. *The Geological Record of Ecological Dynamics: Understanding the Biotic Effects of Future Environmental Change*. Washington, DC: Natl. Acad. Press

Odum E.P. (1971): Fundamentals of ecology. – 574 pp., Philadelphia (W. B. Saunders Co)

Oschmann, W. 1990: Dropstones - Rocky mini-islands in high- latitude pelagic soft substrate environments. *Senckenbergiana maritima 21*, 55-75.

Ott J. (1992). The Adriatic benthos: Problems and perspectives. In G. Colombo, I. Ferrari, V. U. Ceccherelli, & R. Rossi (Eds.), *Marine Eutrophication and Population Dynamics. 25th EMBS* (pp. 367–378). Fredensborg, Denmark: Olsen&Olsen.

Paine R.T., Suchanek T.H. (1983). Convergence of ecological processes between independently evolved competitive dominants: A tunicate-mussel comparison. *Evolution* 37:821-31

Pempkowiak J., Sikora A., & Biernacka E. (1999). Speciation of Heavy Metals in Marine Sediments vs their Bioaccumulation by Mussels. *Chemosphere*, *39*(2), 313–321.

Pennington W. (1973). The recent sediments of Windermere. Freshwater Biology, 3, 363–382.

Pérès, J. M. (1982). Major benthic assemblages. In: Kinne O. (Ed.)*: Marine Ecology*. John Wiley & Sons Ltd., Chichester, 5 (1): 373-522.

Pérès J.M. & Picard J. (1951) Note sur les fonds coralli- gènes de la région de Marseille. – *Archives de zoologie expérimentale et générale*, **88**: 24-38.

Pessani D., Tirelli T. & Flagella S. (2004) Key for the identification of Mediterranean brachyuran megalopae, *Mediterranean Marine Science* Vol. 5/2, 2004, pp 53-64 Torino, Italy

Peterson, R. C. J.: 1986, 'Population and guild analysis for interpretation of heavy metal pollution in streams', in: Cairns, J. Jr. (ed.) *Community Toxicity Testing*, American Society for Testing and Materials, Philadelphia, Spec Tech Publ. 920, pp. 180–198.

Pigorini B. (1968) Sources and dispersion of recent sediments of the Adriatic Sea: Marine Geology, v. 6, p. 187–229.

Porta M., & Zumeta E. (2002). Persistent Organic Pollutants. *Occup Environ Med*, *59*, 651–652.

Reguant S., Vazquez A., Zamarreno I. & Maluquer P. (1985). Significacion de los briozoos en los sedimentos superficiales de la plataforma continental del Cabo de Gata (Almerıa, Espana). *Acta Geol. Hisp*. 20 (1), 69–80.

Rick TC, Lockwood R. 2013. Integrating paleobiology, archeology, and history to inform biological conservation. *Conserv. Biol*. 27:45–54

Riedel B., Zuschin M., Haselmair A., & Stachowitsch M. (2008). Oxygen depletion under glass: Behavioural responses of benthic macrofauna to induced anoxia in the Northern Adriatic. *Journal of Experimental Marine Biology and Ecology*, *367*(1), 17–27. doi:10.1016/j.jembe.2008.08.007

Riedel B., Zuschin M., & Stachowitsch M. (2012). Tolerance of benthic macrofauna to hypoxia and anoxia in

shallow coastal seas: a realistic scenario. *Marine Ecology Progress Series*, *458*, 39–52. doi:10.3354/meps09724

Rios L. M., Moore C., & Jones P. R. (2007). Persistent organic pollutants carried by synthetic polymers in the ocean environment. *Marine Pollution Bulletin*, *54*(8), 1230–7. doi:10.1016/j.marpolbul.2007.03.022

Robson A.J., Neal C. (1997). A summary of regional water quality for Eastern UK Rivers. The Science of the Total Environment 194/195, 15–37.

Samuelsen T.J. (1974). New records of *Upogebia deltaura* and *U. stellata* (Crustacea, Decapoda) from western Norway. *Sarsia*, 56, 131-134.

Sartoretto S., Verlaque M. & Laborel J. (1996) Age of settlement and accumulation rate of submarine "coralligène" (−10 to −60 m) of the northwestern Mediterranean Sea; relation to Holocene rise in sea level. *Marine Geology* 130, 317-331.

Sayer C.D., Bennion H, Davidson TA, Burgess A, Clarke G, et al. 2012. The application of palaeolimnology to evidence-based lake management and conservation: examples from UK lakes. *Aquatic Conserv. Mar. Freshw. Ecosyst.* 22:165–80

Schnedl S. (2014). Down-core changes in molluscan death assemblages as indicators of millennial-scale environmental shifts (Northern Adriatic Sea, Brijuni Islands). Masterthesis, University of Vienna.

Schopf T.J.M. (1969). Paleoecology of Ectoprocts (bryozoans). J. *Paleontol.* 43 (2), 234–244.

Šoštarić R., & Küster H. (2001). Roman plant remains from Veli Brijun (island of Brioni), Croatia. *Vegetation History and Archaeobotany*, *10*(4), 227–233.

Smith A.M. (1995). Palaeoenvironmental interpretation using bryozoans: a review. In: Bosence, D.W.J., Allison, P.A. (Eds.), Marine Palaeoenvironmental Analysis from Fossils. *Geol. Soc. Spec. Publ.* 83, 231–243.

Smol JP. 2008. *The Pollution of Lakes and Rivers: A Palaeoenvironmental Perspective*. Oxford, UK: Blackwell

Stach L.W., (1936). Correlation of zoarial form with habitat. *J. Geol.* 44, 60–66.

Stach L.W., (1937). The application of the Bryozoa in Caino- zoic stratigraphy. Report of the 23rd Meeting, Australia–New Zealand Association of Advanced Science, 23, 80–83.

Stachowitsch M. (1980) The epibiotic and endolithic species associated with the gastropod shells inhabited by the hermit crabs

Stachowitsch M. (1991). Anoxia in the Northern Adriatic Sea: rapid death, slow recovery. In R. V. Tyson & T. H. Pearson (Eds.), *Modern and ancient Continental Shelf Anoxia* (pp. 119–129). Geological Society Special Publications 58,480 pp.

Steller D.L., Riosmena-Rodriguez R., Foster M.S. & Roberts C.A. (2003). Rhodolith bed diversity in the Gulf of

California: the importance of rhodolith structure and consequences of disturbance. *Aquatic Conservation: Marine and Freshwater Ecosystems* 13, S5–S20.

South G.R., Hooper R.G. (1980). A Catalogue and Atlas of the Benthic Marine Algae of the Island of New Foundland. Memorial Univ. Occasional 116. Stephenson, T. A., Stephenson A. Pap. Biol. 3:1-136

Steneck S.R., (1986). The Ecology of Coralline Algal Crusts: Convergent Patterns and Adaptative Strategies, *Annual Review of Ecology and Systematics*, Vol. 17 273-303

Swetnam TW, Allen CG, Betancourt JL. 1999. Applied historical ecology: using the past to manage for the future. *Ecol. Appl.* 9:1189–206

Swift D.J. (1993). The macrobenthic infauna of Sellafield (northeastern Irish Sea) with special reference to bioturbation. *Journal of the Marine Biological Association of the United Kingdom*, 73, 143^162.

Thrush S. F. & Dayton P. K. (2002). Disturbance of marine benthic habitats by trawl- ing and dredging : implications for Marine Biodiversity. *Annual Review of Ecology and Systematics*. 33, 449–473.

Tudela S. (2004). Ecosystem effects of fishing in the Mediterranean: an analysis of the major threats of fishing gear and practices to biodiversity and marine habitats. Number 74. General fisheries commission for the Mediterranean Sea. Rome.

Tunberg B. (1986). Studies on the population ecology of *Upogebia deltaura* (Leach) (Crustacea, Thalassinidea). Estuarine, Costal and Shelf Science. 22(6): 753-765

Turekian K. & Graustein W. (2003). Natural radionuclide in the atmosphere. Treatise on Geochemistry, 4, 261–279.

Vegas-Vilarrubia T, Rull V, Montoya E, Safont E. 2011. Quaternary palaeoecology and nature conservation: a general review with examples from the neotropics. *Quat. Sci. Rev.* 30:2361–88

Wang Y., Shi J., Wang H., Lin Q., Chen X., & Chen Y. (2007). The influence of soil heavy metals pollution on soil microbial biomass, enzyme activity, and community composition near a copper smelter. *Ecotoxicology and Environmental Safety*, *67*(1), 75–81.

Ward M.A. & Thorpe J.P. (1991) Distribution of encrusting bryozoans and other epifauna on the subtidal bivalve *Chlamys opercrilaris*. *Marine Biology 110*, 253-259.

Weber K., & Zuschin M. (2013). Delta-associated molluscan life and death assemblages in the northern Adriatic Sea: Implications for paleoecology , regional diversity and conservation Author ' s personal copy. *Palaeogeography, Palaeoclimatology, Palaeoecology*, *370*, 77–91.

Williams C. (1996). Combating marine pollution from land-based activities: Australian initiatives. Ocean and Coastal Management 33 (1-3), 87–112.

Willis KJ, Bailey RM, Bhagwat SA, Birks HJB. 2010a. Biodiversity baselines, thresholds and resilience: testing predictions and assumptions using palaeoecological data. *Trends Ecol. Evol.* 25:583–91

Willis KJ, Bennett KD, Bhagwat SA, Birks JB. 2010b. 4°C and beyond: What did this mean for biodiversity in the past? *Syst. Biodivers.* 8:3–9

Willis KJ, Bhagwat S. 2010. Questions of importance to the conservation of biological biodiversity. *Clim. Past* 6:759–69

Willis KJ, Birks HJB. 2006. What is natural? The need for a long-term perspective in biodiversity conservation. *Science* 314:1261–65

Wilson S., Blake Ch., Berges A.J. & Maggs A.Ch (2004). Environmental tolerances of free-living coralline algae (maerl): implications for European marine conservation. Biological Conservation 120: 279–289

Wray J.L. (1971). Ecology and geologic distribution. *Geology of Calcareous Algae,* eds. R. Ginsburg R. Rezak J.L. Wray, 1:5.1-5.6.

Zabaler M. & Maluquer P. (1988). Illustration keys for the classification of Mediterranean Bryozoa, Treballs del Museu de Zoologia, Barcelona

Zahra A. Z., Adabi M.H, Burrett C.F. & Quilty G.F. (2004) Bryozoan distribution and growth form associations as a tool in environmental interpretation, Tasmania, Australia. *Sedimentary Geology* 167: 1-15.

Zavatarelli M., Baretta J.W., Baretta-Bekka J.G., & Pinardi N. (2000). The dynamics of the Adriatic Sea ecosystem: An idealized model study. Deep-Sea Research I 47:937-970

Zavatarelli M., Raicich F., Bregant D., Russo A. & Artegiani A. (1998). Climatological biogeochemical characteristics of the Adriatic Sea. *Journal of Marine Systems*, 18, 227–263.

Zeng E.Y., & Vista C.L. (1997). Organic Pollutants in the Coastal Environment off San Diego, California. 1. Source Identification and Assessment by Compositional indices of Polycyclic Aromatic Hydrocarbons. *Environmental Toxicology and Chemistry*, *16*(2), 179–188.

Zonta R., Zaggia L. & Argese E. (1994). Heavy metal and grain-size distributions in estuarine shallow water sediments of the Cona Marsh (Venice Lagoon, Italy). *Science of the Total Environment* 151/1: 19-28.

Zore-Armanda M., & Gacic M. (1987). Effects of bura on the circulation in the North Adriatic. *Annales Geophysicae* 5B:93-102

Zuschin M., Stachowitsch M., Pervesler P., & Kollmann H., (1999) Structural features and taphonomic pathways of a high-biomass epifauna in the northern Gulf of Trieste, Adriatic Sea: Lethaia, v. 32, p. 299–317.

Zuschin M. & Stachowitsch M. (2009). Epifauna-Dominated Benthic Shelf Assemblages: Lessons From the Modern Adriatic Sea. *Palaios*, *24*(4), 211–221. doi:10.2110/palo.2008.p08- 062r

Zuschin M. & Piller W.E. (1997) Gastropod shells recycled - an example from a rocky tidal flat in the Northern Bay of Safaga (Red Sea, Egypt). *Lethaia* 30, 127-134.

Websites:

Oliver P.G., Holmes A.M., Killeen I.J. & Turner J.A. 2010 *Marine Bivalve Shells of the British Isles* (Mollusca: Bivalvia). Amgueddfa Cymru - National Museum Wales. Available online at http://naturalhistory.museumwales.ac.uk/britishbivalves. [Accessed: 14 November 2016].

NOAA: Screening quick reference table: http://response.restoration.noaa.gov/sites/default/files/SQuiRTs.pdf [Accessed: 10 March 2017]

WoRMS: http://www.marinespecies.org/ [Accessed: 14 January 2017]

Program packages

Colwell R.K. (2013). EstimateS: Statistical estimation of species richness and shared species from samples. Version 9. User's Guide and application published at: http://purl.oclc.org/estimates.

Hsieh T. C., Ma K. H. & Anne Chao. (2016). iNEXT: iNterpolation and EXTrapolation for species diversity. R package version 2.0.8, URL: http://chao.stat.nthu.edu.tw/blog/software-download

Kindt R. & Coe R. (2005). Tree diversity analysis. A manual and software for common statistical methods for ecological and biodiversity studies. World Agroforestry Centre (ICRAF), Nairobi. ISBN 92-9059-179-X.

Oksanen J., Guillaume B.F., Kindt R., Legendre P., Minchin P.R., O'Hara R.B., Simpson G.L., Solymos P., Stevens M. & Wagner H. (2015). vegan: Community Ecology Package. R package version 2.3-1. https://CRAN.R-project.org/package=vegan.

PAST: Hammer, Ø., Harper, D.A.T., and Ryan, P.D. (2001) Past: paleontological statistics software package for education and data analysis. Palaeontologia Electronica 4:9

R: R Core Team (2016). R: A language and environment for statistical computing. R Foundation for Statistical Computing, Vienna, Austria; http://www.R-project.org/.

Roberts D.W. (2016). labdsv: Ordination and Multivariate Analysis for Ecology. R package version 1.8-0. https://CRAN.R-project.org/package=labdsv

Simpson G.L. & Oksanen J. (2016). analogue: Analogue matching and Modern Analogue Technique transfer function models. (R package version 0.17-0). (http://cran.r-project.org/package=analogue).

Wickham H., (2009). ggplot2: Elegant Graphics for Data Analysis. Springer-Verlag New York.

APPENDIX

Summary

The current study makes use of tools provided by the relatively new field of conservation paleobiology. The aim is to relate changes in benthic communities to past environmental conditions. This approach allows to define a baseline to estimate impact of changing environmental conditions at a timescale beyond direct human observation by using geo-historical data. Cores of 9cm and 16cm diameter were taken with an UWITEC™ piston corer south to Veliki Brijun, the main island of Brijuni Nationalpark to obtain sufficient material for analysis of hard part remains, sediment and environmental pollutants. Hard part remains within the taxonomic groups of mollusca, echinodermata, crustacea, bryozoa, brachiopoda, foraminifera and corallinaceae were found. Analysis of community composition generally divided the core in two section. The lower part (60-105cm sediment depth) is characterized by coarse sediment, strong reworking and species adapted to moderate to high energy environments. Furthermore, occurrence of terrestrial and limnic snails and frequently found terrestrial material such as woody and reed like plant remains at this section indicate strong terrestrial influence, suggesting a shallow water environment at the onset of the Holocene transgression. Crustacea, mainly the thalassinid mud shrimp *Upogebia cf. deltaura,* Mollusca (Scaphopoda, Gastropoda, Bivalves, Polyplacophora), serpulid worms and Echinoidea are characteristic taxa for this part of the core.

Silt and clay make up the major part at the upper sections of the core. Sea level rise is assumed to have already decelerated at this time period and reached almost todays state. Increase in occurrence of erect bryozoans strongly dominated by *Cellaria salicornioides* and maerl, produced mainly by the free living calcareous alga *Phymatolithon sp.,* both hinting to a deeper setting with lower current intensities. A conspicuous peak of macroids occurrence and bryozoan species richness around 50-60 cm core depth hints to the development of secondary hardbottom like state at 3000-5000 years BP. Increase in nutrient accumulation and fine grain sediment towards the top correlates with shifts in taxonomic composition. Bryozoan diversity displays a hump-shaped pattern along the core with its maximum at about 40cm sediment depth, whereas species richness stays relatively constant. The only exceptions are the aforementioned macroid-layer and the very low species number at the 4-6cm section. Distinctive peaks in heavy metal especially Hg and Pb and organic environmental pollutants (PAH, PCB)

in the uppermost 10cm strongly emphasize anthropogenic origin. Compositional changes of the benthic megafauna displayed a significant relation to concentration of these contaminates. Taxonomic shifts in the upper 20 cm, therefore can possibly be attributed to anthropogenic pressure.

Zusammenfassung

Die gegenwärtige Studie bedient sich der Werkzeuge der relativ neuen Disziplin der „conservation paleobiology". Das Ziel besteht darin, Zusammenhänge zwischen Veränderungen benthischer Artengemeinschaften und Umweltbedingungen zu finden. Dieser Ansatz erlaubt es einen Grundwert zu definieren, um die Auswirkungen sich ändernder Umweltbedingungen einschätzen zu können, welcher einen Zeitraum direkter menschlicher Beobachtung überspannt. Südlich von Veliki Brijuni, der größten Insel des Brijuni Nationalparks, wurden Bohrkerne mit dem Durchmesser 9cm und 16 cm entnommen, um Sediment, Schadstoffgehalt und Material für die Analyse von Schalenrückständen und andere Harteilen zu analysieren. Es wurden Überreste von Mollusken, Echinodermata, Crustacea, Bryozoa, Brachiopoda, Foraminifera und Kalkrotalgen gefunden. Der Bohrkern kann, basierend auf der Analyse der Artengemeinschaft in zwei Bereiche unterteilt werden. Der untere Bereich (60-105cm) ist charakterisiert durch einen erhöhten Anteil an grobkörnigem Sediment und Arten die an mittlere bis starke Wasserbewegungen angepasst sind.

Das Auftreten von terrestrischen und limnischen Gastropoden und ein hoher Gehalt an holzigem und schilfähnlichem terrestrischen Material, weist auf einen starken Einfluss des umgebenden Landes hin. In der Artenverteilung des unteren Teils des Kerns, wird der relativ seichte Bereich zur Zeit der Holozänen Transgression ersichtlich. Crustacaen, die hauptsächlich aus der einen Art des Maulwurfkrebse *Upogebia cf deltaura* bestehen, Mollusken (Scaphopoden, Gastropoden, Bivalven, Polyplacophora), Serpuliden und Echinodermaten sind die charakteristischen taxonomischen Gruppen in diesen tieferen Schichten.

Im jüngeren Teil überwiegt Silt und Ton. Es kann angenommen werden, dass in diesem Bereich sich der Anstieg des Meeresspiegels verlangsamt und sich beinahe auf dem heutigen Niveau befunden hat. Verstärktes Auftreten von Bryozoen, stark dominiert durch die Art *Cellaria salicornioides* und Maerl, großteils gebildet von der frei lebenden Kalkrotalge *Phymatolithon sp.,*

deuten auf einen höheren Wasserstand und geringere Strömungsgeschwindigkeiten hin. Verstärktes Vorkommen von Macroiden und eine hohe Artenvielfalt von Bryozoen in einer Sedimenttiefe von 50-60 cm weisen auf die Entstehung eines sekundären Hartbodens vor 3000-5000 Jahren hin. Es konnte gezeigt werden, dass der Anstieg von Nähstoffen und feinkörnigem Sediment in höheren Schichten mit Veränderungen in der taxonomischen Zusammensetzung korreliert. Die Diversität der Bryozoen erreicht ihr Maximum im mittleren Bereich in einer Schichttiefe von 40cm, während die Artenvielfalt relativ konstant bleibt. Die einzigen Ausnahmen sind die bereits erwähnte Macroid-Schicht und eine sehr geringe Anzahl an Arten in der Schicht zwischen 4-6cm Tiefe. Markante Anstiege an Schwermetallen, besonders von Hg und Pb und organischen Schadstoffen lassen eine anthropogene Ursache vermuten. Veränderungen der Zusammensetzung der benthischen Megafauna zeigt eine signifikante Korrelation zu den gemessenen Konzentrationen im Sediment. Taxonomische Veränderungen in den obersten 20cm ist daher wahrscheinlich auf menschlichen Einfluss zurückzuführen.

List of species

Bryozoa (abundance)

FAMILY	SPECIES	ABUNDANCE	GROWTH-TYPE	HABITUS
Cellariidae	*Cellaria fistulosa*	167	erect	cellariiform
Cellariidae	*Cellaria salicornioides*	383	erect	cellariiform
Cellariidae	*Cellaria sp.*	2	erect	cellariiform
Myriaporidae	*Myriapora truncata*	81	erect	vinculariiform
Phoceanidae	*Phoceana tubulifera*	62	erect	vinculariiform
Margarettidae	*Margaretta cereoides*	4	erect	cellariiform
Schizoporellidae	*Schizoporella magnifica*	1	encrusting	membraniporiform
Schizoporellidae	*Schizoporella dunkeri*	1	encrusting	membraniporiform
Schizoporellidae	*Schizoporella cf. S. tetragona*	1	encrusting	membraniporiform
Schizoporellidae	*Schizobrachiella sanguinea*	6	encrusting	membraniporiform
Microporellidae	*Microporella ciliata*	26	encrusting	membraniporiform
Cryptosulidae	*Cryptosula pallasiana*	2	encrusting	membraniporiform
Escharinidae	*Escharina vulgaris*	1	encrusting	membraniporiform
Cheiloporinidae	*Hagiosynodos cf kirchenpaueri*	19	encrusting	membraniporiform
Phidoloporidae	*Schizotheca serratimargo*	108	erect	adeoniform
Phidoloporidae	*Schizotheca fissa*	3	encrusting	membraniporiform
Phidoloporidae	*Dentiporella sardonica*	63	encrusting	celleporiform

Family	Species	Count	Growth	Morphotype
Phidoloporidae	*Rhynchozoon neapolitanum*	13	encrusting	celleporiform
Phidoloporidae	*Reteporella cf. grimaldii*	58	erect	reteporiform
Celleporidae	*Turbicellepora avicularis*	29	encrusting/erect	celleporiform
Celleporidae	*Turbicellepora camera*	14	encrusting/erect	celleporiform
Celleporidae	*Celleporina siphuncula*	6	encrusting	celleporiform
Celleporidae	*Celleporina sp.*	10	encrusting	celleporiform
Celleporidae	*Celleporina caminata*	31	encrusting	celleporiform
Celleporidae	*Buskea nitida*	5	erect	vinculariiform
Celleporidae	*Cellepora adriatica*	9	encrusting	celleporiform
Celleporidae	*Lagenipora sp.*	1	encrusting	membraniporiform
Smittinidae	*Smittina cervicornis*	121	erect	adeoniform
Smittinidae	*Parasmittina cf rouvillei*	39	encrusting	membraniporiform
Smittinidae	*Prenantia cheilostoma*	2	encrusting	membraniporiform
Bitectiporidae	*Pentapora fascialis*	129	erect	eschariform
Bitectiporidae	*Schizomavella auriculata/ asymetrica*	28	encrusting	membraniporiform
Bitectiporidae	*Schizomavella linearis*	44	encrusting	membraniporiform
Bitectiporidae	*Schizomavella cornuta*	65	encrusting	membraniporiform
Bitectiporidae	*Schizomavella rudis*	3	encrusting	membraniporiform
Bitectiporidae	*Hippoporina pertusa*	1	encrusting	membraniporiform
Watersiporidae	*Watersipora cucullata*	1	encrusting	membraniporiform
Adeonellidae	*Adeonella pallasii*	183	erect	adeoniform
Adeonidae	*Reptadeonella violacea*	34	encrusting	membraniporiform
Microporidae	*Calpensia nobilis*	63	encrusting	membraniporiform
Candidae	*Scrupocellaria scruposa*	3	erect	cellariiform
Chorizoporidae	*Chorizopora brongniartii*	28	encrusting	membraniporiform
Calloporidae	*Copidozoum tenuirostre*	78	encrusting	membraniporiform
Calloporidae	*Ellisina gautieri*	1	encrusting	membraniporiform
Antroporidae	*Rosseliana rosselii*	2	encrusting	membraniporiform
Cribrilinidae	*Collarina balzaci*	1	encrusting	membraniporiform
Cribrilinidae	*Puellina sp.*	3	encrusting	membraniporiform
Cribrilinidae	*Puellina hincksi*	2	encrusting	membraniporiform
Exochellidae	*Escharoides mamillata*	2	encrusting	membraniporiform
Romancheinidae	*Escharella rylandi*	6	encrusting	membraniporiform
Romancheinidae	*Escharella sp. #2*	4	encrusting	membraniporiform
Umbonulidae	*Umbonula ovicellata*	1	encrusting	membraniporiform
unidentified	*Species 1*	3	erect	adeoniform
unidentified	*Species 2*	1	encrusting	membraniporiform
unidentified	*Species3*	1	encrusting	membraniporiform

FAMILY	SPECIES		GROWTH-TYPE	HABITUS
unidentified	*Species 4*	1	encrusting	membraniporiform
unidentified	*Species 5*	2	encrusting	membraniporiform
Annectocymidae	*Entalophoroecia sp.*	17	creeping/erect	vinculariiform
Annectocymidae	*Annectocyma cf. major*	80	encrusting/erect	vinculariiform
Annectocymidae	*Annectocyma arcuata*	4	erect	vinculariiform
Tubuliporidae	*Exidmonea coerula*	39	erect	vinculariiform
Tubuliporidae	*Tubulipora cf. liliacea*	89	Encrusting/semierect	membraniporiform
Stomatoporidae	*Stomatopora gingrina*	1	erect	/
Plagioeciidae	*Plagioecia sp.*	1	encrusting	membraniporiform
Plagioeciidae	*Plagioecia sarniensis*	2	encrusting	membraniporiform
Plagioeciidae	*Plagioecia dorsalis*	5	Encrusting/semierect	membraniporiform
Plagioeciidae	*Plagioecia patina*	29	encrusting	membraniporiform
Diastoporidae	*Diplosolen obelium*	15	encrusting	membraniporiform
Diastoporidae	*Cardioecia watersi*	2	erect	vinculariiform
Lichenoporidae	*Disporella sp.*	5	encrusting	membraniporiform
Lichenoporidae	*Lichenopora cf. radiata*	19	encrusting	membraniporiform
Lichenoporidae	*Lichenopora sp. 2*	8	encrusting	/
Frondiporidae	*Frondipora verrucosa*	20	erect	reteporiform
Crisiidae	*Crisia ramosa*	1	erect	cellariiform
Horneridae	*Hornera sp.*	1	erect	vinculariiform

Bryozoa (weight)

FAMILY	SPECIES	WEIGHT (g)	GROWTH-TYPE	HABITUS
Cellariidae	*Cellaria fistulosa*	0.2504	erect	cellariiform
Cellariidae	*Cellaria salicornioides*	0.6219	erect	cellariiform
Cellariidae	*Cellaria sp.*	0.0025	erect	cellariiform
Myriaporidae	*Myriapora truncata*	1.8642	erect	vinculariiform
Phoceanidae	*Phoceana tubulifera*	0.3763	erect	vinculariiform
Margarettidae	*Margaretta cereoides*	0.0174	erect	cellariiform
Schizoporellidae	*Schizoporella magnifica*	0.0016	encrusting	membraniporiform
Schizoporellidae	*Schizoporella dunkeri*	0.014	encrusting	membraniporiform
Microporellidae	*Microporella ciliata*	0.0139	encrusting	membraniporiform
Cryptosulidae	*Cryptosula pallasiana*	0.0009	encrusting	membraniporiform
Phidoloporidae	*Schizotheca serratimargo*	1.7512	erect	adeoniform
Phidoloporidae	*Dentiporella sardonica*	1.565	encrusting	celleporiform
Phidoloporidae	*Rhynchozoon neapolitanum*	0.1615	encrusting	celleporiform
Phidoloporidae	*Reteporella cf. grimaldii*	0.1236	erect	reteporiform
Celleporidae	*Turbicellepora avicularis*	0.1829	encrusting/erect	celleporiform
Celleporidae	*Turbicellepora camera*	0.24	encrusting/erect	celleporiform

Celleporidae	*Celleporina siphuncula*	0.0091	encrusting	celleporiform
Celleporidae	*Celleporina sp.*	0.0286	encrusting	celleporiform
Celleporidae	*Celleporina caminata*	0.3191	encrusting	celleporiform
Celleporidae	*Buskea nitida*	0.0096	erect	vinculariiform
Celleporidae	*Cellepora adriatica*	0.0346	encrusting	celleporiform
Celleporidae	*Lagenipora sp.*	0.0006	encrusting	membraniporiform
Smittinidae	*Smittina cervicornis*	0.9485	erect	adeoniform
Smittinidae	*Parasmittina cf rouvillei*	0.0869	encrusting	membraniporiform
Smittinidae	*Prenantia cheilostoma*	0.0153	encrusting	membraniporiform
Bitectiporidae	*Pentapora fascialis*	1.463	erect	eschariform
Bitectiporidae	*Schizomavella auriculata/ asymetrica*	0.0253	encrusting	membraniporiform
Bitectiporidae	*Schizomavella linearis*	0.0448	encrusting	membraniporiform
Bitectiporidae	*Schizomavella cornuta*	0.3536	encrusting	membraniporiform
Bitectiporidae	*Schizomavella rudis*	0.0033	encrusting	membraniporiform
Adeonellidae	*Adeonella pallasii*	1.2006	erect	adeoniform
Adeonidae	*Reptadeonella violacea*	0.0144	encrusting	membraniporiform
Microporidae	*Calpensia nobilis*	0.0212	encrusting	membraniporiform
Candidae	*Scrupocellaria scruposa*	0.0011	erect	cellariiform
Chorizoporidae	*Chorizopora brongniartii*	0.0004	encrusting	membraniporiform
Calloporidae	*Copidozoum tenuirostre*	0.0001	encrusting	membraniporiform
Cribrilinidae	*Puellina hincksi*	0.0007	encrusting	membraniporiform
Exochellidae	*Escharoides mamillata*	0.0017	encrusting	membraniporiform
/	*Species 1*	0.0074	erect	adeoniform
/	*Species 4*	0.0019	encrusting	membraniporiform
/	*Species 5*	0.0038	encrusting	membraniporiform
Annectocymidae	*Entalophoroecia sp.*	0.0206	creeping/erect	vinculariiform
Annectocymidae	*Annectocyma cf. major*	0.2113	encrusting/erect	vinculariiform
Annectocymidae	*Annectocyma arcuata*	0.0059	erect	vinculariiform
Tubuliporidae	*Exidmonea coerula*	0.0676	erect	vinculariiform
Tubuliporidae	*Tubulipora cf. liliacea*	0.3099	Encrusting/semierect	membraniporiform
Stomatoporidae	*Stomatopora gingrina*	0.0002	erect	/
Plagioeciidae	*Plagioecia sp.*	0.0008	encrusting	membraniporiform
Plagioeciidae	*Plagioecia sarniensis*	0.0021	encrusting	membraniporiform
Plagioeciidae	*Plagioecia dorsalis*	0.0176	Encrusting/semierect	membraniporiform
Plagioeciidae	*Plagioecia patina*	0.0487	encrusting	membraniporiform
Diastoporidae	*Diplosolen obelium*	0.0259	encrusting	membraniporiform
Diastoporidae	*Cardioecia watersi*	0.0087	erect	vinculariiform
Lichenoporidae	*Disporella sp.*	0.0079	encrusting	membraniporiform
Lichenoporidae	*Lichenopora cf. radiata*	0.0525	encrusting	membraniporiform

Lichenoporidae	*Lichenopora sp. 2*	0.0868	encrusting	/
Frondiporidae	*Frondipora verrucosa*	0.1413	erect	reteporiform
Crisiidae	*Crisia ramosa*	0.0004	erect	cellariiform

Gastropoda

FAMILY	ABUNDANCE	WEIGHT (g)	SUBSTRATRELATION
Lottidae	53	0.2204	Epifaunal
Fissurellidae	17	0.3444	Epifaunal
Scissurellidae	36	0.0608	Epifaunal
Phasianellidae	2	0.0904	Epifaunal
Trochidae	218	2.8647	Epifaunal
Turbinidae	3	0.0136	Epifaunal
Rissoidae	819	7.4291	Epifaunal
Aporrhaidae	9	0.1249	Semiinfaunal
Tornidae	33	0.2338	Host
Vanikoridae	4	0.0057	Epifaunal
Calyptraeidae	26	0.0691	Epifaunal
Hydrobiidae	41	0.2871	Epifaunal
Iravadiidae	4	0.01	Semiinfaunal
Naticidae	24	0.6002	Infaunal
Capulidae	37	0.7416	Epifaunal
Cerithiidae	607	5.2212	Epifaunal
Turritellidae	18	0.1893	Semiinfaunal
Epitoniidae	26	0.4351	Host
Aclididae	6	0.0219	Host
Eulimidae	20	0.1649	Host
Muricidae	55	0.9837	Epifaunal
Cystiscidae	5	0.0387	Epifaunal
Costellariidae	3	0.0885	Infaunal
Fasciolariidae	6	0.1026	Epifaunal
Nassariidae	138	2.9747	Epifaunal
Columbellidae	9	0.2851	Epifaunal
Conoidae	56	0.7626	Epifaunal
Cerithiopsidae	92	0.9497	Epifaunal
Triphoridae	72	1.079	Host
Pyramidellidae	67	0.5409	Host
Haminoeidae	2	0.1009	Epifaunal
Philinidae	2	0.0036	Epifaunal
Retusidae	2	0.0152	Infaunal
Neritidae (Theodoxus fluviatilis)	13	0.2435	limnic
Succineidae	3	0.0672	terrestrial
Limnic snails	49	0.804	limnic

Bivalvia

FAMILY	ABUNDACE	WEIGHT (g)	SUBSTRATERELATION
Nuculanidae	70	0.46552	Infaunal
Nuculidae	381	5.93844	Infaunal
Arcidae	84	3.7311	Epifaunal
Noetinae	499	2.374	Epifaunal
Glycymerididae	66	0.1175	Infaunal
Crenellinae	33	0.0256	Host
Modiolinae	404	1.2363	Semiinfaunal
Pectinidae	374	5.5499	Epifaunal
Anomioidea	951	1.5889	Epifaunal
Limidae	138	0.3902	Epifaunal
Ostreidae	131	5.2887	Epifaunal
Chamidae	17	0.0196	Epifaunal
Lucinidae	33	0.344	Infaunal
Thyasiridae	26	0.018	Infaunal
Lasaeidae	51	0.0223	Host
Kellidae	121	0.0272	Host
Montacutidae	10	0.01288	Host
Cardiidae	1106	2.913	Infaunal
Semelidae	130	0.2083	Infaunal
Tellinidae	122	0.6763	Infaunal
Veneridae	1710	10.3295	Infaunal
Trapezidae	12	0.106	Infaunal
Corbulidae	439	2.857	Infaunal
Gastrochaenidae	69	0.4517	Borer
Hiatellidae	204	0.4851	Nestler
Cuspidariidae	1	0.0025	Infaunal
Thraciidae	16	0.052	Infaunal

Remaining taxonomic groups

TAXA	WEIGHT (g)
Macroids	112.8136
Corallinaceae	34.9183
Polychaeta	7.8456
Polyplacophora	0.50311
Scaphopoda	0.3347
Ophiurida	0.09343
Echinoidea	6.7015
Brachiopoda	0.078
Foraminifera	0.2818
Crustacea	8.5032